

N-body & Hydrodynamic Simulations

Stefano Borgani

Dept. of Physics - University of Trieste

INAF – Astronomical Observatory of Trieste & INFN - Trieste

- I. N-body methods
- II. Hydrodynamical Methods
 - i. Lagrangian methods (SPH)
 - ii. Eulerian Methods
- III. Applications to formation of cosmic structures
 - i. Including astrophysics of galaxy formation
 - ii. Cosmology with galaxy clusters and simulations



Part I: N-body simulations

Based on:

Springel 2005, MNRAS, 364, 1005

Dolag, SB+, 2008, Sp.Sc.Rev., 2008, 134

Springel, arXiv:1412:5187

What is an N-body code?



Problem: solve the dynamics of a self-gravitating collisionless system

Collisionless Boltzmann (Vlasov) + Poisson equations:

$$\frac{\partial f}{\partial t} + \frac{\mathbf{p}}{ma^2} \nabla f - m \nabla \Phi \frac{\partial f}{\partial \mathbf{p}} = 0 \quad f(\mathbf{x}, \mathbf{p}, t) : \text{Phase-space distrib. function}$$

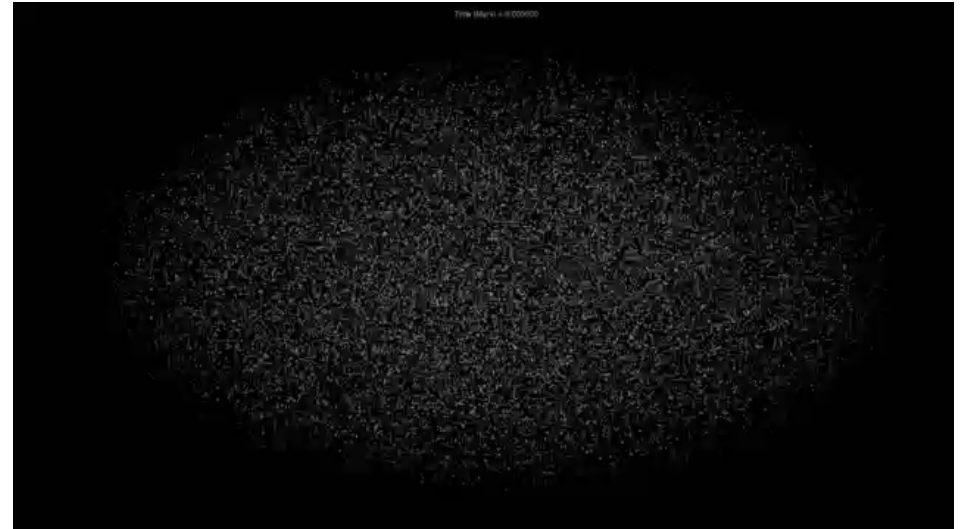
$$\nabla^2 \Phi(\mathbf{x}, t) = 4\pi G a^2 [\rho(\mathbf{x}, t) - \bar{\rho}(t)]$$

$$\rho(\mathbf{x}, t) = \int f(\mathbf{x}, \mathbf{p}, t) d^3 p$$

→ Tough to deal with: it's in 6D!

N-body approximation:

- sample the initial phase space with N discrete fluid elements
- integrate their eqs. of motion in the collective gravity field
- equivalent to solving the characteristic eqs., describing curves in phase space where $f(\mathbf{x}, \mathbf{p}, t)$ is constant



What is an N-body code?

- Integrate the equations of motions of the N particles:

$$\frac{d\mathbf{p}}{dt} = -m\nabla\Phi \qquad \frac{d\mathbf{x}}{dt} = \frac{\mathbf{p}}{ma^2}$$

Direct N-body code: For each particle compute the contribution to the potential from all the other N-1 particles:

$$\Phi(\mathbf{r}) = -G \sum_j \frac{m_j}{(|\mathbf{r} - \mathbf{r}_j|^2 + \epsilon^2)^{\frac{1}{2}}}$$

ϵ : softening parameter ($\sim 1/20$ - $1/50$ MIS)

→ To reduce spurious two-body relaxation when a finite particle number is used to describe a collisionless fluid

→ $N(N-1)/2$ operations!!!

Solutions:

- Resort to special purpose hardware solutions (e.g. GPUs)
- Resort to faster integration methods, always implying a lower accuracy

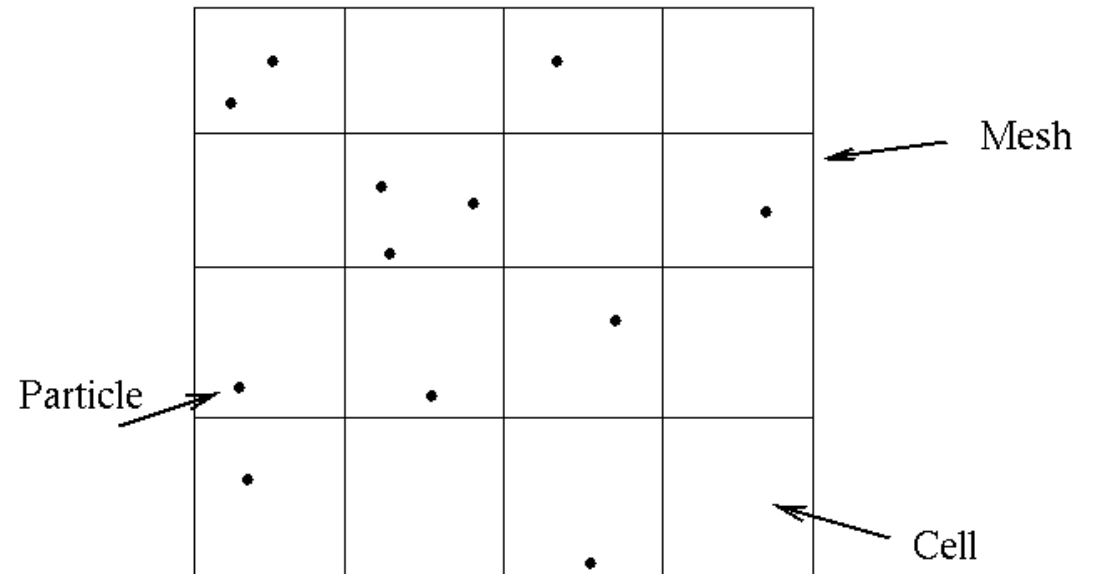


Particle-Mesh (PM)

1st STEP: assign densities to the mesh from particle positions

$$\rho_m = \frac{1}{h^3} \sum_i m_i W(\mathbf{x}_i - \mathbf{x}_m)$$

$W(\mathbf{x}_m - \mathbf{x}_i)$: weighting function



2nd STEP: solve the Poisson equation in Fourier space

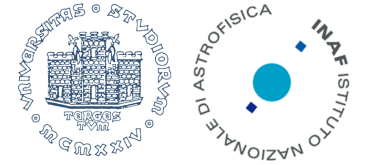
$$\Phi(\mathbf{x}) = \int g(\mathbf{x} - \mathbf{x}') \rho(\mathbf{x}') d\mathbf{x}'$$

Solution of the Poisson eq. with
 $g(\mathbf{x}) = -G/|\mathbf{x}|$: Green's function of the Laplacian

→ Use FFT to compute $\hat{\Phi}(\mathbf{k}) = \hat{g}(\mathbf{k}) \hat{\rho}(\mathbf{k})$

→ Transform back to compute $\Phi(\mathbf{x})$

Particle-Mesh (PM)



3rd STEP: compute the force on the grid: $\mathbf{f}(\mathbf{x}) = -\nabla\Phi(\mathbf{x})$

Use a finite differentiation: $f_{i,j,k}^{(x)} = -\frac{\Phi_{i+1,j,k} - \Phi_{i-1,j,k}}{2h}$

4th STEP: interpolate back forces to particles positions, using the same weighting scheme:

$$\mathbf{f}(\mathbf{x}_i) = \sum_m W(\mathbf{x}_i - \mathbf{x}_m) \mathbf{f}_m$$

5th STEP: update particle positions and velocities
E.g. using the “leapfrog” scheme to integrate $\ddot{\mathbf{x}} = \mathbf{f}(\mathbf{x})$

Kick-Drift-Kick

$$\mathbf{v}_{n+1/2} = \mathbf{v}_n + \mathbf{f}(\mathbf{x}_n)\Delta t/2$$

$$\mathbf{x}_{n+1} = \mathbf{x}_n + \mathbf{v}_{n+1/2}\Delta t$$

$$\mathbf{v}_{n+1} = \mathbf{v}_{n+1/2} + \mathbf{f}(\mathbf{x}_{n+1})\Delta t/2$$

Drift-Kick-Drift

$$\mathbf{x}_{n+1/2} = \mathbf{x}_n + \mathbf{v}_n\Delta t/2$$

$$\mathbf{v}_{n+1} = \mathbf{v}_n + \mathbf{f}(\mathbf{x}_{n+1/2})\Delta t$$

$$\mathbf{x}_{n+1} = \mathbf{x}_{n+1/2} + \mathbf{v}_{n+1}\Delta t/2.$$

$$\Delta t = \alpha \sqrt{\epsilon/|\mathbf{a}|}$$

$$\alpha \approx 0.1$$

N + N_g log N_g operations now required !

Tree codes

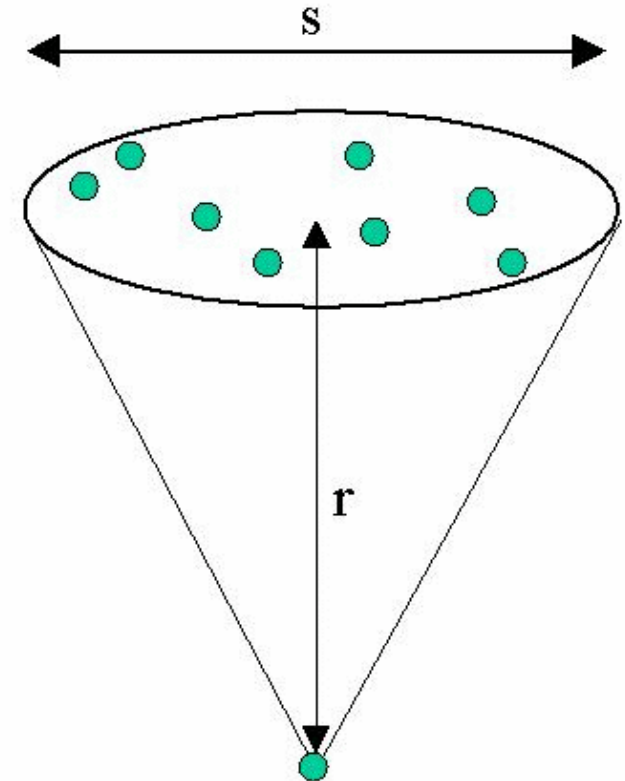
Barnes & Hut 86

Basic idea: treat a distant group of particles as a single “macro-particle”

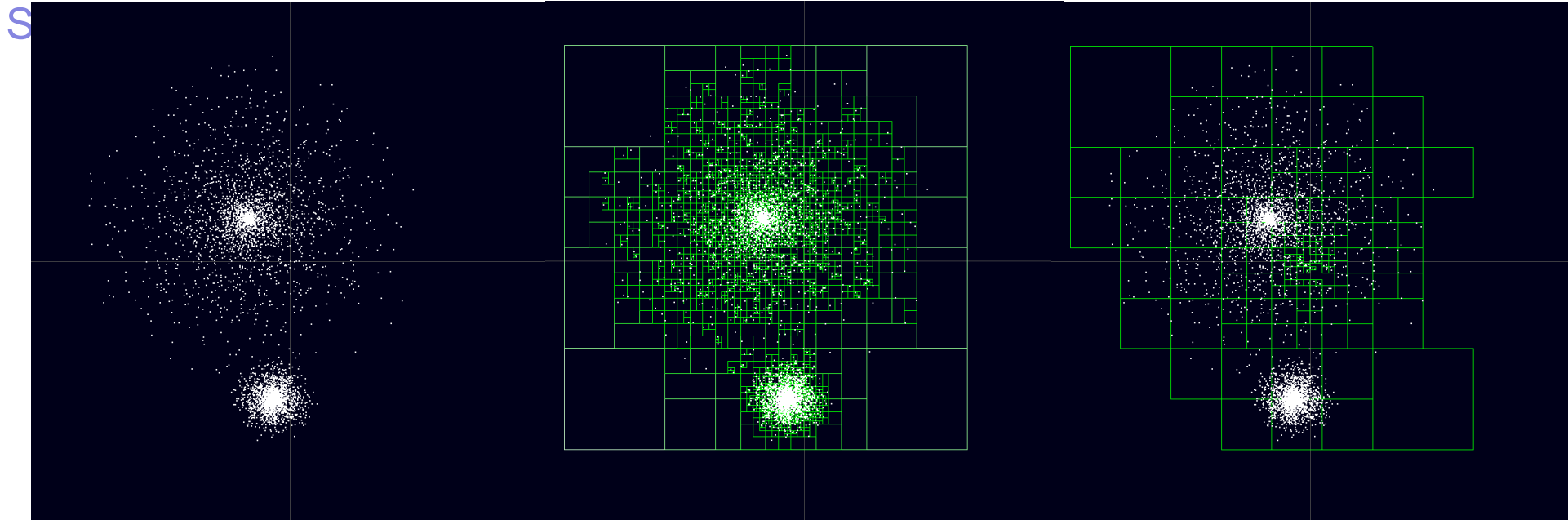
Precision regulated by the value of the “critical opening angle”: $s > r/\theta_c$ ($\theta_c \sim 0.5$)

→ $N \log N$ operations required, but:

- Pre-factor depending on how clustered is the particle distribution
- Need to construct and store the structure a hierarchical binary tree.



Tree codes



→ Recursively divide the simulation box in sub-domains until each “leaf” of the “tree” contains either one or zero particles

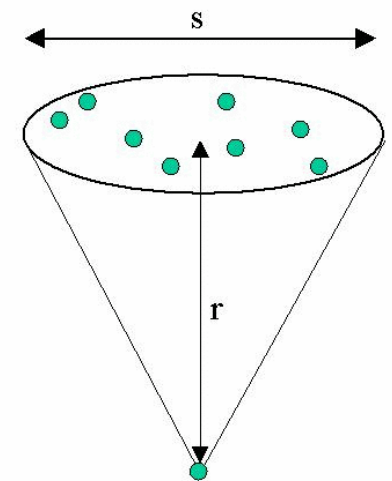
→ “Walk” the tree for each particle, starting from the top-node.

r : spatial extent of the node.

s : distance of the center of mass of the node from the particle

$\theta_c < r/s$ → open the node and iterate

$\theta_c > r/s$ → compute the force from the node on the particle



TreePM (e.g. Bagla 02):

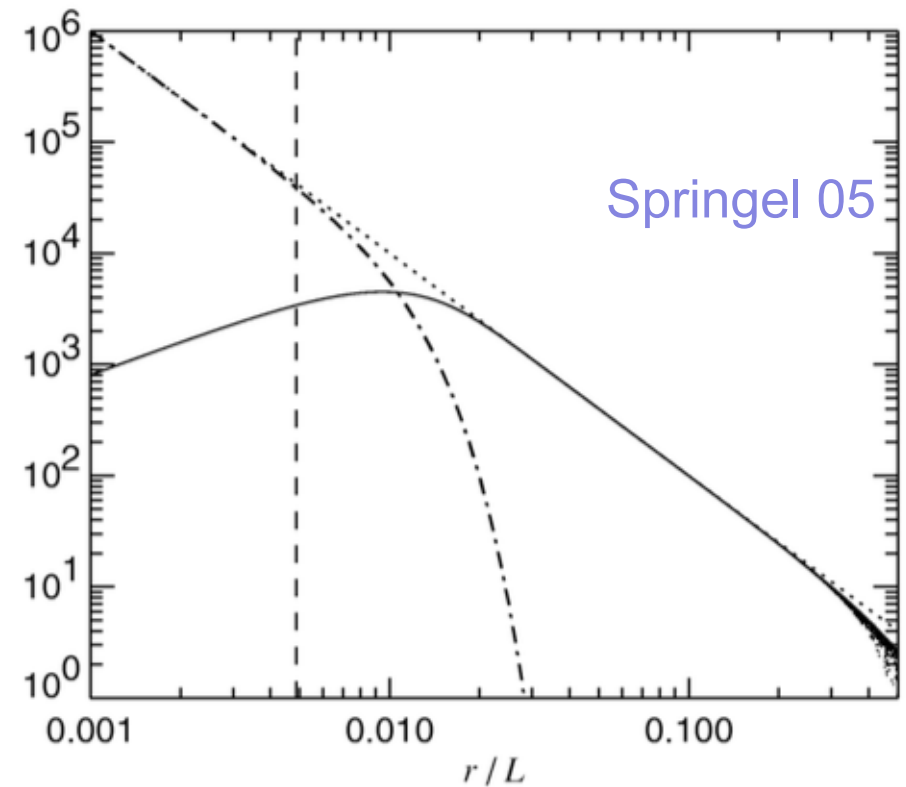
$$\Phi_{\mathbf{k}} = \Phi_{\mathbf{k}}^{\text{long}} + \Phi_{\mathbf{k}}^{\text{short}}$$

$$\Phi_{\mathbf{k}}^{\text{long}} = \Phi_{\mathbf{k}} \exp(-\mathbf{k}^2 r_s^2)$$

→ from the PM method
 r_s : splitting scale

$$\Phi^{\text{short}}(\mathbf{x}) = -G \sum_i \frac{m_i}{r_i} \operatorname{erfc} \left(\frac{r_i}{2r_s} \right)$$

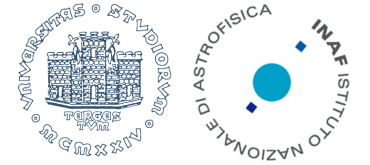
→ from the Tree part



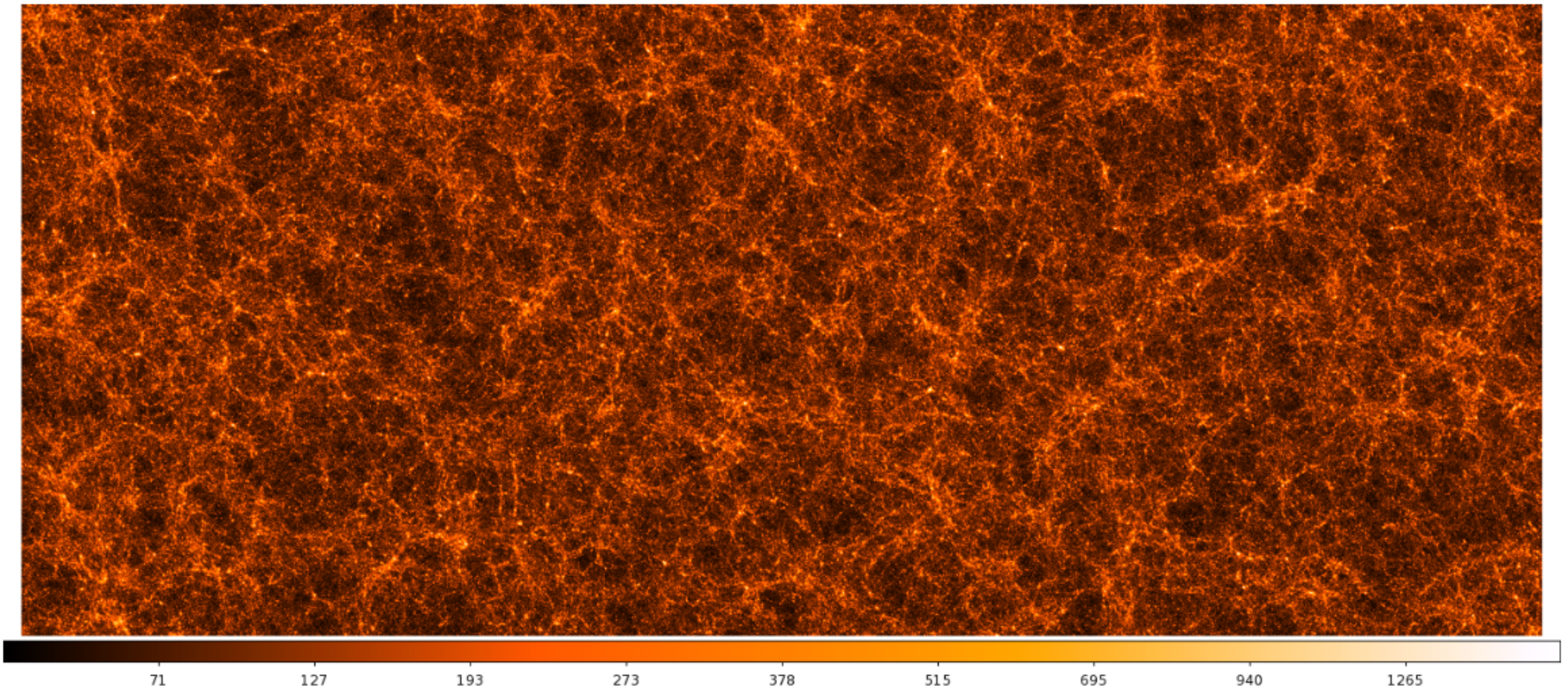
P3M (e.g. Efstathiou+85): same as TreePM with $\Phi_{short}(\mathbf{x})$ computed from direct integration

AP3M/ATreePM (e.g. Couchman 91, Springel 05): same as above, with Adaptive PM

The record



Dark Sky Simulations; Skillman+14
 10240^3 particles; Box size = $8 h^{-1}$ Gpc



→ Past-light cone between $z=0.9$ and 1.0

Part II: Hydrodynamical Methods

Based on:

Monaghan, Rep. Prog. Phys., 2005, 68, 1793

Rosswog, NewA, 2009, 53, 78

Dolag, SB+, 2008, Sp.Sc.Rev., 2008, 134

Springel, arXiv:1412:5187

- To follow the formation and evolution of *baryonic structures* inside the potential wells of Dark Matter in non-linear regime
- Two large classes of numerical methods: **Lagrangian** and **Eulerian**
- **Eulerian** methods: follow the *fluxes* of gas and energies in space. Derivatives evaluated at fixed points in space
- **Lagrangian** methods: follow the evolution of *fluid elements*. Derivatives in a coordinate system following the fluid element

ρ : fluid density
 \mathbf{v} : fluid velocity
 P : pressure;
 u : internal energy;

Euler equations for a non-viscous fluid:

$$\frac{d\rho}{dt} = -\rho \nabla \cdot \vec{v}.$$

Continuity equation; mass conservation

$$\frac{d\vec{v}}{dt} = -\frac{\nabla P}{\rho} + \vec{f}, \quad \vec{f} = -\vec{\nabla} \Phi$$

Euler equation; momentum conservation

$$\frac{du}{dt} = \frac{P}{\rho^2} \frac{d\rho}{dt} = -\frac{P}{\rho} \nabla \cdot \vec{v}.$$

Energy conservation; 1st law of thermodynamics

$$dU = dQ - PdV,$$

$$P = (\gamma - 1)\rho u, \quad \gamma = c_p/c_v$$

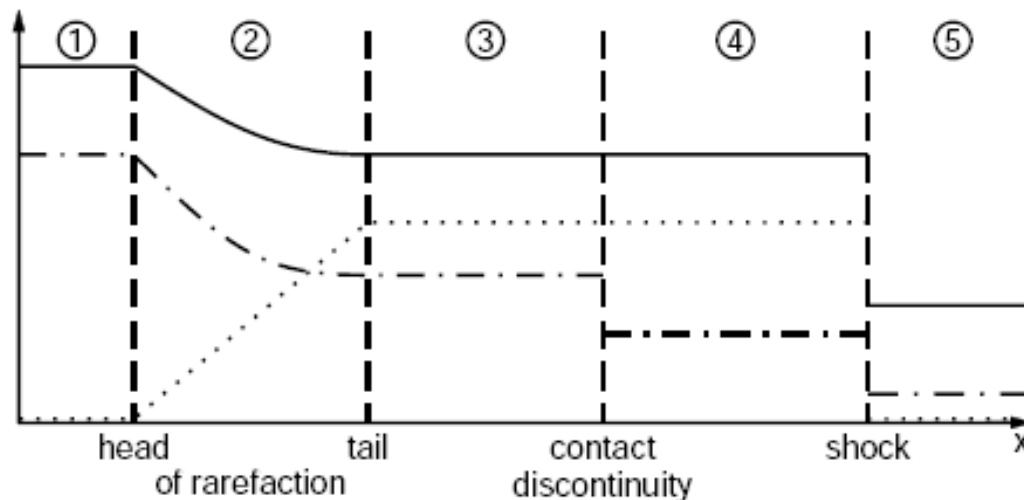
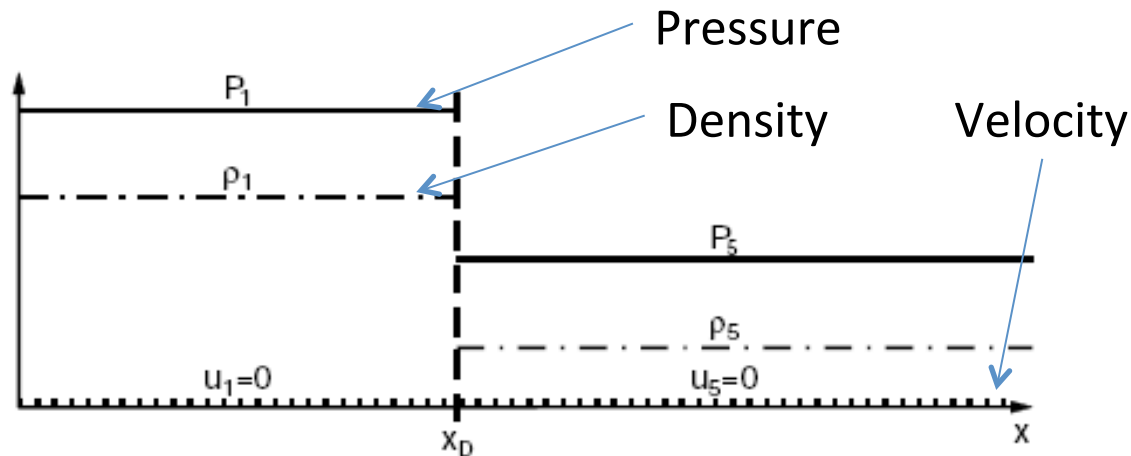
Equation of state

$\gamma=5/3$ for an ideal monoatomic gas

$$\frac{d}{dt} = \frac{dx^i}{dt} \frac{\partial}{\partial x^i} + \frac{\partial}{\partial t} = \vec{v} \cdot \nabla + \frac{\partial}{\partial t}$$

Lagrangian derivative

Eulerian methods – The Riemann problem



What is the Riemann problem:

- Initial value problem for a hyperbolic system

$$\frac{\partial U}{\partial t} + \nabla \cdot \mathbf{F} = 0$$

- Two piece-wise constant states with an interface at $t=0$

$$U_L = \begin{pmatrix} \rho_L \\ P_L \\ \mathbf{v}_L \end{pmatrix}, \quad U_R = \begin{pmatrix} \rho_R \\ P_R \\ \mathbf{v}_R \end{pmatrix}$$

$\mathbf{v}_L = \mathbf{v}_R = 0$: Sod shock tube

Shock: irreversible conversion of mechanical into thermal energy

Contact discontinuity: original separation plane

Rarefaction wave: smoothly connects two states

Eulerian methods - Discretization



Equations of fluido-dynamics:

$$\frac{\partial \mathbf{U}}{\partial t} + \nabla \cdot \mathbf{F} = 0$$

$$P = (\gamma - 1)\rho u$$

State variable

$$\mathbf{U} = \begin{pmatrix} \rho \\ \rho \mathbf{v} \\ \rho e \end{pmatrix},$$

Fluxes

$$\mathbf{F} = \begin{pmatrix} \rho \mathbf{v} \\ \rho \mathbf{v} \mathbf{v}^T + P \\ (\rho e + P)\mathbf{v} \end{pmatrix}, \quad e = u + \mathbf{v}^2/2$$

$$\mathbf{U}_i = \frac{1}{V_i} \int_{\text{cell } i} \mathbf{U}(\mathbf{x}) dV. : \text{average state within a cell}$$

	$P_i, V_i,$ u_i, ρ_i	$P_j, V_j,$ u_j, ρ_j

→ Integration of conservation law within a cell in a given time interval

$$\int_{x_{i-\frac{1}{2}}}^{x_{i+\frac{1}{2}}} dx \int_{t_n}^{t_{n+1}} dt \left(\frac{\partial \mathbf{U}}{\partial t} + \frac{\partial \mathbf{F}}{\partial x} \right) = 0.$$

$$\rightarrow \int_{x_{i-\frac{1}{2}}}^{x_{i+\frac{1}{2}}} dx [\mathbf{U}(x, t_{n+1}) - \mathbf{U}(x, t_n)] + \int_{t_n}^{t_{n+1}} dt [\mathbf{F}(x_{i+\frac{1}{2}}, t) - \mathbf{F}(x_{i-\frac{1}{2}}, t)] = 0.$$

Cell-average at the n -th time-step:
$$\mathbf{U}_i^{(n)} \equiv \frac{1}{\Delta x} \int_{x_{i-\frac{1}{2}}}^{x_{i+\frac{1}{2}}} \mathbf{U}(x, t_n) dx.$$

$$\rightarrow \Delta x [\mathbf{U}_i^{(n+1)} - \mathbf{U}_i^{(n)}] + \int_{t_n}^{t_{n+1}} dt [\mathbf{F}(x_{i+\frac{1}{2}}, t) - \mathbf{F}(x_{i-\frac{1}{2}}, t)] = 0.$$

Godunov scheme:

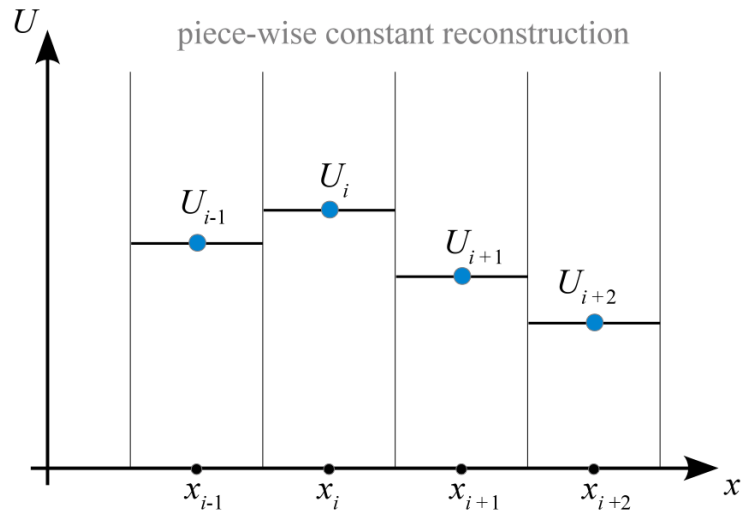
$\mathbf{F}(x_{i+\frac{1}{2}}, t)$ \rightarrow Solution of the Riemann problem with $\mathbf{U}_i^{(n)}$ as left state and $\mathbf{U}_{i+1}^{(n)}$ as right state:

$$\mathbf{F}_{i+\frac{1}{2}}^* = \mathbf{F}_{\text{Riemann}}(\mathbf{U}_i^{(n)}, \mathbf{U}_{i+1}^{(n)})$$

\rightarrow Advancement of the state:

$$\mathbf{U}_i^{(n+1)} = \mathbf{U}_i^{(n)} + \frac{\Delta t}{\Delta x} [\mathbf{F}_{i-\frac{1}{2}}^* - \mathbf{F}_{i+\frac{1}{2}}^*]$$

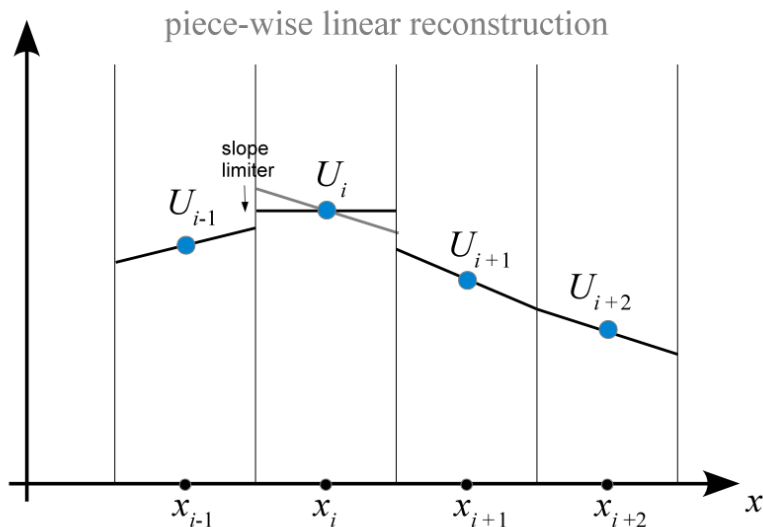
Reconstruct-Evolve-Average



Reconstruct: define the run of a quantity U^n in a cell to compute the cell-averaged value

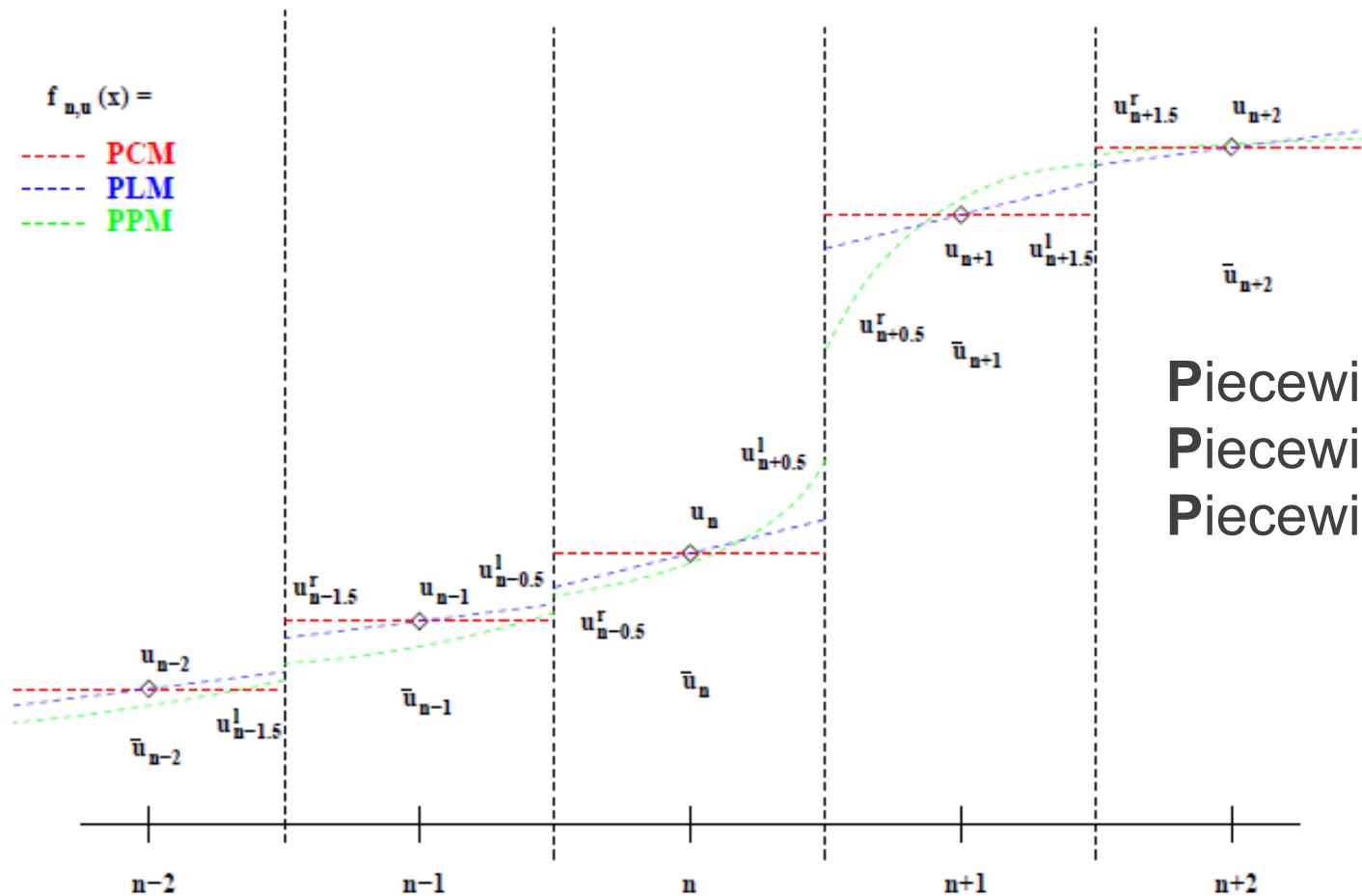
Evolve the reconstructed state by solving the Riemann problem at the cell interface and use this to evolve by Δt

Average: account for the fluxes entering and leaving the cell volume to compute the evolved cell-averaged state U^{n+1}



Slope Limiters: additional constraint on reconstruction, to prevent new extrema and unphysical oscillations in the solution

Reconstruction accuracy



Piecewise **C**onstant **M**ethod
Piecewise **L**inear **M**ethod
Piecewise **P**arabolic **M**ethod

- **Newer schemes:** (W)ENO: (Weighted) Essentially Non Oscillatory, MP: Monotonicity Preserving; Use more grid points with higher-order reconstruction in smooth part of the fluid, and sharp discontinuities at the shocks.

Extension to multiple dimensions



Euler equations in 3D:

$$\partial_t \begin{pmatrix} \rho \\ \rho u \\ \rho v \\ \rho w \\ \rho e \end{pmatrix} + \partial_x \begin{pmatrix} \rho u \\ \rho u^2 + P \\ \rho uv \\ \rho uw \\ \rho u(\rho e + P) \end{pmatrix} + \partial_y \begin{pmatrix} \rho v \\ \rho v^2 + P \\ \rho vw \\ \rho v(\rho e + P) \end{pmatrix} + \partial_z \begin{pmatrix} \rho w \\ \rho w^2 + P \\ \rho w(\rho e + P) \end{pmatrix} = 0,$$

$$e = e_{\text{therm}} + (u^2 + v^2 + w^2)/2 : \text{total specific energy}$$

$$\partial_t \mathbf{U} + \partial_x \mathbf{F} + \partial_y \mathbf{G} + \partial_z \mathbf{H} = 0 \quad \mathbf{F}, \mathbf{G}, \mathbf{H}: \text{fluxes along } x, y, z$$

Dimensional splitting:

$$\partial_t \mathbf{U} + \partial_x \mathbf{F} = 0,$$

$$\partial_t \mathbf{U} + \partial_y \mathbf{G} = 0,$$

$$\partial_t \mathbf{U} + \partial_z \mathbf{H} = 0.$$

- Differentiation in one dimension each
- Flux updates made sequentially

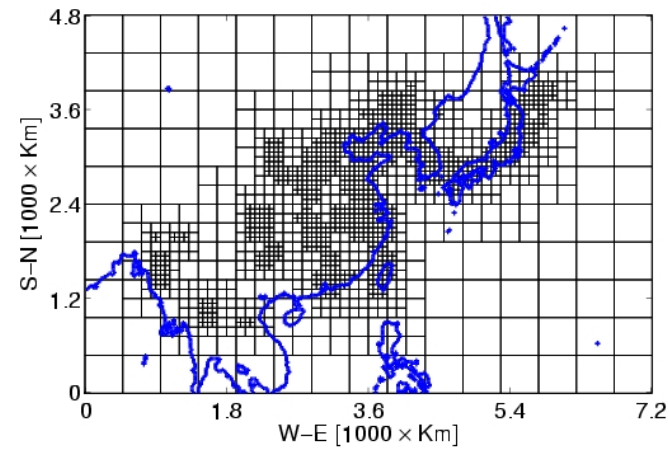
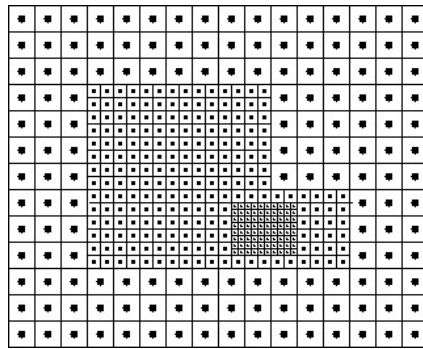
Unsplit scheme: flux updates applied simultaneously

For the 2D Cartesian case:

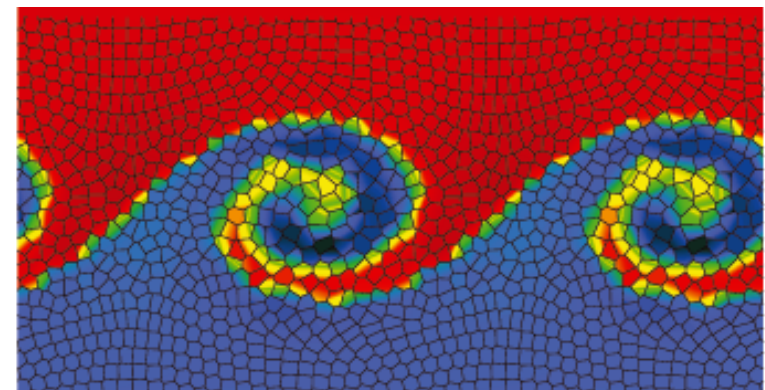
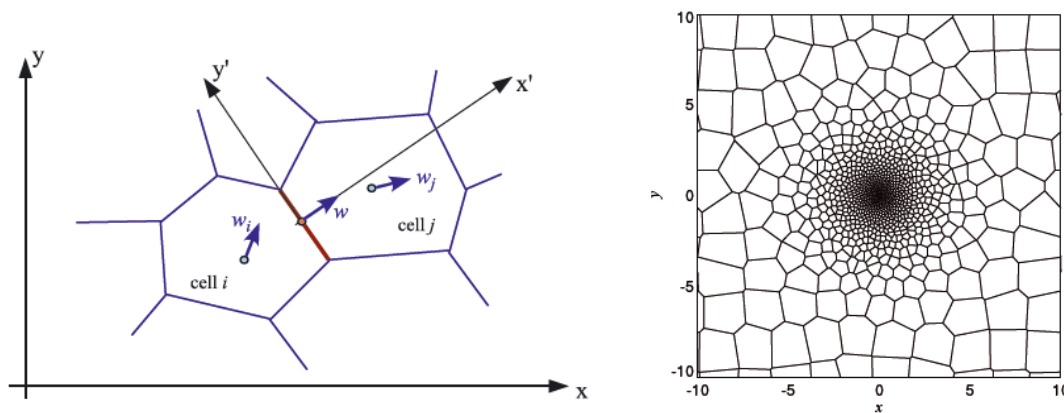
$$U_{i,j}^{n+1} = U_{i,j}^n + \frac{\Delta t}{\Delta x} \left(\mathbf{F}_{i-\frac{1}{2},j} - \mathbf{F}_{i+\frac{1}{2},j} \right) + \frac{\Delta t}{\Delta y} \left(\mathbf{G}_{i,j-\frac{1}{2}} - \mathbf{G}_{i,j+\frac{1}{2}} \right)$$

Different Eulerian codes

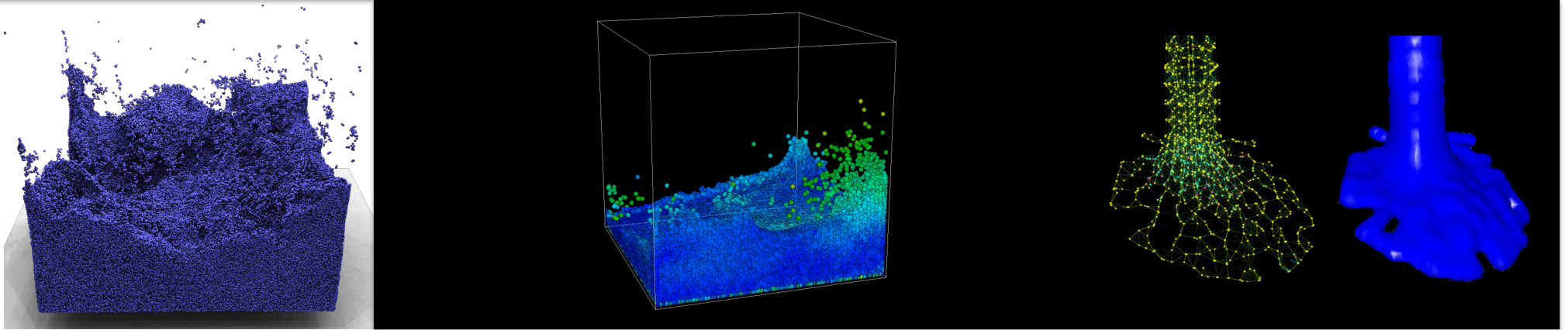
- Uniform grid: fixed resolution.
- AMR, Adaptive Mesh Refinement: hierarchy of nested grids to increase resolution where needed



- Moving mesh (e.g., AREPO)



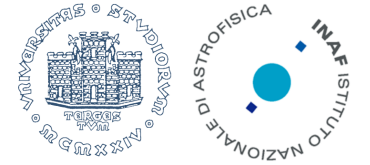
- ...meshless (e.g. GSPH).



Basic principles:

- Fluid sampled with points (*particles*)
- Hydrodynamic quantities are carried by each particle, but their values are *smoothed* over a given number of neighbouring particles
- Particles move under the Euler equations making use of the smoothed quantities
- After each *time-step*, quantities are re-evaluated

Smoothing kernel & interpolating function



→ Interpolating function: $\tilde{f}_h(\vec{r}) = \int f(\vec{r}') W(\vec{r} - \vec{r}', h) d^3r'$

$W(r)$: interpolating kernel

h : *smoothing length*

→ Properties of the kernel:

$$\lim_{h \rightarrow 0} \tilde{f}_h(\vec{r}) = f(\vec{r}) \quad \text{and} \quad \int W(\vec{r} - \vec{r}', h) d^3r' = 1$$

To recover the original function in the limit of small h

→ Discretization:

$$\tilde{f}_h(\vec{r}) = \int \frac{f(\vec{r}')}{\rho(\vec{r}')} W(\vec{r} - \vec{r}', h) \rho(\vec{r}') d^3r' \quad \rightarrow \quad f(\vec{r}) = \sum_b \frac{m_b}{\rho_b} f_b W(\vec{r} - \vec{r}_b, h)$$

$$f(\vec{r}) = \rho(\vec{r}) \quad \rightarrow \quad \rho(\vec{r}) = \sum_b m_b W(\vec{r} - \vec{r}_b, h)$$

Kernel function: additional properties

- Radial kernel for conservation of angular momentum

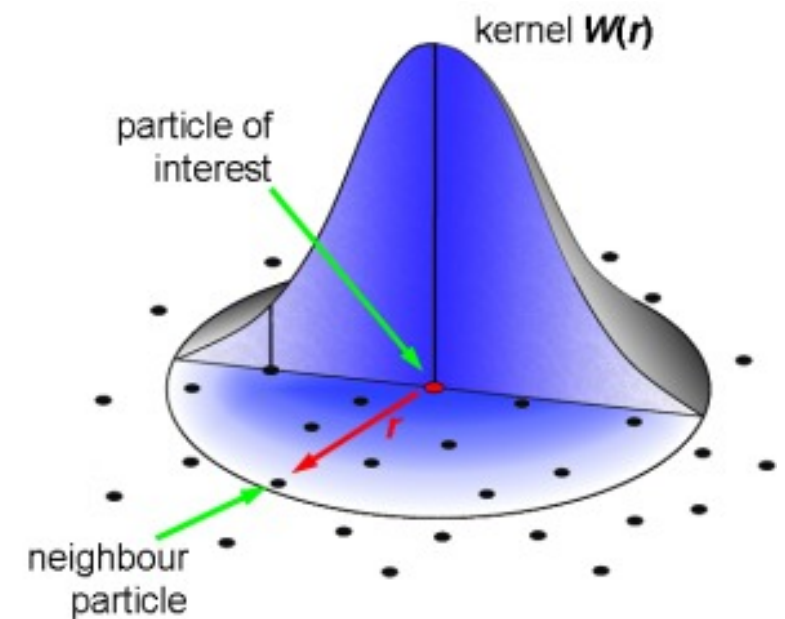
$$W(\vec{r} - \vec{r}', h) = W(|\vec{r} - \vec{r}'|, h)$$

- Compact support to avoid n^2 interactions per particle

→ Widely used **cubic spline kernel**:

$$W(q) = \frac{1}{\pi h^3} \begin{cases} 1 - \frac{3}{2}q^2 + \frac{3}{4}q^3 & \text{for } 0 \leq q \leq 1 \\ \frac{1}{4}(2 - q)^3 & \text{for } 1 < q \leq 2 \\ 0 & \text{for } q > 2 \end{cases} \quad q = |\vec{r} - \vec{r}'|/h$$

→ Gaussian kernel: useful for analytic computations but no compact support



→ Differentiate the discretized equation: $\nabla f(\vec{r}) = \sum_b \frac{m_b}{\rho_b} f_b \nabla W(\vec{r} - \vec{r}_b, h)$
 It doesn't vanish for $f(r) = \cos t$

→ To enforce it: $\frac{\partial A}{\partial x} = \frac{1}{\Phi} \left(\frac{\partial(\Phi A)}{\partial x} - A \frac{\partial \Phi}{\partial x} \right)$

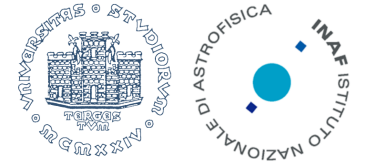
→ In SPH this is: $\left(\frac{\partial A}{\partial x} \right)_a = \frac{1}{\Phi_a} \sum_b m_b \frac{\Phi_b}{\rho_b} (A_b - A_a) \frac{\partial W_{ab}}{\partial x_a}$
 $W_{ab} = W(\vec{r}_a - \vec{r}_b, h)$

$$\Phi = 1 \quad \frac{\partial A_a}{\partial x_a} = \sum_b \frac{m_b}{\rho_b} (A_b - A_a) \frac{\partial W_{ab}}{\partial x_a} \quad \Phi = \rho \quad \frac{\partial A_a}{\partial x_a} = \frac{1}{\rho_a} \sum_b m_b (A_b - A_a) \frac{\partial W_{ab}}{\partial x_a}$$

→ The continuity equation becomes:

$$\frac{d\rho}{dt} = -\rho \nabla \cdot \vec{v}. \quad \frac{d\rho_a}{dt} = \rho_a \sum_b \frac{m_b}{\rho_b} \mathbf{v}_{ab} \cdot \nabla_a W_{ab} \quad \mathbf{V}_{ab} = \mathbf{V}_a - \mathbf{V}_b$$

Euler equation in SPH



$$\frac{d\vec{v}}{dt} = -\frac{\nabla P}{\rho}$$

→ Brute force differentiation of pressure: $\frac{d\vec{v}_a}{dt} = -\frac{1}{\rho_a} \sum_b \frac{m_b}{\rho_b} P_b \nabla_a W_{ab}$

$$\vec{F}_{ba} = \left(m_a \frac{d\vec{v}_a}{dt} \right)_b = -\frac{m_a m_b}{\rho_a \rho_b} P_b \nabla_a W_{ab}$$

If $P_a \neq P_b \Rightarrow \vec{F}_{ba} \neq -\vec{F}_{ab}$

$$\vec{F}_{ab} = \left(m_b \frac{d\vec{v}_b}{dt} \right)_a = -\frac{m_b m_a}{\rho_b \rho_a} P_a \nabla_b W_{ba} = \frac{m_a m_b}{\rho_a \rho_b} P_a \nabla_a W_{ab}$$

→ Momentum not conserved

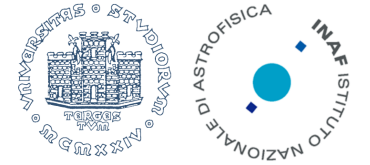
→ Use instead: $\nabla \left(\frac{P}{\rho} \right) = \frac{\nabla P}{\rho} - P \frac{\nabla \rho}{\rho^2}$

$$\begin{aligned} \frac{d\vec{v}_a}{dt} &= -\frac{P_a}{\rho_a^2} \sum_b m_b \nabla_a W_{ab} - \sum_b \frac{m_b P_b}{\rho_b \rho_b} \nabla_a W_{ab} \\ &= -\sum_b m_b \left(\frac{P_a}{\rho_a^2} + \frac{P_b}{\rho_b^2} \right) \nabla_a W_{ab}. \end{aligned}$$

→ Pressure part manifestly symmetric

→ Momentum now conserved

Energy equation in SPH



$$\frac{du}{dt} = \frac{P}{\rho^2} \frac{d\rho}{dt} = -\frac{P}{\rho} \nabla \cdot \vec{v}.$$

$$\frac{du_a}{dt} = \frac{P_a}{\rho_a^2} \frac{d\rho_a}{dt} = \frac{P_a}{\rho_a^2} \frac{d}{dt} \left(\sum_b m_b W_{ab} \right) = \frac{P_a}{\rho_a^2} \sum_b m_b \vec{v}_{ab} \cdot \nabla_a W_{ab}$$

Based on using:

$$\frac{dW_{ab}}{dt} = \frac{\partial W_{ab}}{\partial r_{ab}} \frac{dr_{ab}}{dt} = \frac{\partial W_{ab}}{\partial r_{ab}} \frac{(\vec{r}_a - \vec{r}_b) \cdot (\vec{v}_a - \vec{v}_b)}{r_{ab}} = \frac{\partial W_{ab}}{\partial r_{ab}} \hat{e}_{ab} \cdot \vec{v}_{ab} = \vec{v}_{ab} \cdot \nabla_a W_{ab}.$$

Equation of state: $P_a = (\gamma - 1) \rho_a u_a$

...these make a full set of SPH equations!

→ Entropy-conserving formulation:

$$P = A(s)\rho^\gamma, \quad s: \text{specific entropy of the fluid element}$$
$$A(s): \text{entropic function}$$

In the absence of any cooling or viscosity terms:

$$\frac{dA(s)}{dt} = 0 \quad \rightarrow \quad \text{Entropy conservation enforced at the particle level, then internal energy computed from}$$

$$u = \frac{A(s)}{\gamma - 1} \rho^{\gamma-1}$$

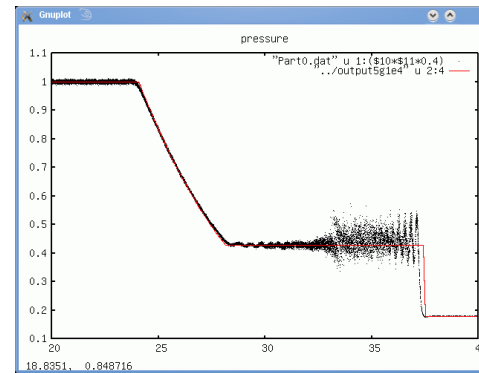
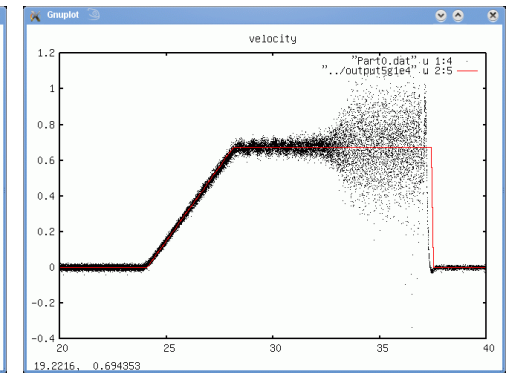
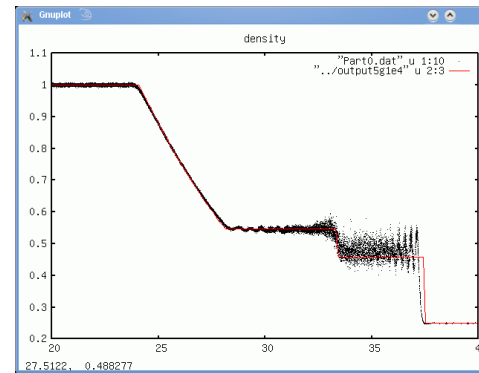
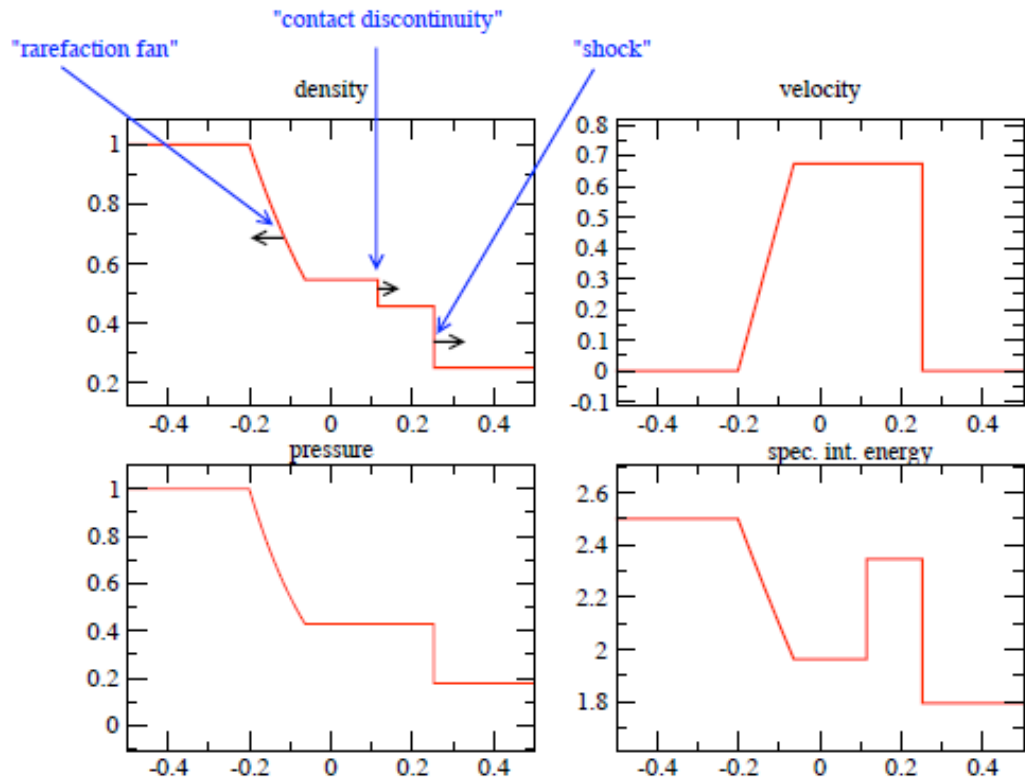
→ Adaptive softening: $\rho_i h_i^3 = \text{const}$: enforce constant mass within the kernel

$$\frac{d\mathbf{v}_i}{dt} = - \sum_{j=1}^N m_j \left[f_i \frac{P_i}{\rho_i^2} \nabla_i W_{ij}(h_i) + f_j \frac{P_j}{\rho_j^2} \nabla_i W_{ij}(h_j) \right] \quad f_i = \left[1 + \frac{h_i}{3\rho_i} \frac{\partial \rho_i}{\partial h_i} \right]^{-1}$$

$$\frac{du_i}{dt} = f_i \frac{P_i}{\rho_i^2} \sum_j m_j (\mathbf{v}_i - \mathbf{v}_j) \cdot \nabla W_{ij}(h_i)$$

→ To account for local softening

Sode shock tube: SPH solution



- Velocity noise in the pre-shock region
- Lack of diffusion of momentum
- Need to convert mechanical energy into thermal energy

Artificial viscosity



→ Add an “artificial” viscous contribution to pressure in the Euler eq.:

$$q_{\text{visc}} = -c_1 \rho c_s l (\nabla \cdot \vec{v}) + c_2 \rho l^2 (\nabla \cdot \vec{v})^2$$

Bulk viscosity

Von Neumann-Richtmyer viscosity

$l (\nabla \cdot \vec{v}) \sim$ velocity jump between two fluid elements; c_s : adiabatic sound speed

→ SPH translation:
$$\left(\frac{P_a}{\rho_a^2} + \frac{P_b}{\rho_b^2} \right) \rightarrow \left(\frac{P_a}{\rho_a^2} + \frac{P_b}{\rho_b^2} + \Pi_{ab} \right)$$

$$\Pi_{ab} = \Pi_{ab,\text{bulk}} + \Pi_{ab,\text{NR}} = \begin{cases} \frac{-\alpha \bar{c}_{ab} \mu_{ab} + \beta \mu_{ab}^2}{\bar{\rho}_{ab}} & \text{for } \vec{r}_{ab} \cdot \vec{v}_{ab} < 0 \\ 0 & \text{otherwise} \end{cases} \quad \mu_{ab} = \frac{\bar{h}_{ab} \vec{r}_{ab} \cdot \vec{v}_{ab}}{r_{ab}^2 + \epsilon \bar{h}_{ab}^2}$$

$\alpha \approx 1$, $\beta \approx 2$ and $\epsilon \approx 0.01$ from numerical experiments

→ SPH equations with artificial viscosity:

$$\frac{d\vec{v}_a}{dt} = - \sum_b m_b \left(\frac{P_a}{\rho_a^2} + \frac{P_b}{\rho_b^2} + \Pi_{ab} \right) \nabla_a W_{ab}$$

$$\frac{du_a}{dt} = \frac{P_a}{\rho_a^2} \sum_b m_b \vec{v}_{ab} \cdot \nabla_a W_{ab} + \frac{1}{2} \sum_b m_b \Pi_{ab} \vec{v}_{ab} \cdot \nabla_a W_{ab}$$

Artificial viscosity

→ Spurious viscous force in the absence of shocks (e.g. in shear flows)

$$\mu_{ab} = \frac{\bar{h}_{ab} \vec{r}_{ab} \cdot \vec{v}_{ab}}{r_{ab}^2 + \epsilon \bar{h}_{ab}^2}$$

“Balsara switch”:

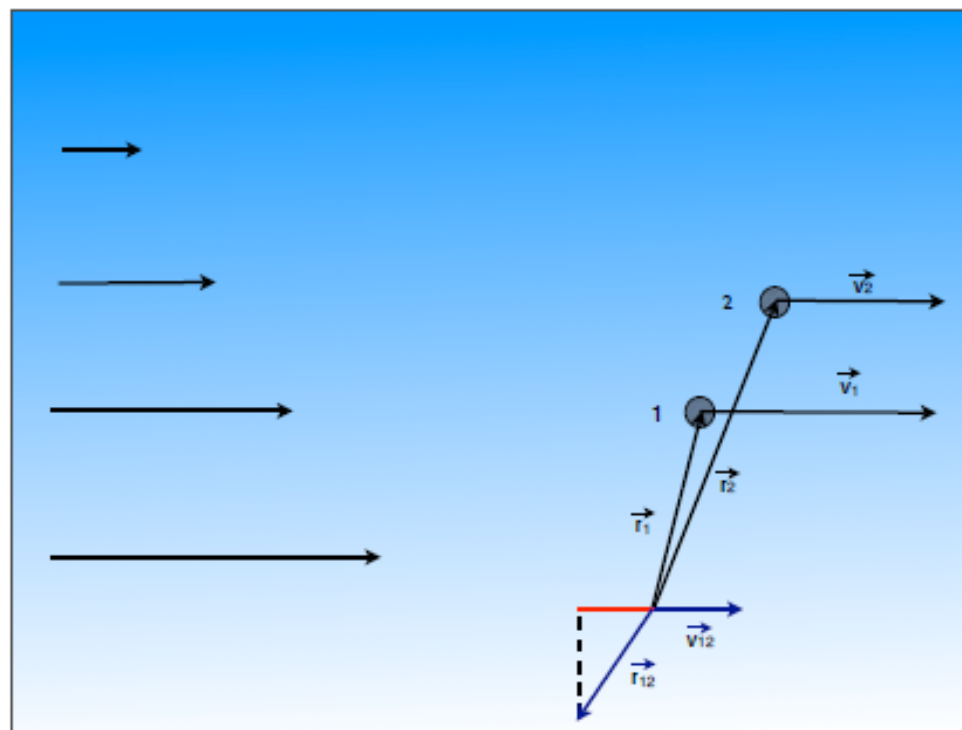
$$f_a = \frac{|\langle \nabla \cdot \vec{v} \rangle_a|}{|\langle \nabla \cdot \vec{v} \rangle_a| + |\langle \nabla \times \vec{v} \rangle_a| + 0.0001 c_{s,a} / h_a}$$

$$\Pi'_{ab} = \Pi_{ab} \bar{f}_{ab}$$

$$\bar{f}_{ab} = (f_a + f_b) / 2$$

=0 in shear flows

=0 in purely compressional flows



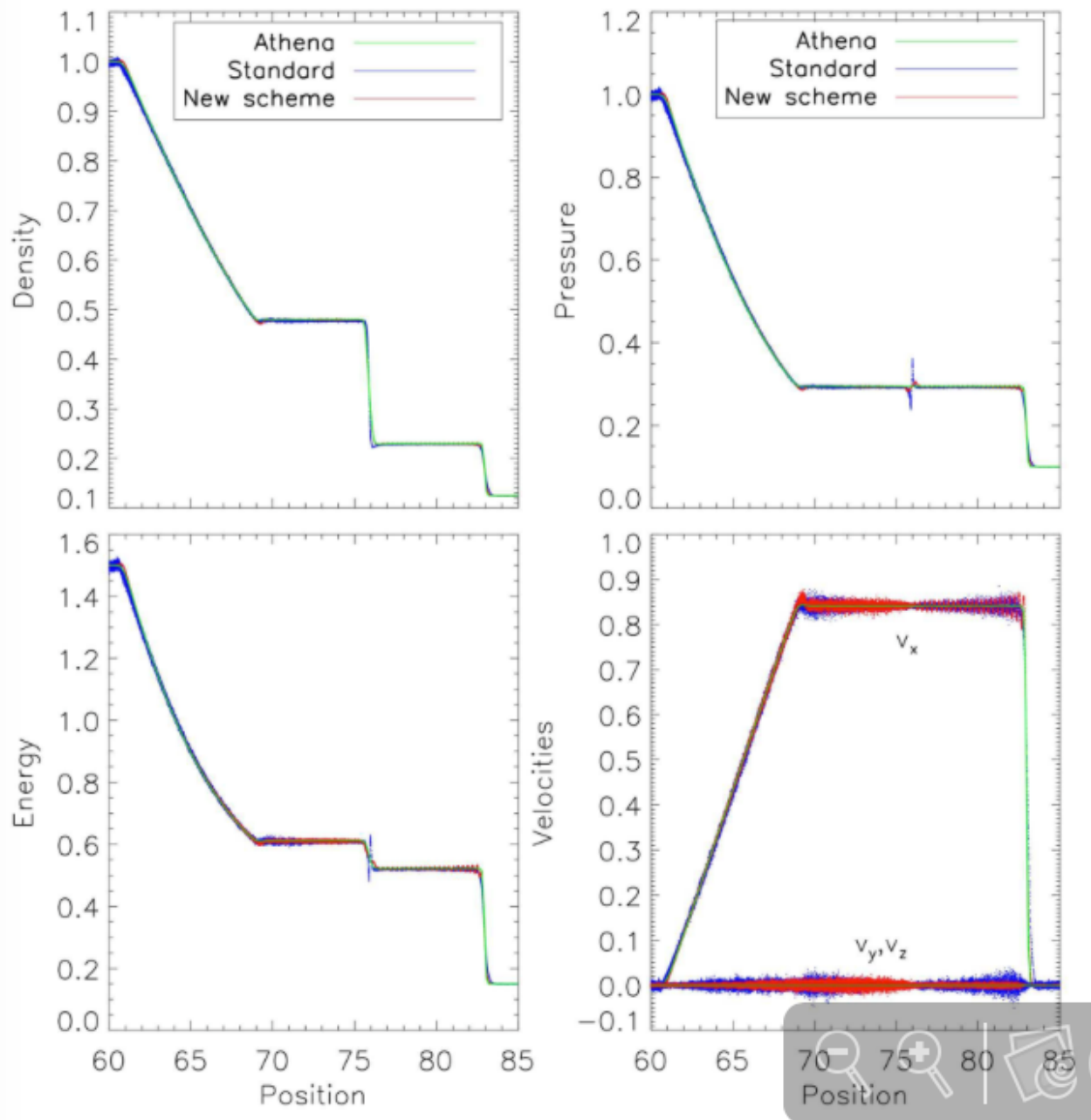
→ Time-dependent viscosity: to make viscosity decay away from shocks

$$\frac{d\alpha_a}{dt} = -\frac{\alpha_a - \alpha_{\min}}{\tau_a} + S_a$$

$$\tau_a = \frac{h_a}{\xi c_{s,a}} \rightarrow \text{Decay time-scale of viscosity}$$

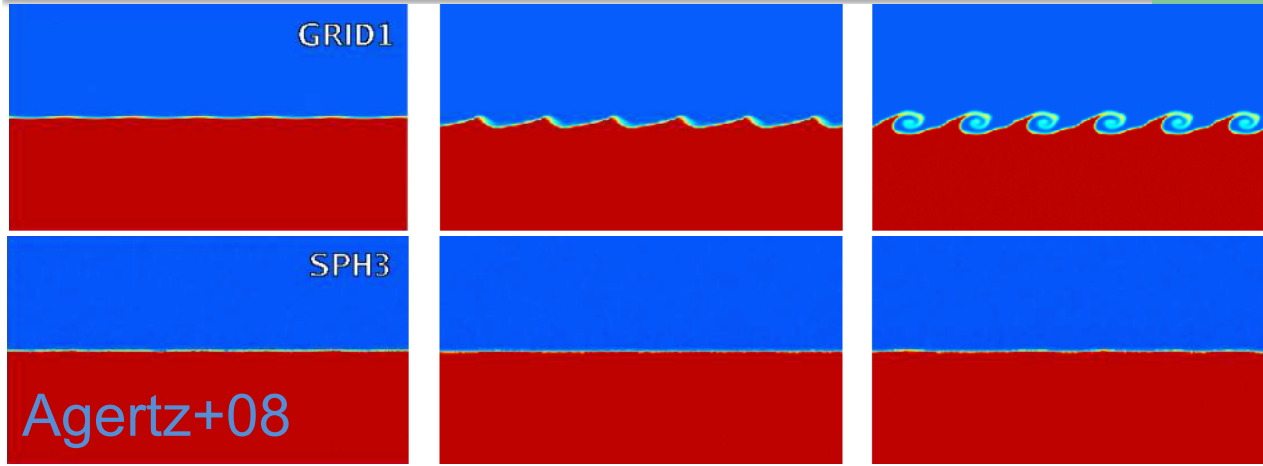
$$S_a = \max[-(\vec{\nabla} \cdot \vec{v})_a, 0] \rightarrow \text{Source term}$$

Artificial viscosity: shock tube test



- Analytic solution better recovered
- ➔ Pre-shock velocity noise much reduced
- Blip in pressure and energy at the contact discontinuity
- Spurious pressure force causing “surface tension”
- ➔ Entropy preserved at the particle level
- ➔ No diffusion of energy across the discontinuity

Kelvin-Helmholtz instability

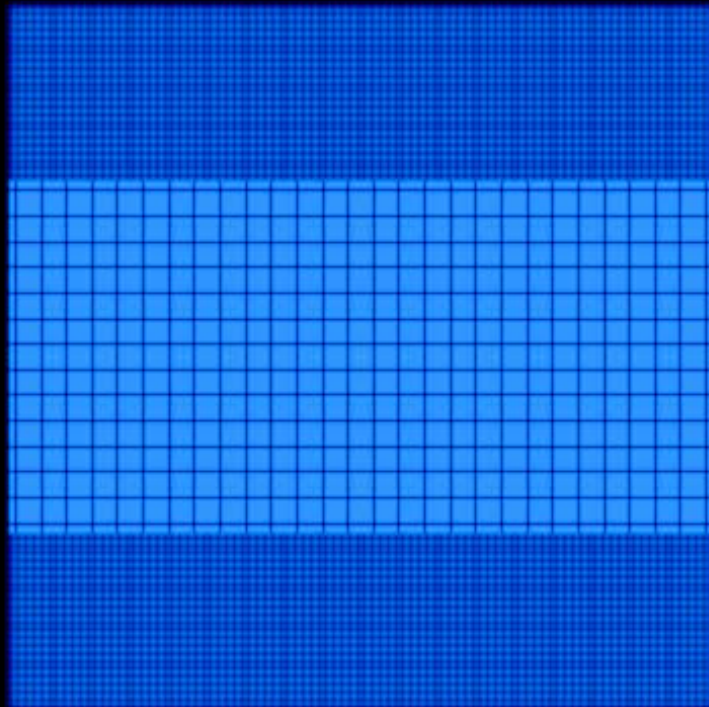


$$\chi = \rho_b / \rho_t = T_t / T_b = c_t^2 / c_b^2$$

$$v_y(x) = \delta v_y \sin(\lambda 2\pi x)$$

$$\tau_{KH} = \frac{\lambda(\rho_b + \rho_t)}{(v_b + v_t)(\rho_b \rho_t)^{1/2}}$$

Time: 0.000E+00



- SPH: surface tension prevents the development of instabilities
- KH instability followed by Eulerian schemes

They happen in real life!!



Artificial thermal energy diffusion



➔ Dissipation term for a conserved scalar quantity A :

$$\left(\frac{dA_a}{dt}\right)_{\text{diss}} = \sum_b m_b \frac{\alpha_{A,b} v_{\text{sig}}}{\bar{\rho}_{ab}} (A_a - A_b) \hat{e}_{ab} \cdot \nabla_a W_{ab}$$

$\alpha_{A,b}$: amount of dissipation
 v_{sig} : maximum signal velocity between a and b

$$\left(\frac{d\vec{v}_a}{dt}\right)_{\text{diss}} = \sum_b m_b \frac{\alpha v_{\text{sig}} (\vec{v}_a - \vec{v}_b) \cdot \hat{e}_{ab}}{\bar{\rho}_{ab}} \nabla_a W_{ab} \quad \text{in the momentum equation}$$

$$\left(\frac{du_a}{dt}\right)_{\text{diss}} = - \sum_b \frac{m_b}{\bar{\rho}_{ab}} \left[\alpha v_{\text{sig}} \frac{1}{2} (\vec{v}_{ab} \cdot \hat{e}_{ab})^2 + \alpha_u v_{\text{sig}}^u (u_a - u_b) \right] \hat{e}_{ab} \cdot \nabla_a W_{ab} \quad \text{in the energy equation}$$

Artificial viscosity

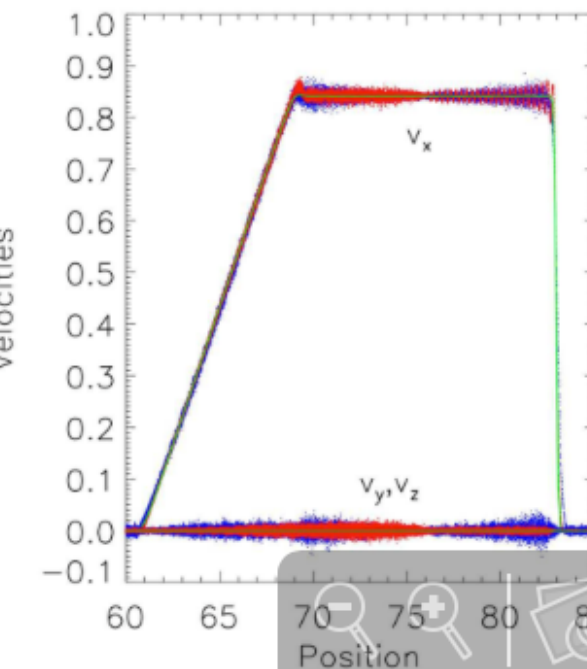
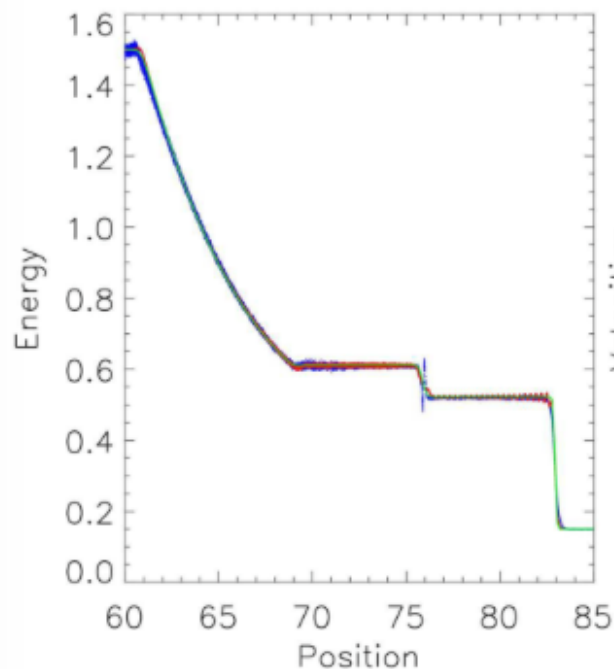
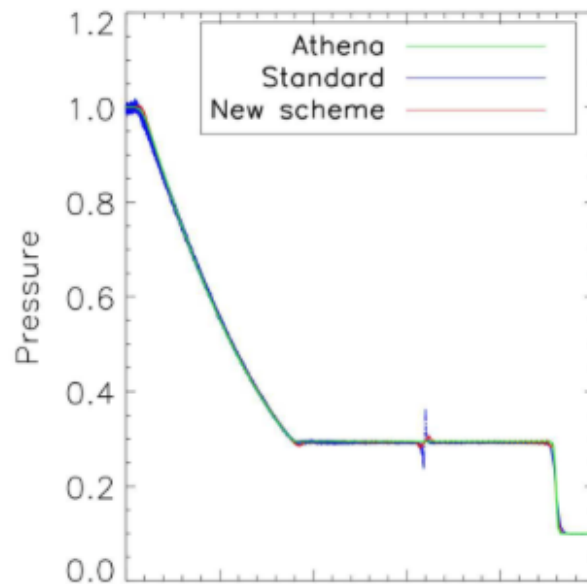
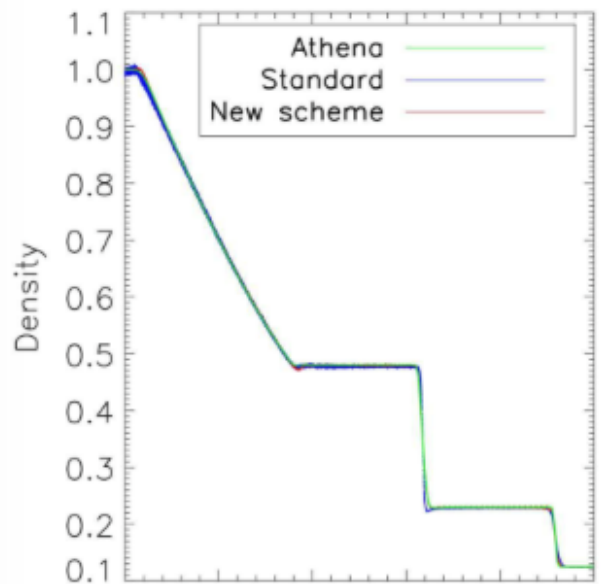
Thermal energy diffusion

$$v_{\text{sig}} = c_{s,a} + c_{s,b} - \vec{v}_{ab} \cdot \hat{e}_{ab} \quad : \text{signal velocity for momentum diffusion (Monaghan 97)}$$

$$v_{\text{sig}}^u = \sqrt{\frac{|P_a - P_b|}{\bar{\rho}_{ab}}} \quad : \text{signal velocity for thermal energy diffusion (Price 08)}$$

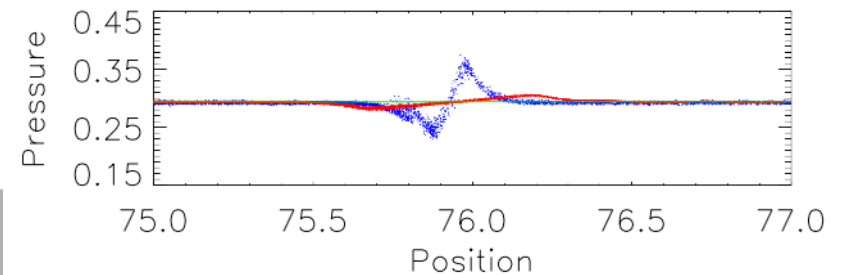
Need to be corrected in the presence of an external (gravitational) potential

Shock tube test – Thermal diffusion in SPH

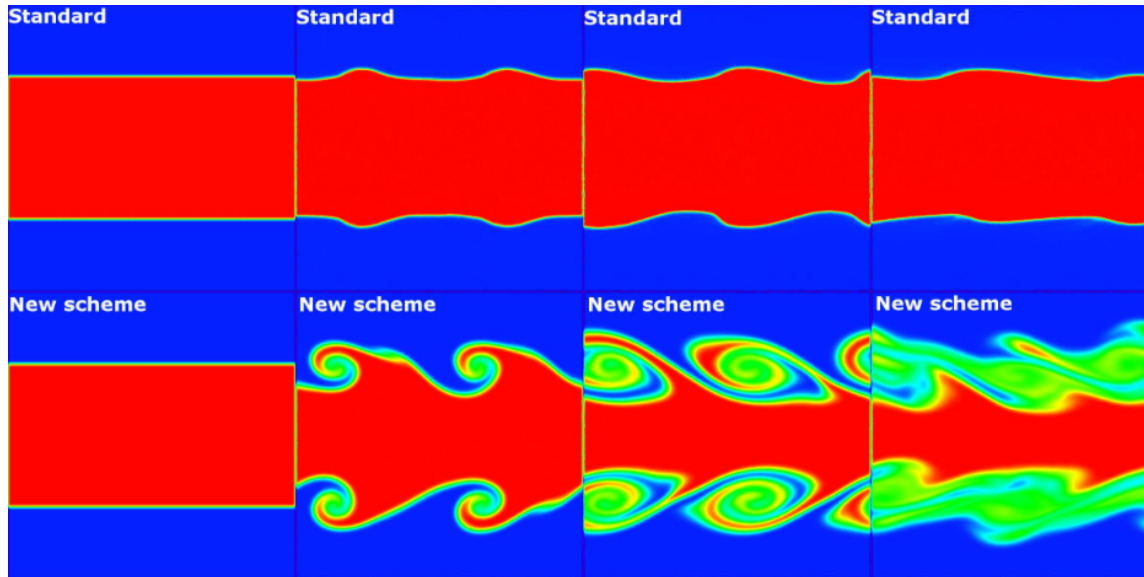


Beck+15

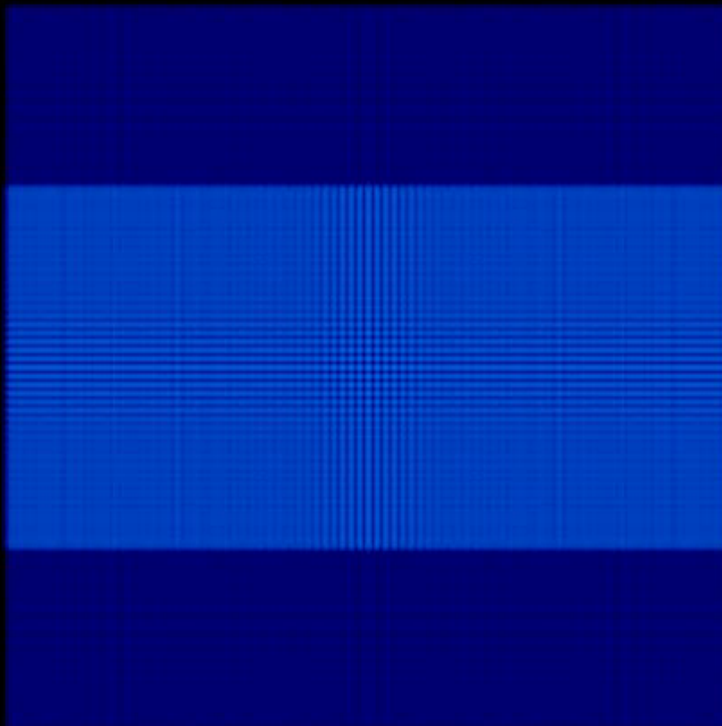
- Blip in pressure and energy much reduced by diffusion
- “Surface tension” reduced
- Particle noise also reduced



KH test with thermal diffusion



Time: 0.000E+00



Beck+15

- Removal of surface tension allows development of instabilities
- Instabilities followed for several characteristic time-scales
- SPH and Eulerian results virtually indistinguishable

SPH pros

- Increases resolution where needed
- Easily coupled to N-Body codes
- Intrinsically Galilean-invariant

SPH cons

- Low-order accuracy for treatment of contact discontinuities
- Sub-sonic velocity noise
- Poor shock resolution
- Difficulty in following hydro instabilities

Eulerian pros

- Sharp discontinuities and shocks accurately captured
- Hydrodynamical instabilities followed for several characteristic times

Eulerian cons

- Not manifestly Galilean invariant
- Preference of spatial directions
- Adaptive resolution not trivial
- Degree of diffusivity not easily controlled

➔ Need “ad-hoc” switches

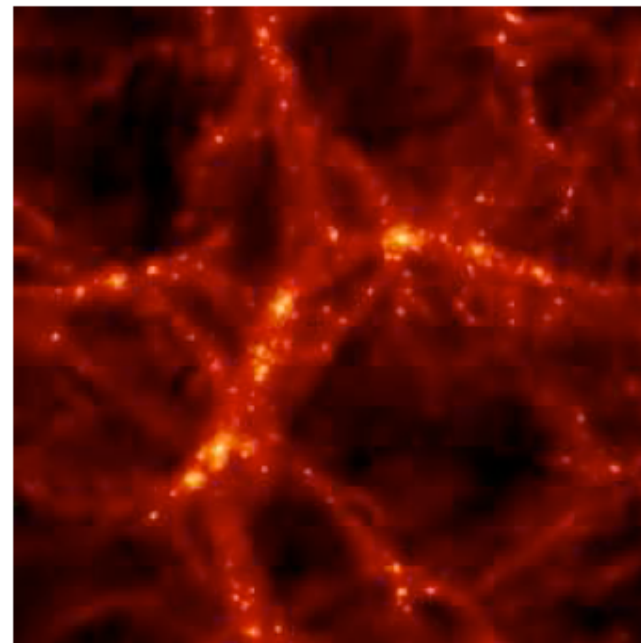
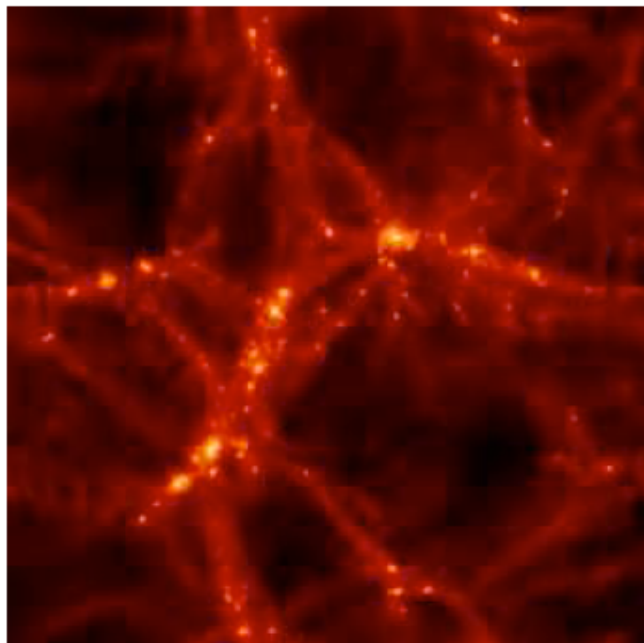
➔ Need control of diffusivity

O'Shea+05

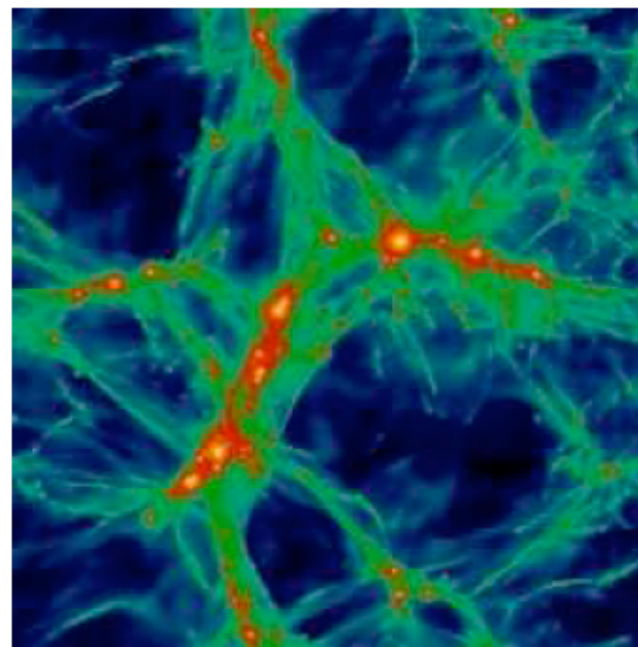
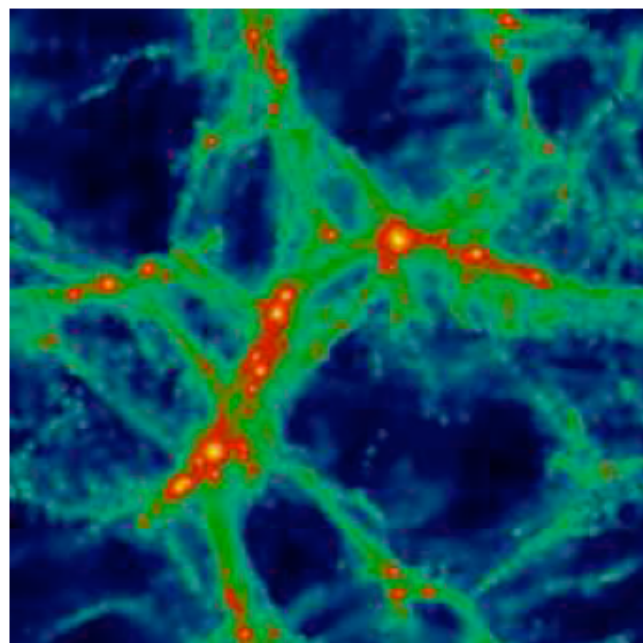
GADGET

ENZO

DM

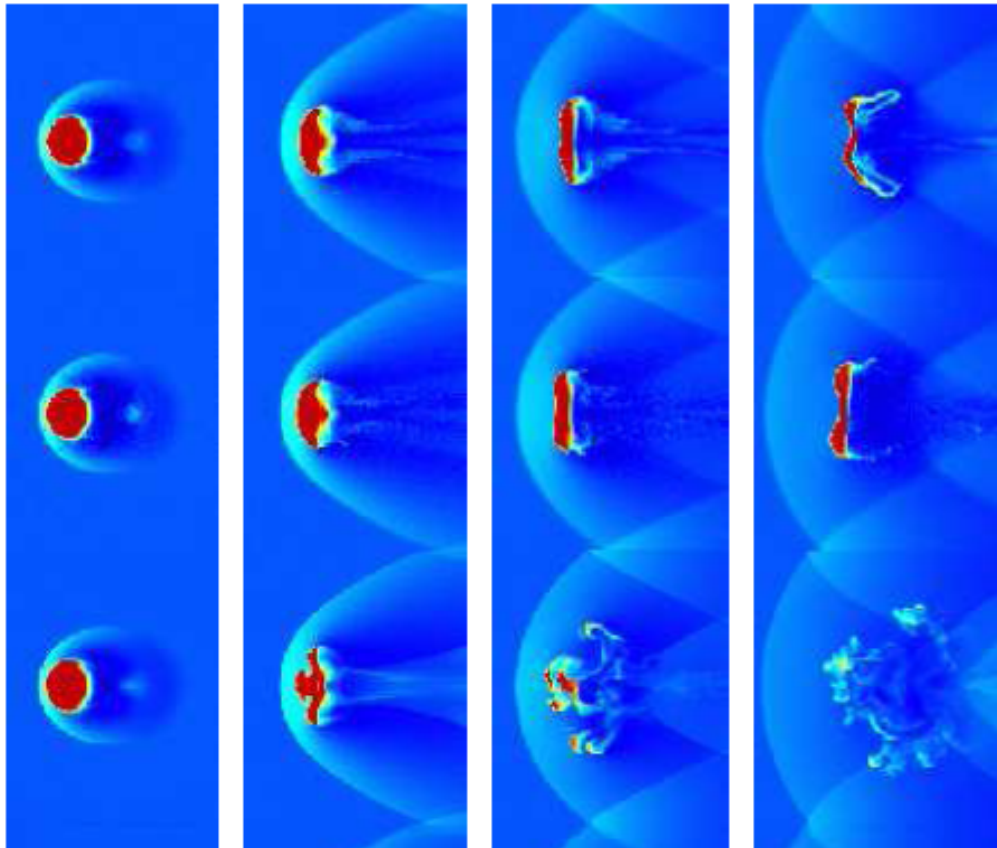


GAS



The test of the “cold blob”

Agertz+08



Gasoline
SPH

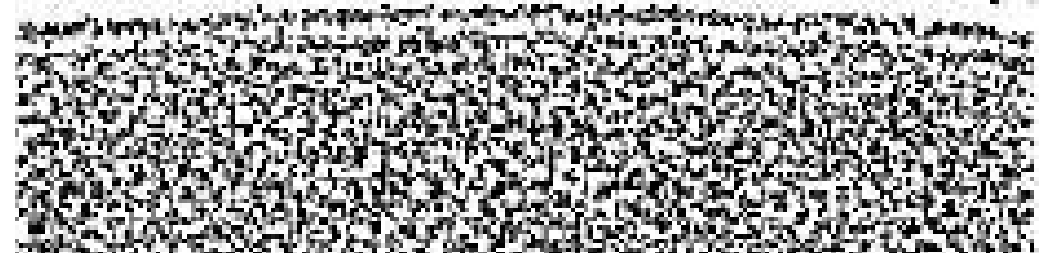
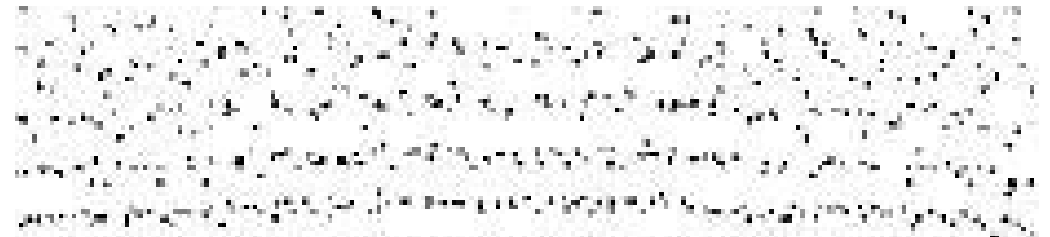
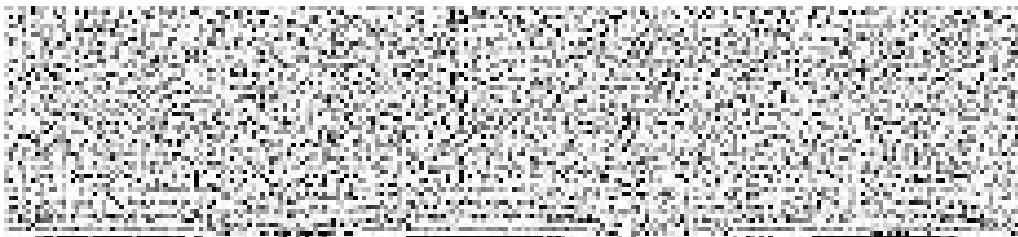
Cold dense cloud moving in a low-density hot medium in pressure equilibrium

Gadget-2
SPH

Spurious pressure forces in SPH at density discontinuities;

ENZO
Grid

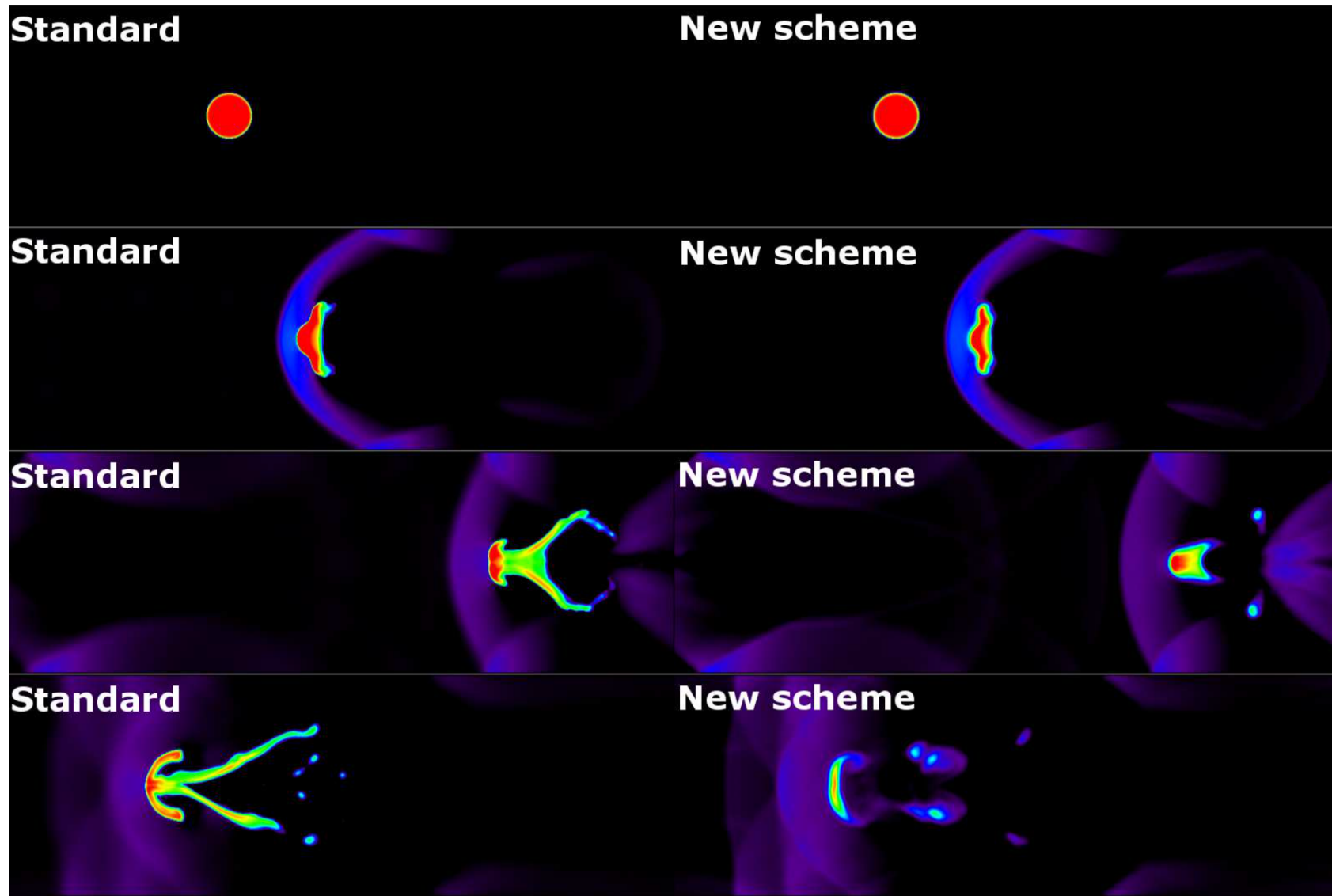
→ Suppression of KH and RT instabilities.



Cold blob with “diffusive” SPH

Beck+15

→ Artificial thermal diffusion promotes mixing, breaks the tension force and allows dissociation of the cloud



Idealised merger between two clusters



From Mitchell+09

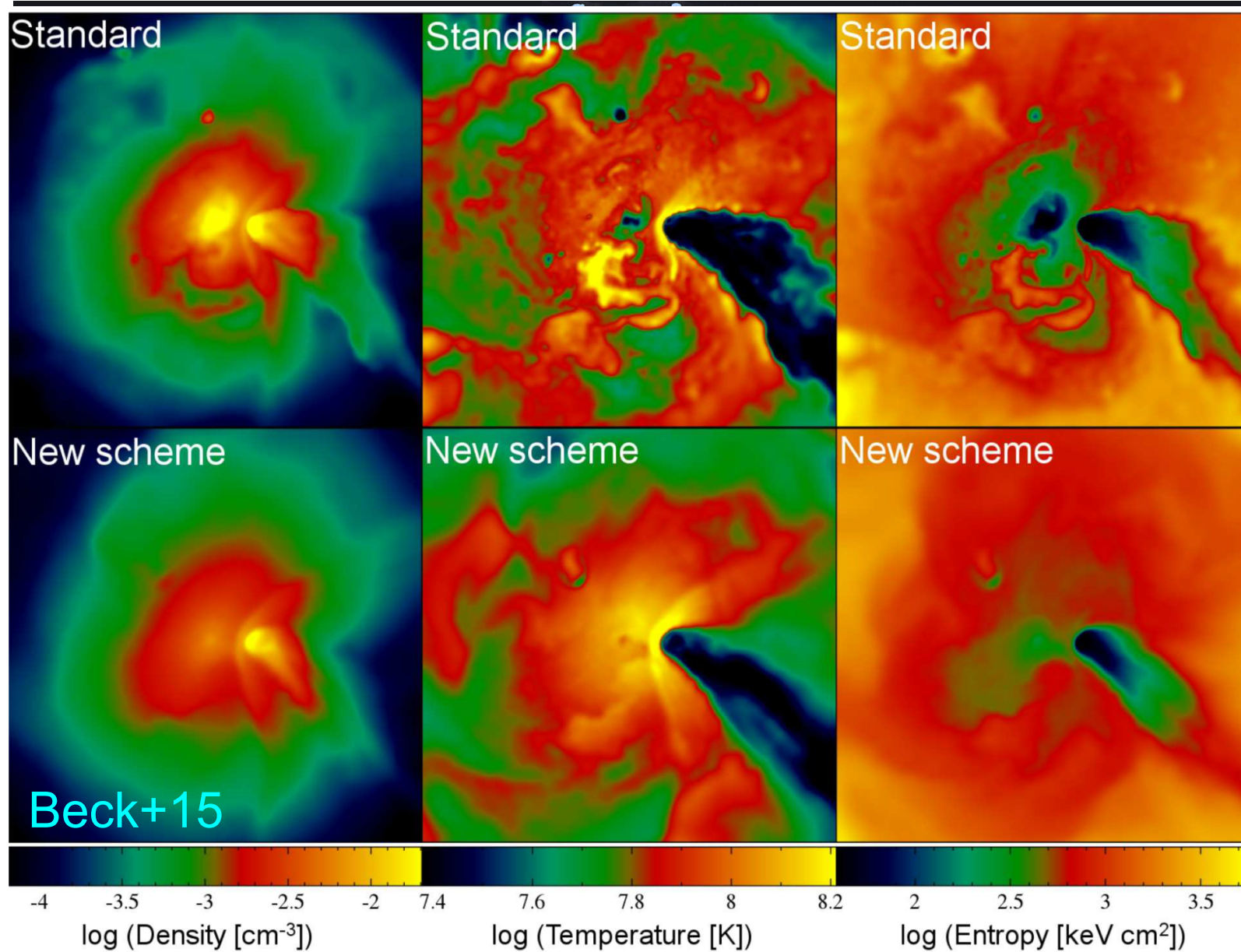
GADGET-2

FLASH

$t = 0.0 \text{ Gyr}$

Santa Barbara cluster

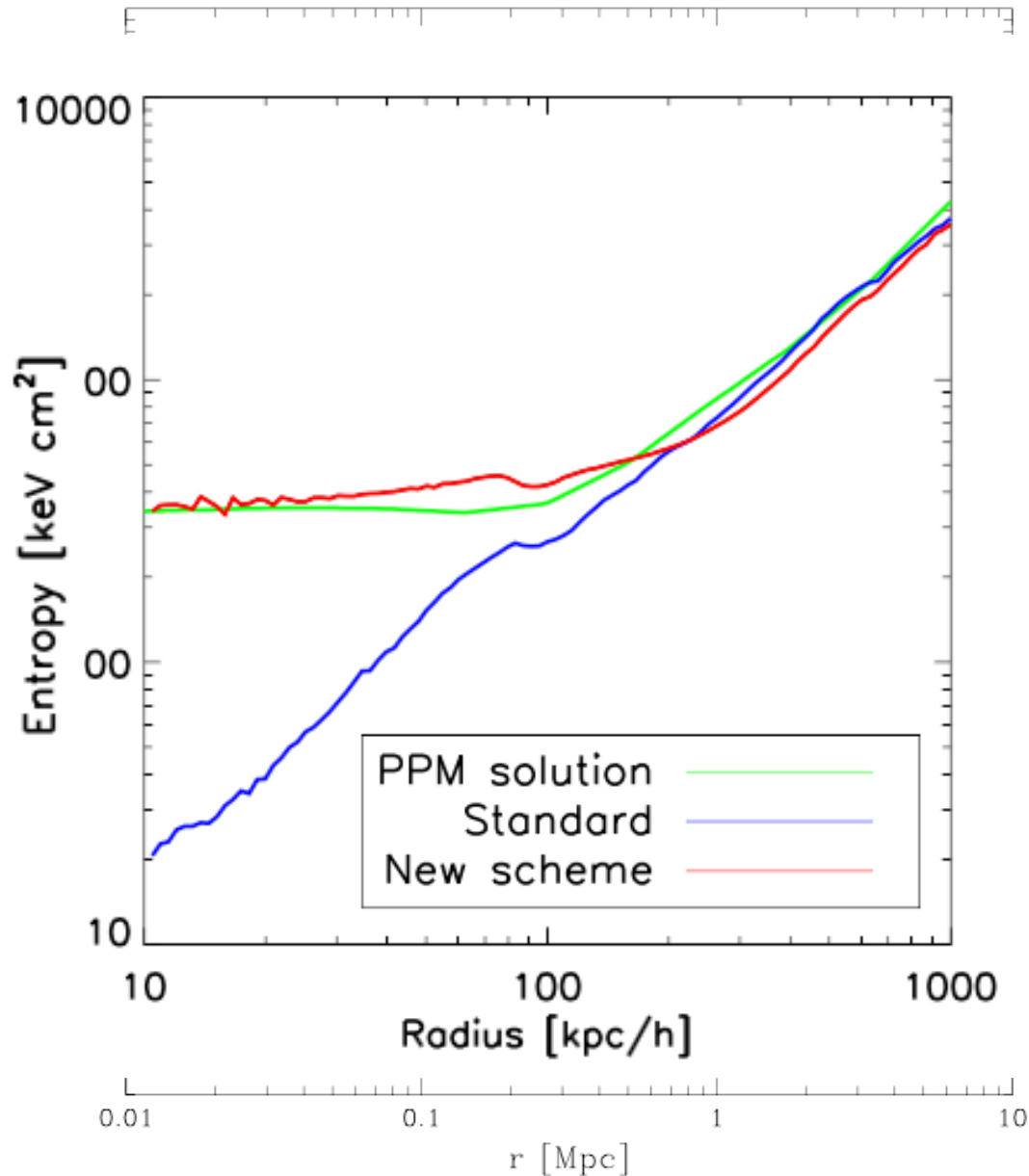
- Cosmological build-up of a massive cluster in an EdS CDM Universe (Frenk+99)



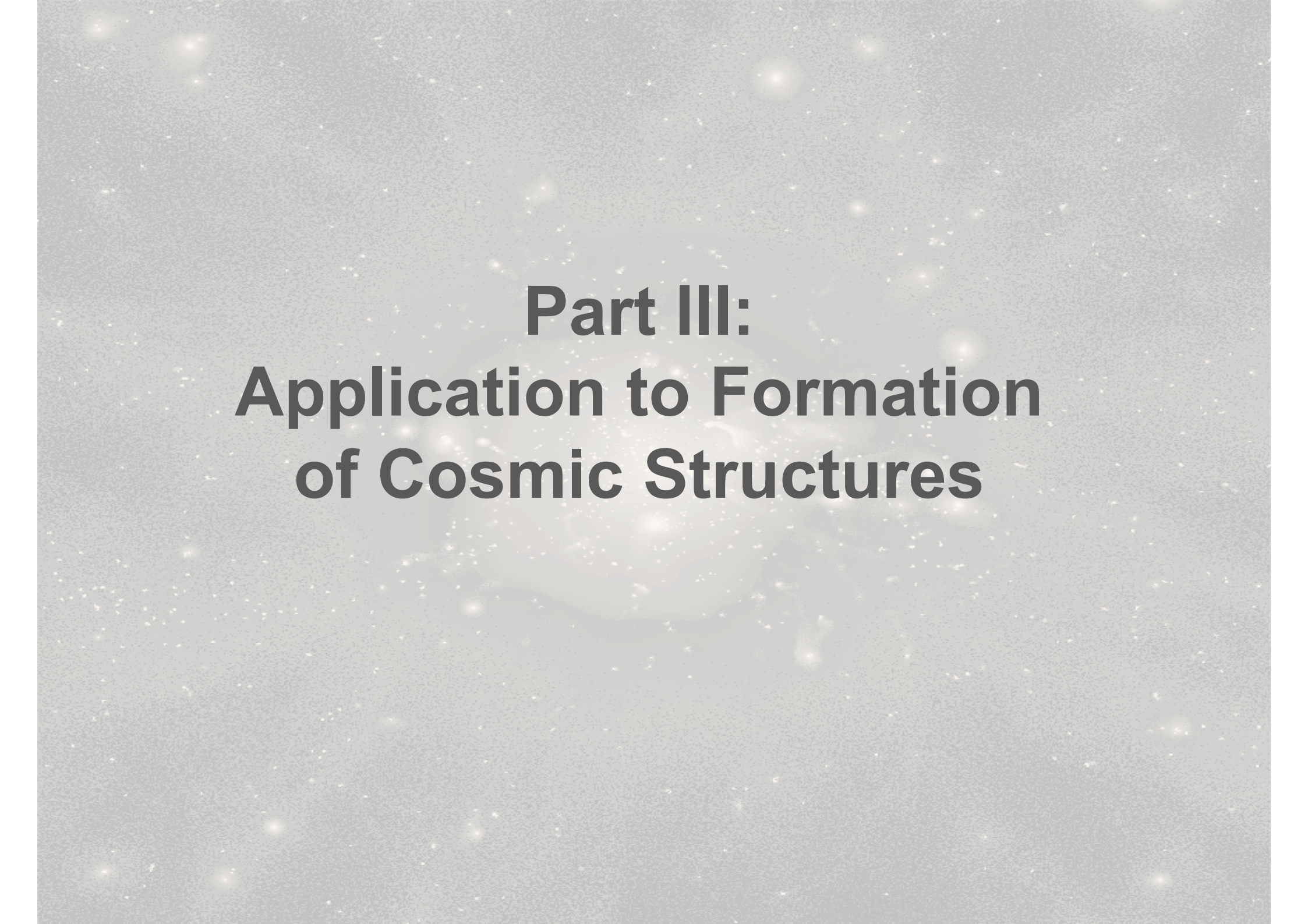
Entropy profiles



$$K(r) = \frac{T(r)}{[\rho_{gas}(r)]^{2/3}}$$

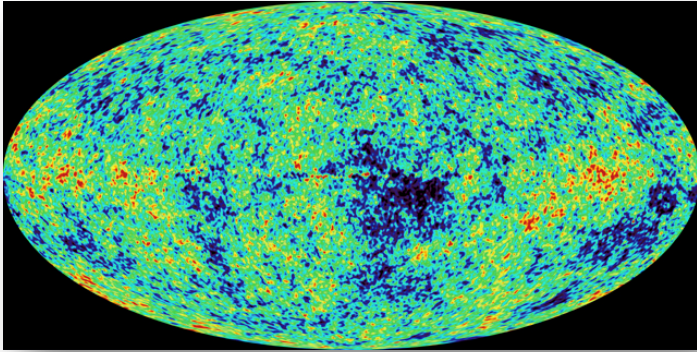


- Frenk+99: SB cluster comparison
→ 1st evidence for AMR to produce entropy cores wrt SPH
- Beck+15: effect of thermal diffusion in SPH
→ TD to promote mixing and creation of entropy cores
→ Now SPH and Eulerian quite close
- Sembolini+15: comparison of a variety of SPH and Eulerian codes

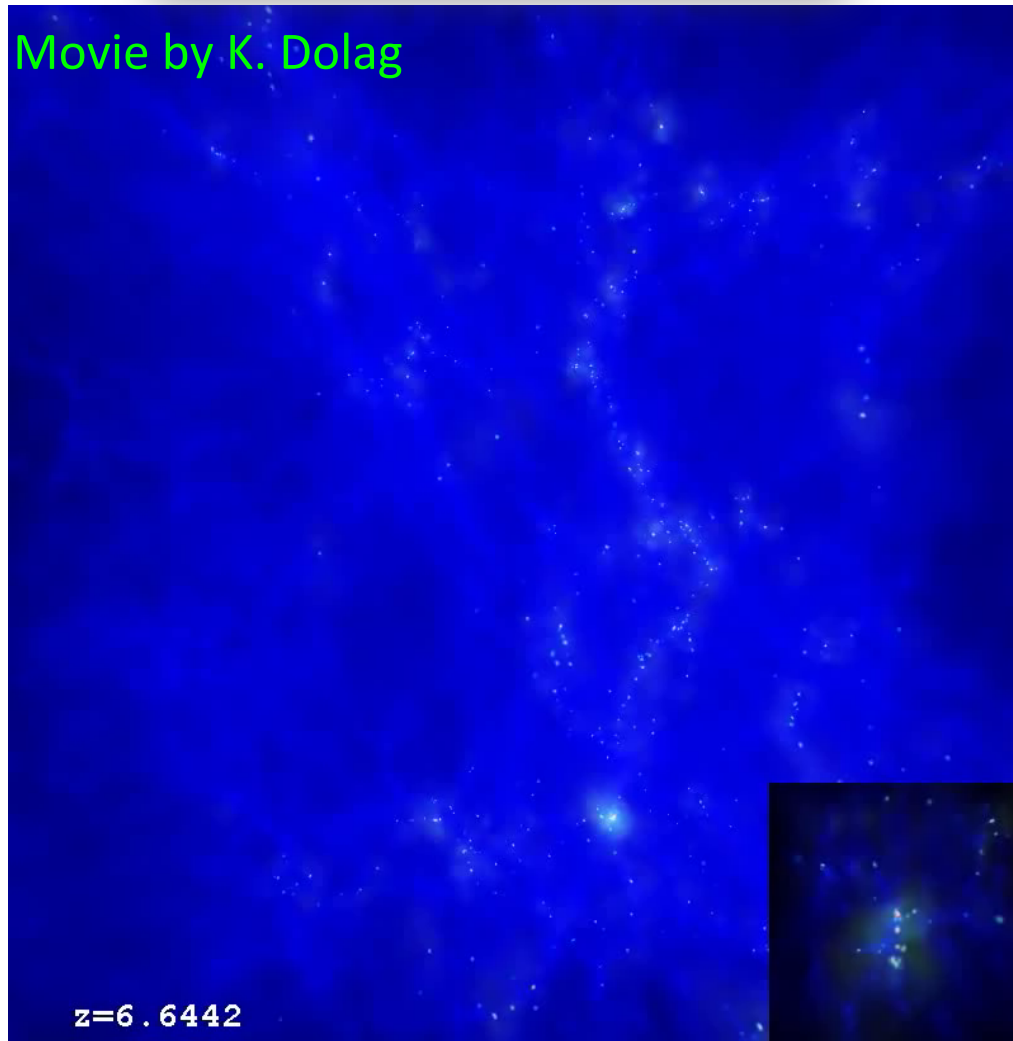


**Part III:
Application to Formation
of Cosmic Structures**

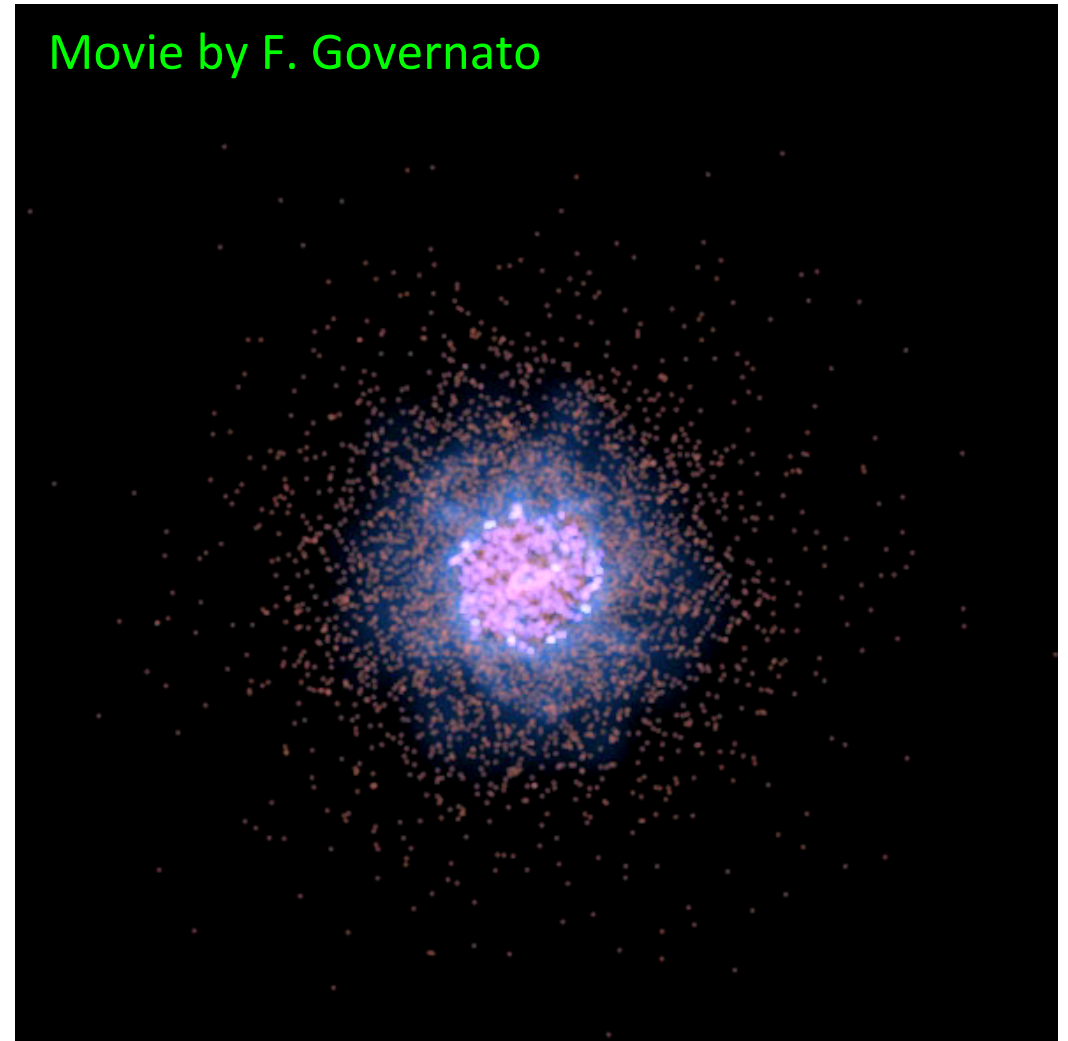
What's a cosmological simulation?



Movie by K. Dolag



Movie by F. Governato



Problem: generate a distribution of particles whose positions and velocities are a realization of a **Gaussian** random field with a given **power spectrum**:

$$\hat{\delta}_{\mathbf{k}} = |\hat{\delta}_{\mathbf{k}}| e^{i\theta_{\mathbf{k}}} \quad P(|\hat{\delta}_{\mathbf{k}}|, \vartheta_{\mathbf{k}}) = \frac{|\hat{\delta}_{\mathbf{k}}|}{P(\mathbf{k})} \exp\left(-\frac{|\hat{\delta}_{\mathbf{k}}|^2}{P(\mathbf{k})}\right) d\hat{\delta}_{\mathbf{k}} d\vartheta_{\mathbf{k}}$$

→ Rayleigh distribution for $|\delta_{\mathbf{k}}|$ and uniform distribution for $\theta_{\mathbf{k}}$

Step 1: generate a Gaussian $\delta_{\mathbf{k}}$ on a grid in Fourier space:

$$\hat{\delta}_{\mathbf{k}} = \sqrt{-2P(\mathbf{k}) \ln r_1} e^{i2\pi r_2} \quad ; \quad r_1, r_2 : \text{random in } [0, 2\pi]$$

Step 2: FT to generate the potential on a grid in configuration space:

$$\Phi(\vec{q}) = \sum_{\vec{k}} \frac{\hat{\delta}_{\mathbf{k}}}{k^2} e^{i\vec{k} \cdot \vec{q}}$$

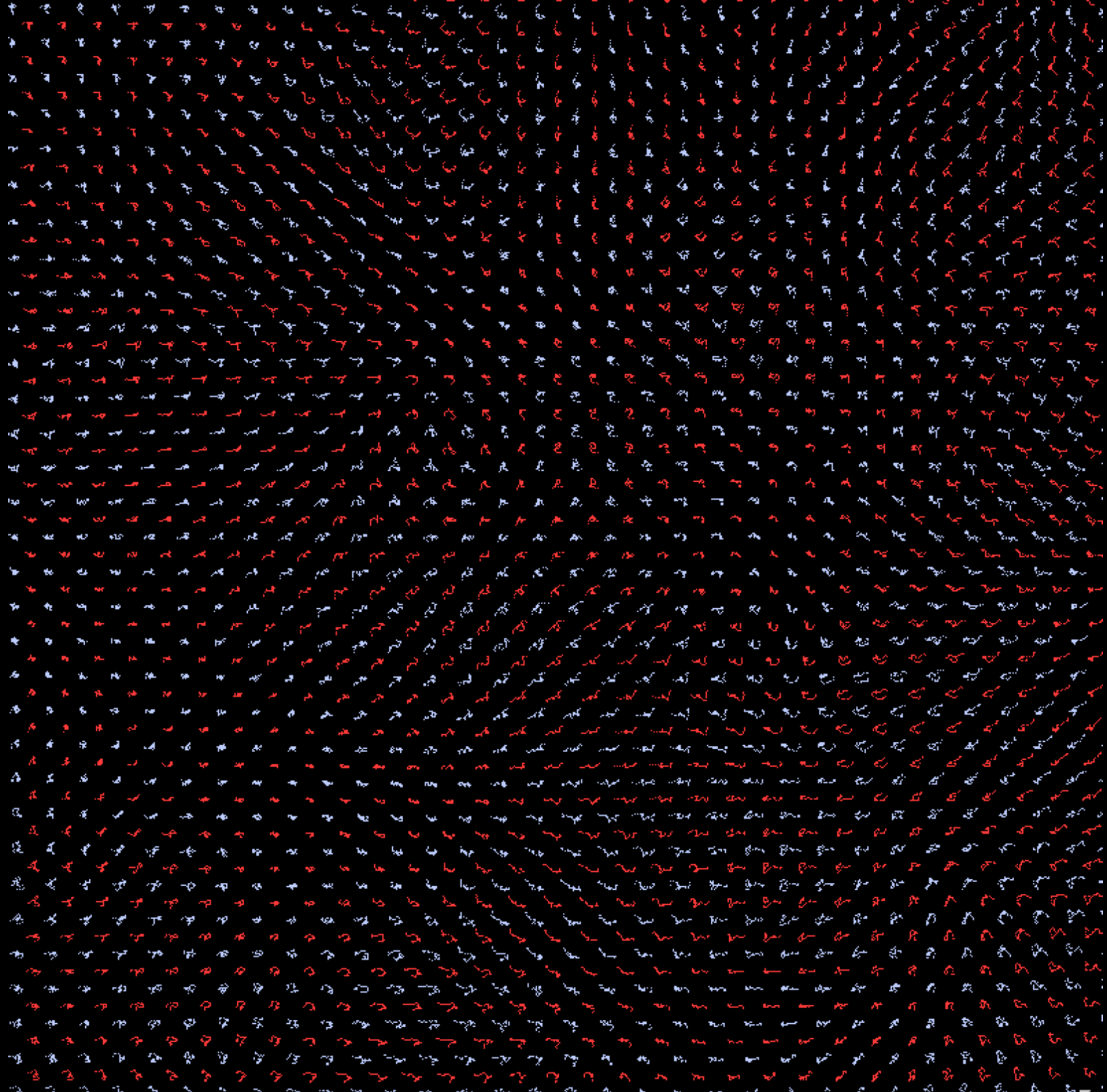
Step 3: compute the linear-theory velocity field on the grid and displace particles from the grid positions using the **Zeldovich** approximation:

$$\vec{u} = -\dot{D}(z) \vec{\nabla} \Phi(\vec{q}) \quad ; \quad \vec{x} = \vec{q} - D(z) \Phi(\vec{q})$$

- ICS generated at high enough redshift to guarantee no shell crossing on the grid scale
- Golden rule: $\sigma_{\text{displ}} = 0.1 \times \text{grid-spacing}$

Refinements:

- Generate ICS on a “glass” rather than on a regular grid (White 1993)
- Use 2LPT instead of Zeldovich approximation (1LPT)



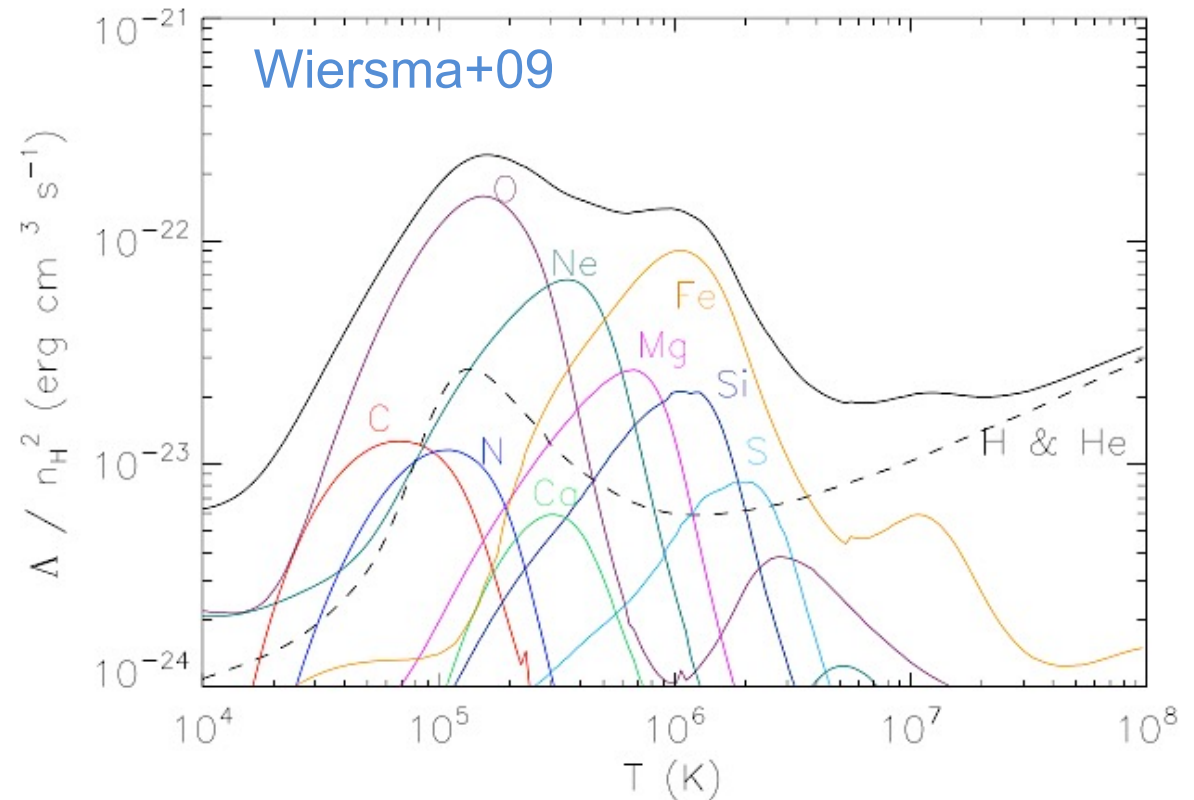
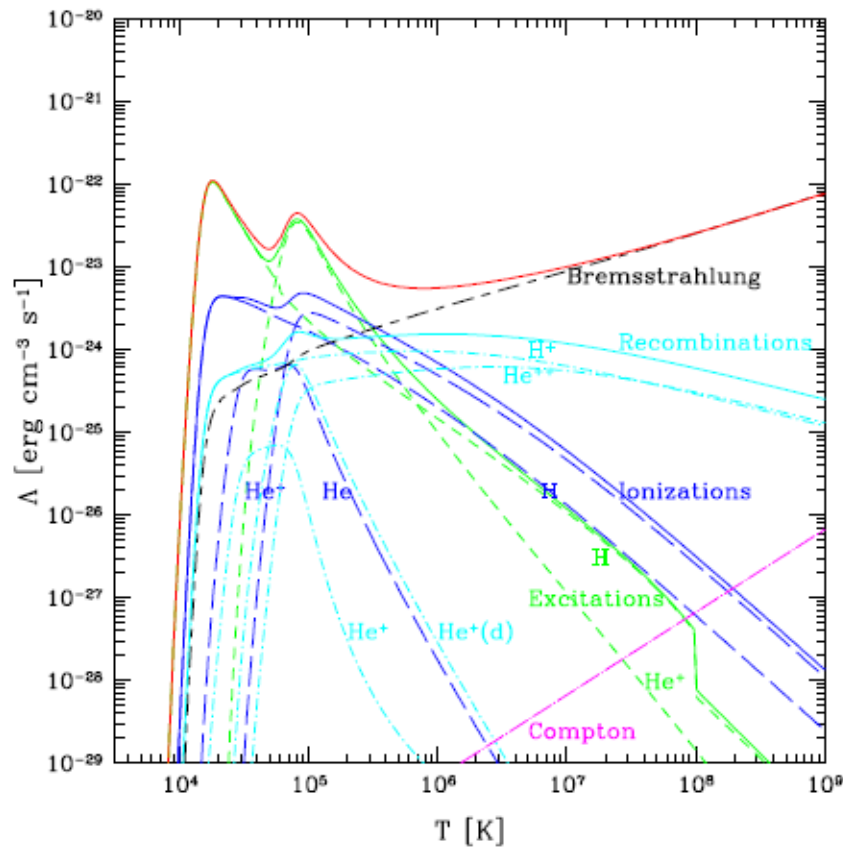
Including Astrophysics – Gas cooling



- Include an additional term to the energy equation:

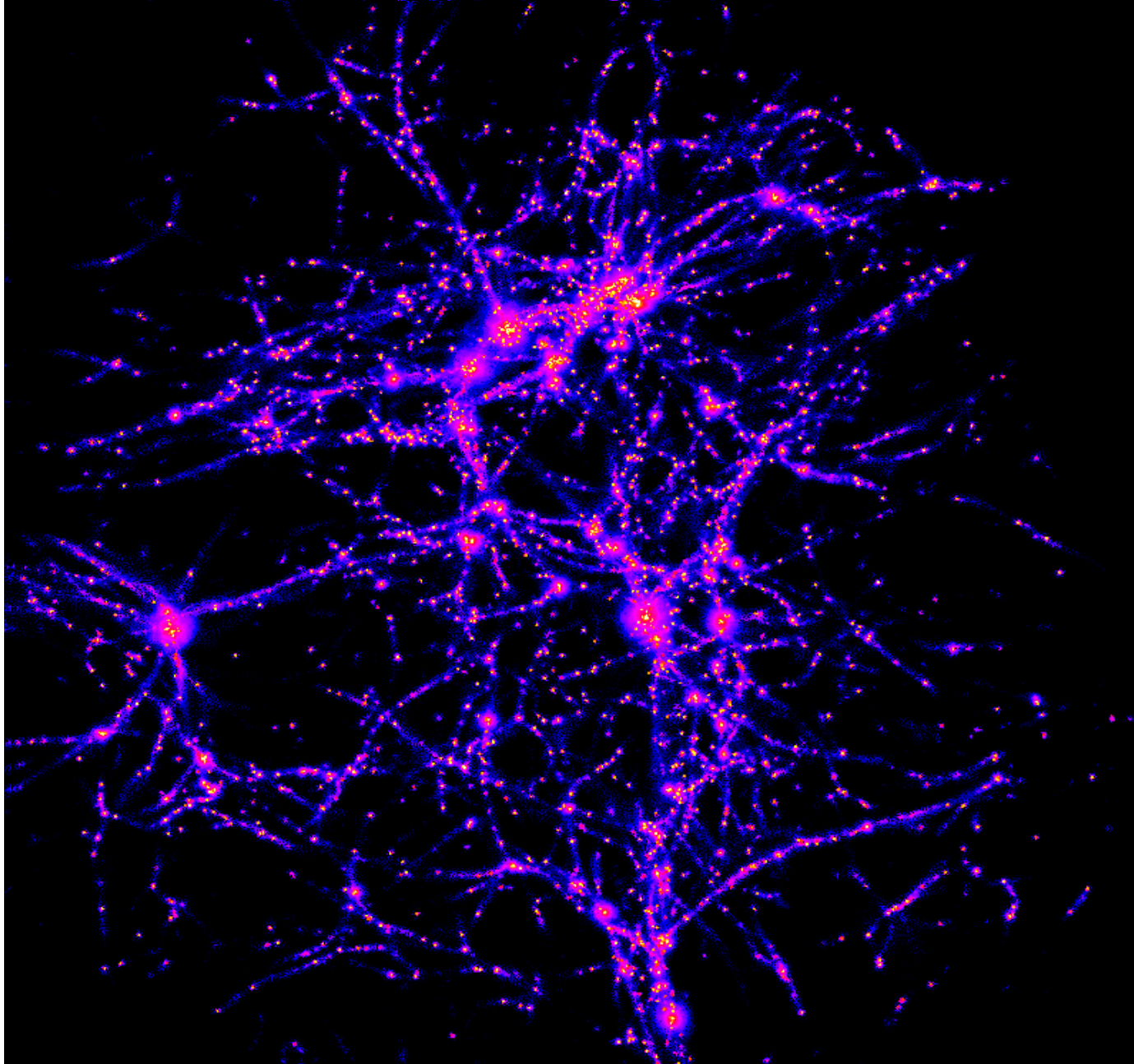
$$\frac{du}{dt} = -\frac{P}{\rho} \vec{\nabla} \cdot \vec{v} + \frac{H - \Lambda}{\rho}; \quad \Lambda(u, \rho, Z) \quad \text{Cooling function: rate of energy loss per unit volume}$$

- Assuming gas optically thin, in ionization equilibrium, ignoring three-body cooling



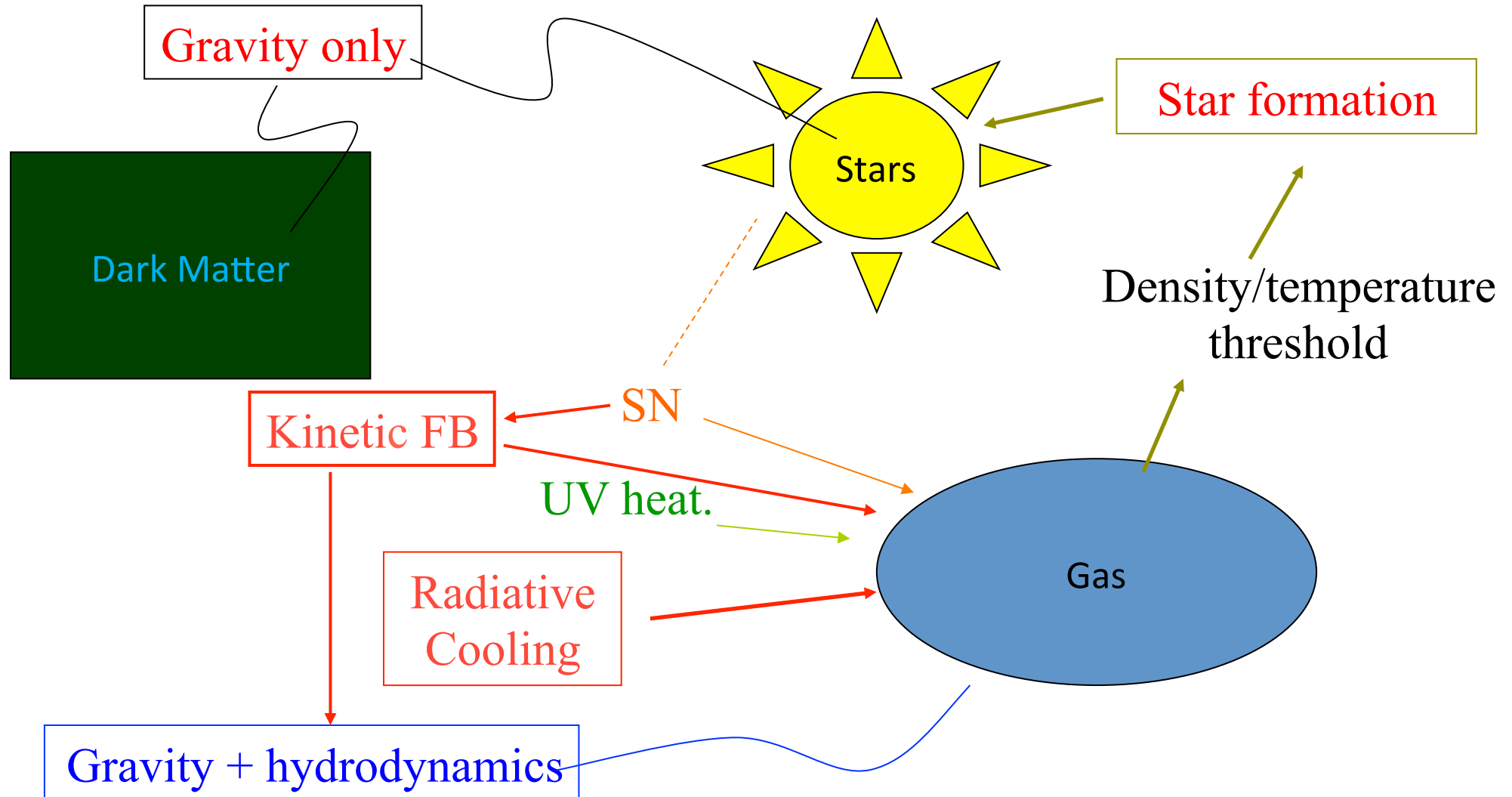
The effect of radiative cooling

A protocluster region @ $z=2$



Star formation and feedback

- Everything happens well below the numerically resolved scales (<1 pc)
- Effects important at resolved scales (>10 kpc)
- ➔ Need to resort to phenomenological “sub-resolution” models



Star formation and feedback



A simple scheme: convert cold dense gas particles into stars (Katz+96; KWH)

- Density criterion: $n_{\text{H}} > 0.1 \text{ cm}^{-3}$

- Jeans instability criterion: $\frac{h_i}{c_i} > \frac{1}{\sqrt{4\pi G \rho_i}}$

- Star formation rate: $\frac{d\rho_{\star}}{dt} = -\frac{d\rho_g}{dt} = \frac{c_{\star}\rho_g}{t_g}$

c_{\star} : star formation efficiency ; t_g : gas consumption time scale

- Gas elements stochastically converted into collisionless star particles within Δt with probability

$$p = 1 - \exp(-c_{\star} \Delta t / t_g)$$

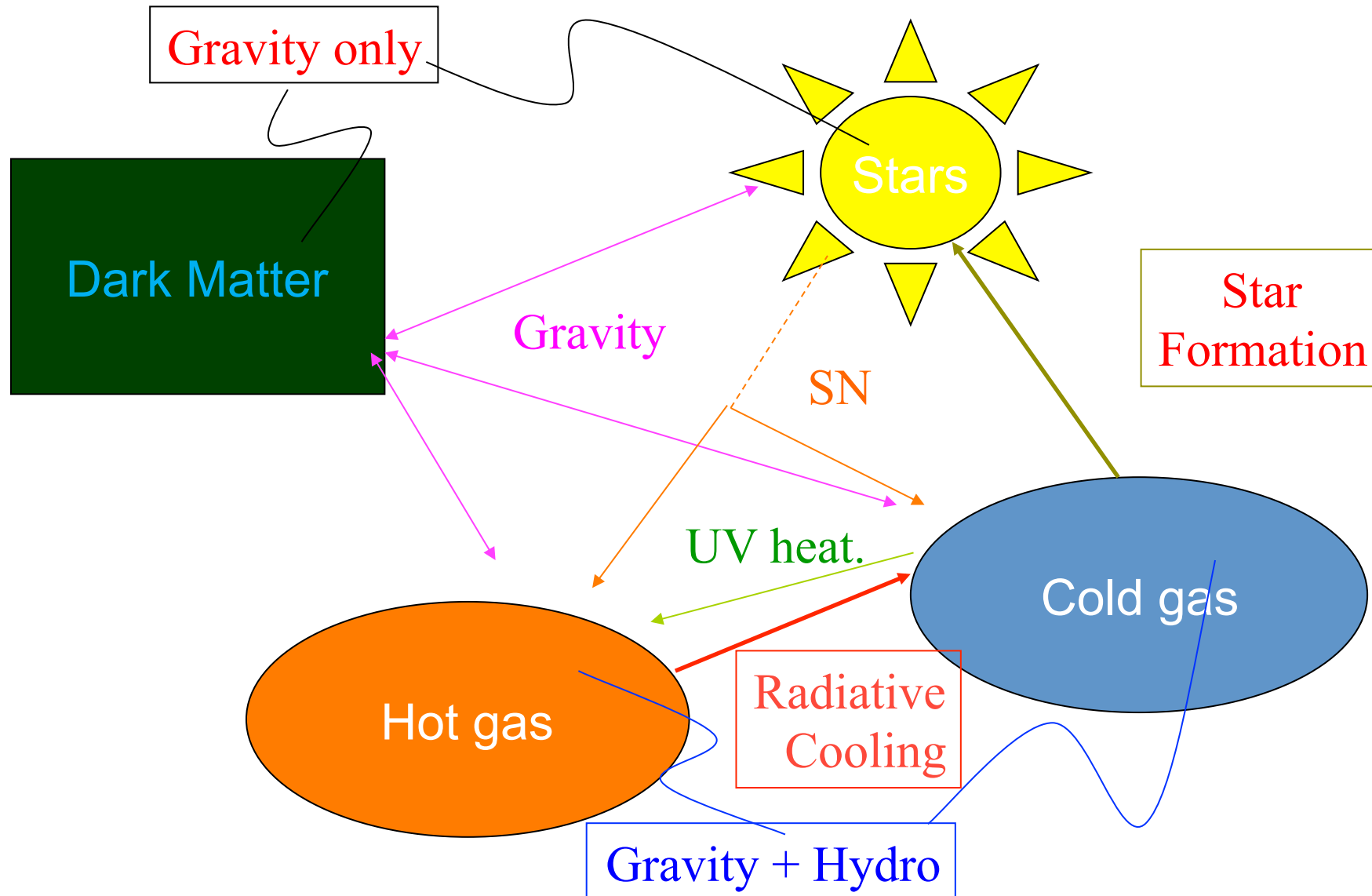
- Number of SNe from an assumed IMF, each SN providing 10^{51} erg

Limitations:

- No description of the ISM, unless extremely high resolution is reached
- Thermal energy from SNe given to nearby high density gas particles
 - ➔ Promptly radiated away
 - ➔ Inefficient feedback
 - ➔ Cooling runaway and exceedingly high star formation

Multi-phase schemes for star formation

- Hot and cold phases co-existing in pressure equilibrium within dense gas elements



A multi-phase star formation model



Springel & Hernquist 2003

$$\frac{d\rho_\star}{dt} = \frac{\rho_c}{t_\star} - \beta \frac{\rho_c}{t_\star} = (1 - \beta) \frac{\rho_c}{t_\star}$$

Stars form from COLD gas
 β : star mass fraction in supernovae

$$\left. \frac{d}{dt}(\rho_h u_h) \right|_{\text{SN}} = \epsilon_{\text{SN}} \frac{d\rho_\star}{dt} = \beta u_{\text{SN}} \frac{\rho_c}{t_\star}$$

SNe energy heats up HOT gas
 ϵ_{SN} : average SN energy per M_\odot of stars formed

$$\left. \frac{d\rho_c}{dt} \right|_{\text{EV}} = A \beta \frac{\rho_c}{t_\star}$$

SNe evaporate a fraction of COLD gas
A: evaporation efficiency

$$\left. \frac{d\rho_c}{dt} \right|_{\text{TI}} = - \left. \frac{d\rho_h}{dt} \right|_{\text{TI}} = \frac{1}{u_h - u_c} \Lambda_{\text{net}}(\rho_h, u_h)$$

HOT gas cools to COLD gas
 u_c : specific energy of the cold clouds ($T_c=1000$ K assumed)

$$\frac{d\rho_c}{dt} = - \frac{\rho_c}{t_\star} - A \beta \frac{\rho_c}{t_\star} + \frac{1 - f}{u_h - u_c} \Lambda_{\text{net}}(\rho_h, u_h)$$

$$\frac{d\rho_h}{dt} = \beta \frac{\rho_c}{t_\star} + A \beta \frac{\rho_c}{t_\star} - \frac{1 - f}{u_h - u_c} \Lambda_{\text{net}}(\rho_h, u_h)$$

$f=0$ for $\rho < \rho_{th}$

$f=1$ for $\rho > \rho_{th}$

ρ_{th} : threshold density for the onset of star formation

A multi-phase star formation model



$$\frac{d}{dt} (\rho_c u_c) = -\frac{\rho_c}{t_\star} u_c - A\beta \frac{\rho_c}{t_\star} u_c + \frac{(1-f)u_c}{u_h - u_c} \Lambda_{\text{net}},$$

$$\frac{d}{dt} (\rho_h u_h) = \beta \frac{\rho_c}{t_\star} (u_{\text{SN}} + u_c) + A\beta \frac{\rho_c}{t_\star} u_c - \frac{u_h - f u_c}{u_h - u_c} \Lambda_{\text{net}}.$$

Evolution of energy of cold and hot phases

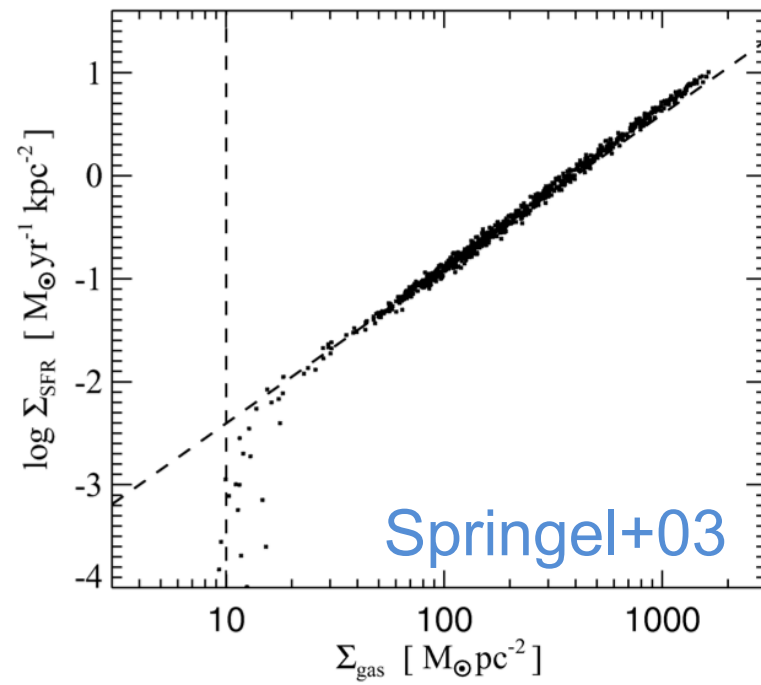
Assume:

- Self-regulated star formation
- Hot and Cold phases in pressure equilibrium
- Constant temperature of the cold phase

Solve the system of equations to calculate star formation rate:

→
$$\frac{\rho_c}{t_\star} = \frac{\Lambda_{\text{net}}(\rho_h, u_h)}{\beta u_{\text{SN}} - (1 - \beta)u_c}$$

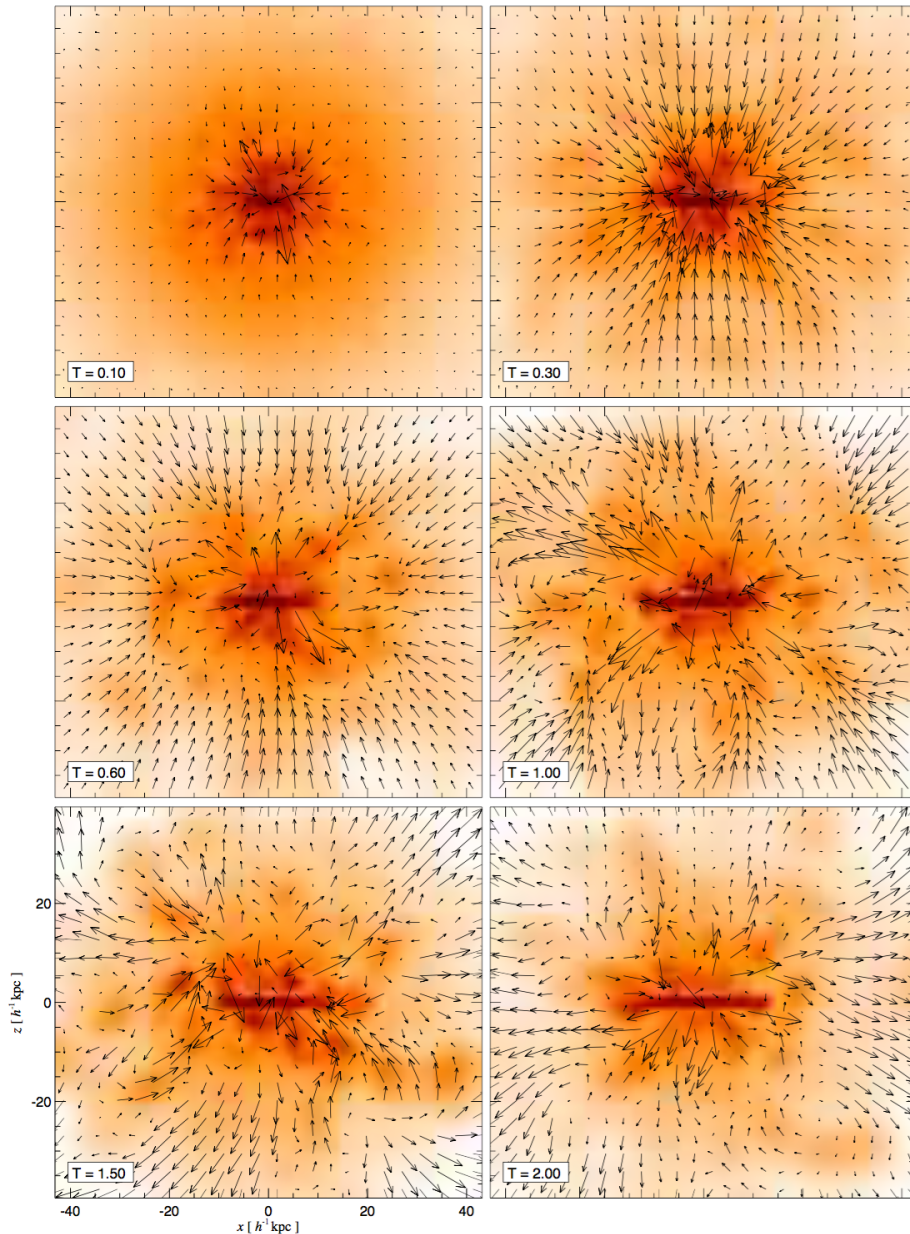
Model parameters fixed so as to reproduce the observed $\Sigma_{\text{SFR}} - \Sigma_{\text{gas}}$ Schmidt-Kennicutt relation:



SN-driven galactic winds

- To deposit energy away from gas with short cooling time
- Gas particles «kicked» with a given velocity and from the ambient gas

M8



Energy-driven winds:
(e.g. Springel & Hernquist 2003)

$$\dot{M}_w = \eta \dot{M}_* \quad ; \quad \frac{1}{2} \dot{M}_w v_w^2 = \chi \epsilon_{SN} \dot{M}_*$$

$$\rightarrow v_w = \sqrt{\frac{2\beta\chi u_{SN}}{\eta(1-\beta)}} \approx (300 - 600) \text{ km / s}$$

$\eta \sim 2-3$: mass-upload factor

$\chi \sim 0.5-1$: feedback efficiency

Momentum-driven winds:

Arising from radiation pressure (e.g. Oppenheimer & Dave' 2006)

$$v_w \approx 3\sigma \quad ; \quad \eta = \sigma / \sigma_0$$

σ : galaxy velocity dispersion

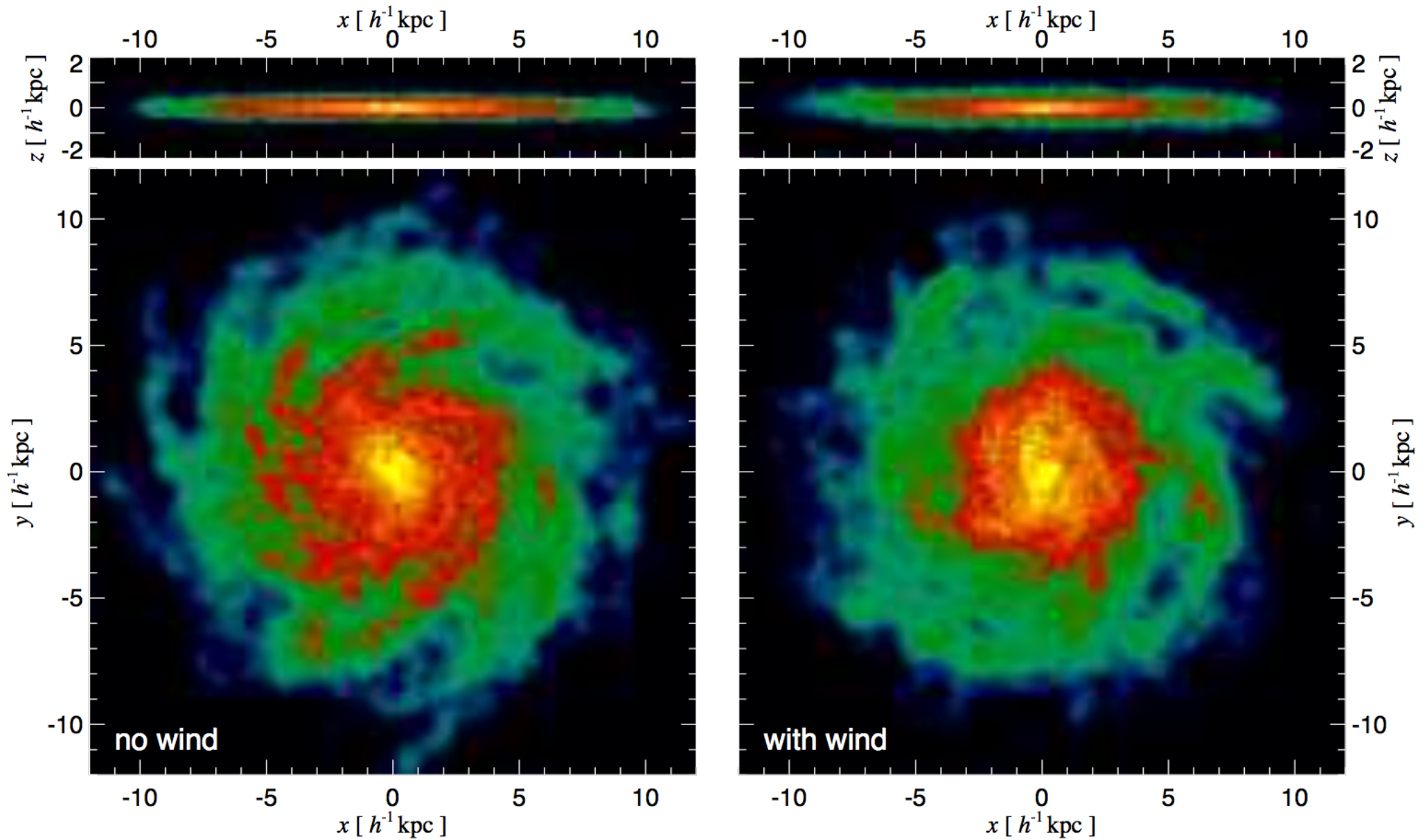
$\sigma_0 \sim 300 \text{ km s}^{-1}$

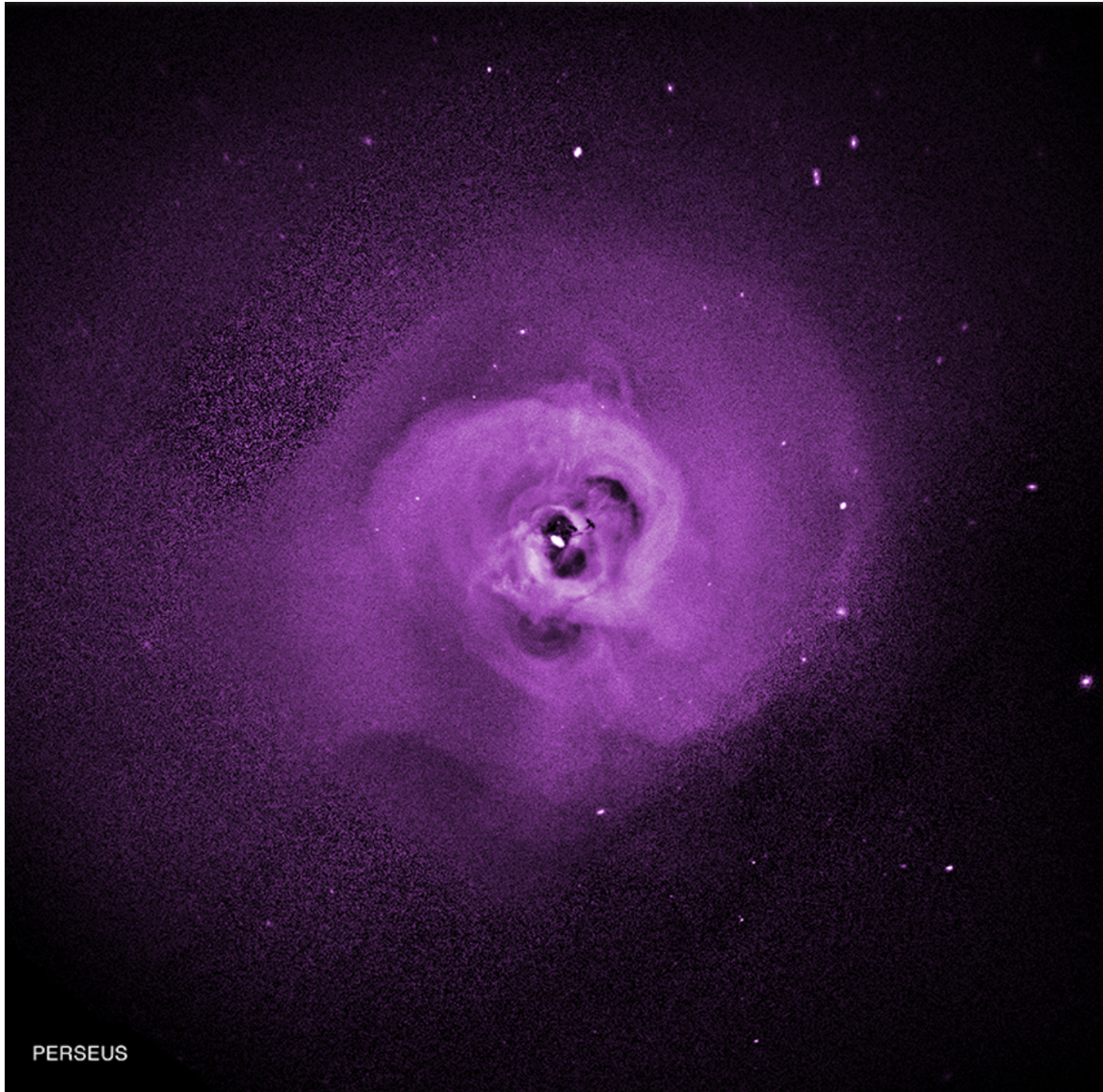
- Stronger feedback in more massive galaxies

Cre

SN-driven galactic winds

Springel & Hernquist 2003





- Suppress the bright end of the galaxy luminosity function
- Quench star formation in massive galaxies at low z
- Steepen the L_X - T relation in galaxy clusters and groups
- Establish the cool-core structure within relaxed galaxy clusters

➔ Requires an energy feedback mechanism of non-stellar origin

Original implementation: Springel+05

- Include BHs as sink particles
- Seeded in resolved DM halo
- Growing by merging and gas swallowing:

Bondi-Hoyle accretion: $\dot{M}_B = \frac{4\pi\alpha G^2 M_{\text{BH}}^2 \rho}{(c_s^2 + v^2)^{3/2}}$

α : fudge factor to account for unresolved density at the Bondi radius (~ 100 originally)

ρ : gas density at the BH position

Eddington-limited: $\dot{M}_{\text{Edd}} \equiv \frac{4\pi G M_{\text{BH}} m_p}{\epsilon_r \sigma_T c}$

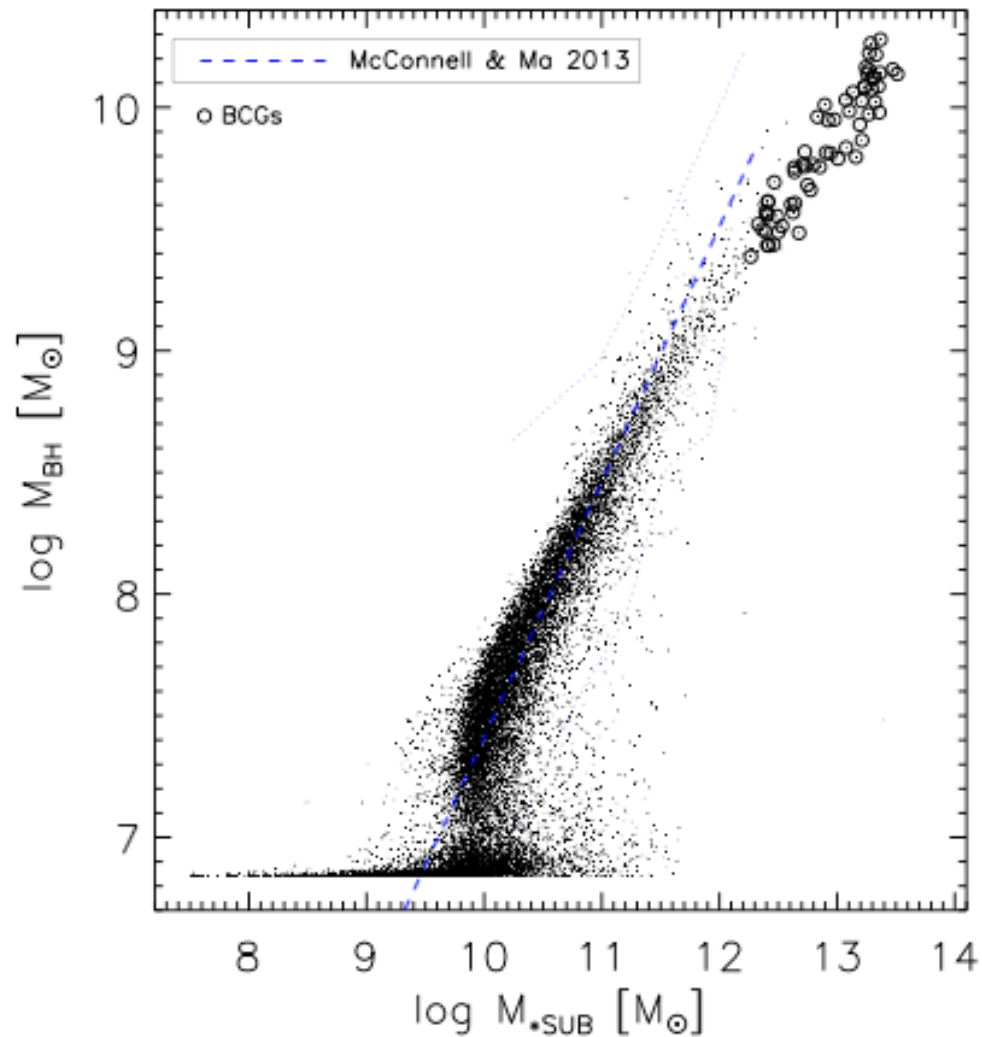
$\epsilon_r = \frac{L_r}{\dot{M}_{\text{BH}} c^2}$: radiative efficiency ~ 0.1

- Thermal energy to surrounding gas: $\dot{E}_{\text{feed}} = \epsilon_f L_r = \epsilon_f \epsilon_r \dot{M}_{\text{BH}} c^2$

ϵ_f : feedback efficiency ~ 0.05

- Model parameters tuned to as to reproduce observational results (e.g. $M_{\text{bulge}}-M_{\text{BH}}$ relation; e.g. Magorrian+98; Marconi & Hunt 03)

Ragone-Figueroa+14

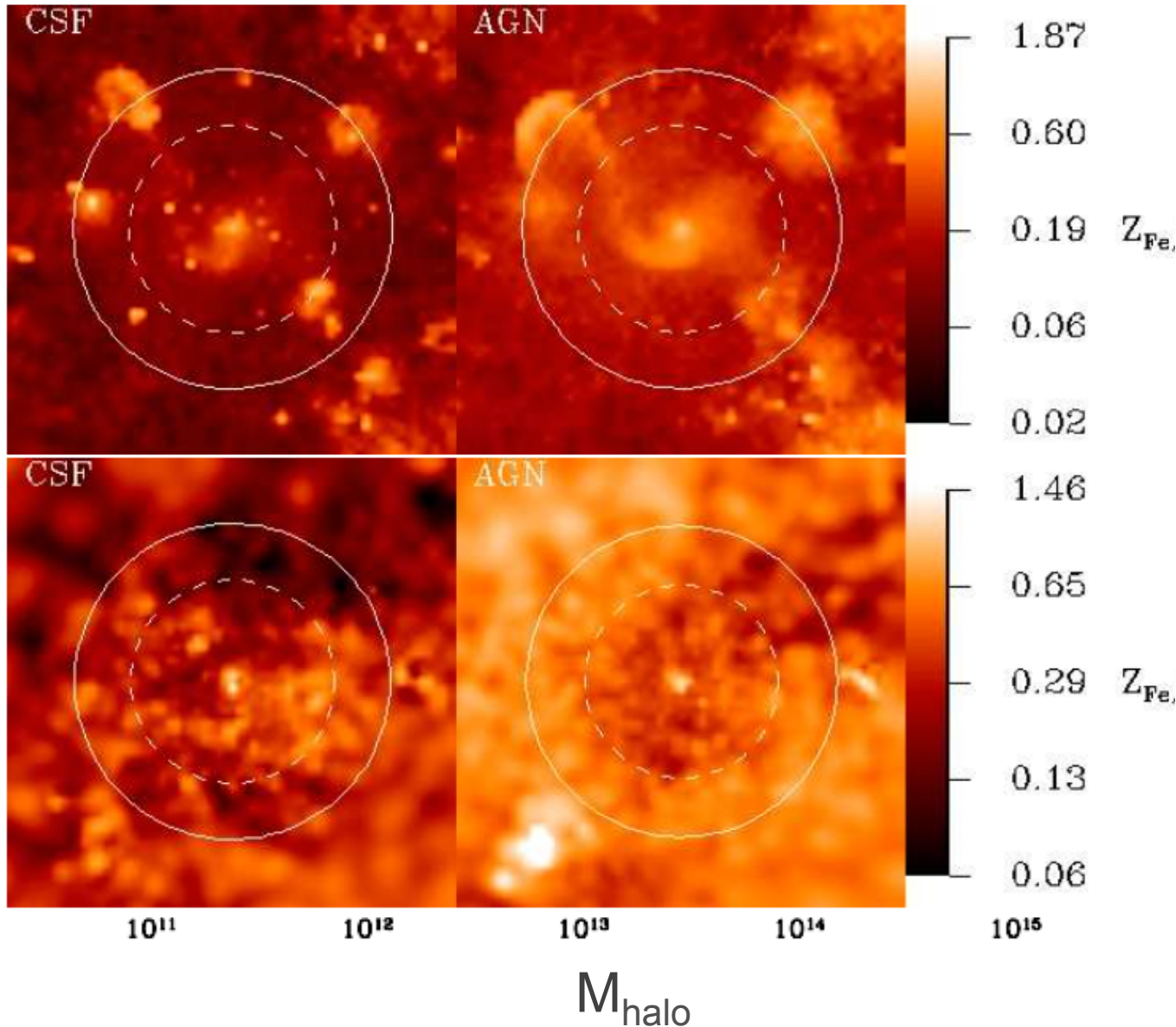


A number of variants:

- Purely Bondi accretion not realistic (e.g. cold & hot accretion modes; e.g. [Steinborn+15](#))
- Make α variable to account for resolved accretion ([Booth & Schaye 09](#))
- Different modes (i.e. QSO and radio) in different regimes (e.g. [Sijacki & Springel 06](#); [Fabjan+10](#))
- Energy thermalization:
 - Mimic injection of [low-entropy bubbles](#) ([Sijacki & Springel 07](#))
 - Describe explicitly sub-relativistic jets ([Dubois+12](#); [Barai+13](#))

....

Planelles+13



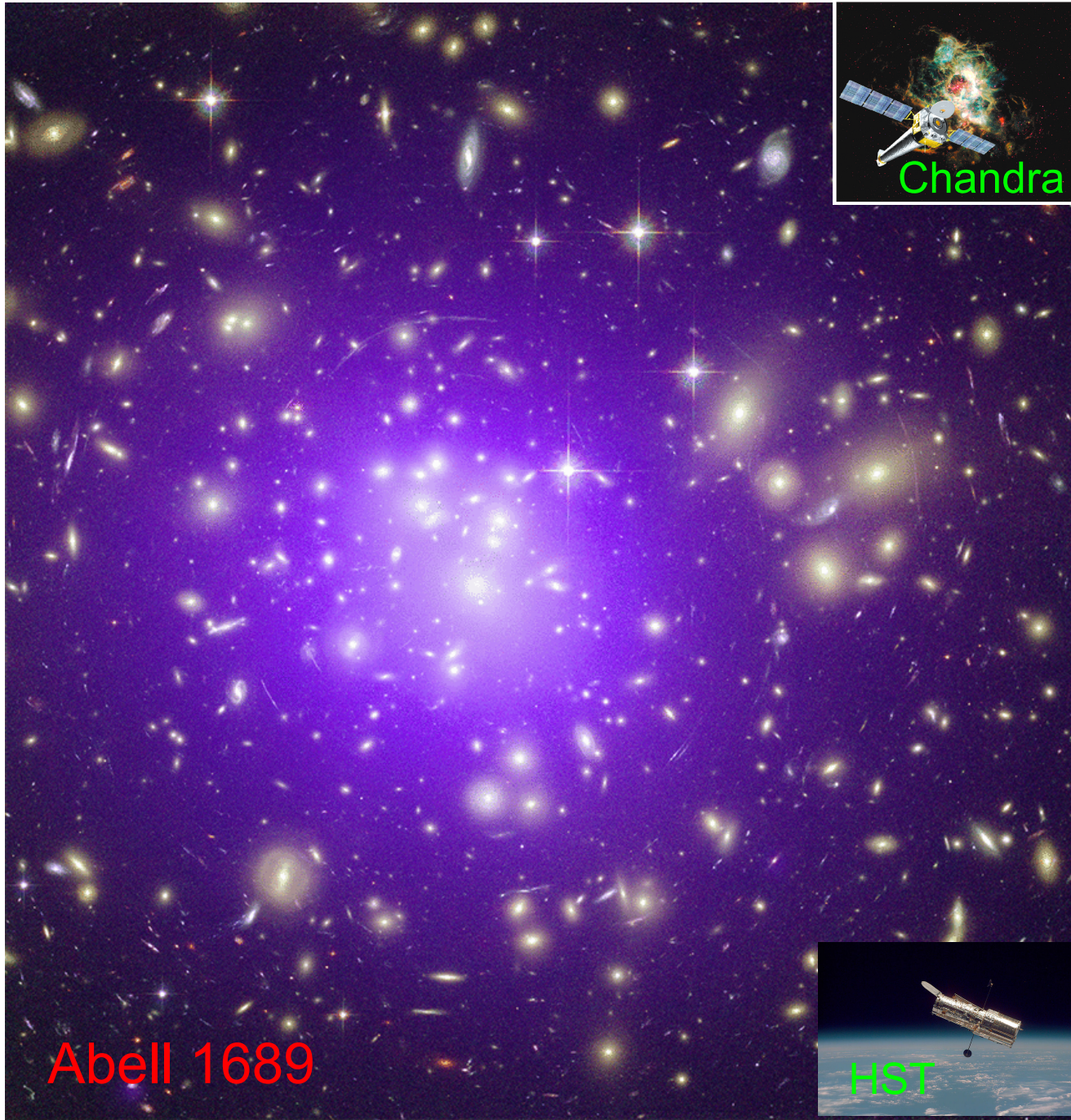
- Suppress star formation efficiency in the most massive galaxies (e.g. [Martizzi+12](#))
- Selectively remove X-ray emitting gas from galaxy groups and steepen the L_X - T relation (e.g. [Puchwein+08](#), [Fabjan+10](#))
- Change the pattern of chemical enrichment in galaxy clusters (e.g. [McCarthy+13](#), [Planelles+13](#))

What I won't talk about?



- Stellar evolution and chemical enrichment
- Radiative transfer
- Magnetic fields
- Plasma effects:
 - Spitzer thermal conduction
 - Spitzer-Braginsky viscosity
 - Electron-ion equilibration
 - Particle acceleration at shocks and non-thermal emission
-

Applications to cluster cosmology



Concentrations of $\sim 10^3$ galaxies

$\sigma_v \sim 500-1000 \text{ km s}^{-1}$

Size: $\sim 1-2 \text{ Mpc}$

Mass: $\sim 10^{14}-10^{15} M_\odot$
 $\rightarrow \lambda_i \approx 10 \text{ Mpc}$

Baryon content:

\rightarrow cosmic share in
hydrostatic equilibrium

ICM temperature:

$\rightarrow T \sim 2-10 \text{ keV}$

\rightarrow fully ionized plasma;

Thermal bremsstrahlung

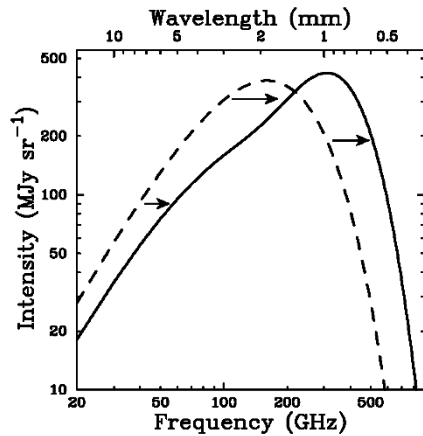
$\rightarrow n_e \sim 10^{-2}-10^{-4} \text{ cm}^{-3}$

$\rightarrow L_X \sim 10^{45} \text{ erg s}^{-1}$

Abell 1689



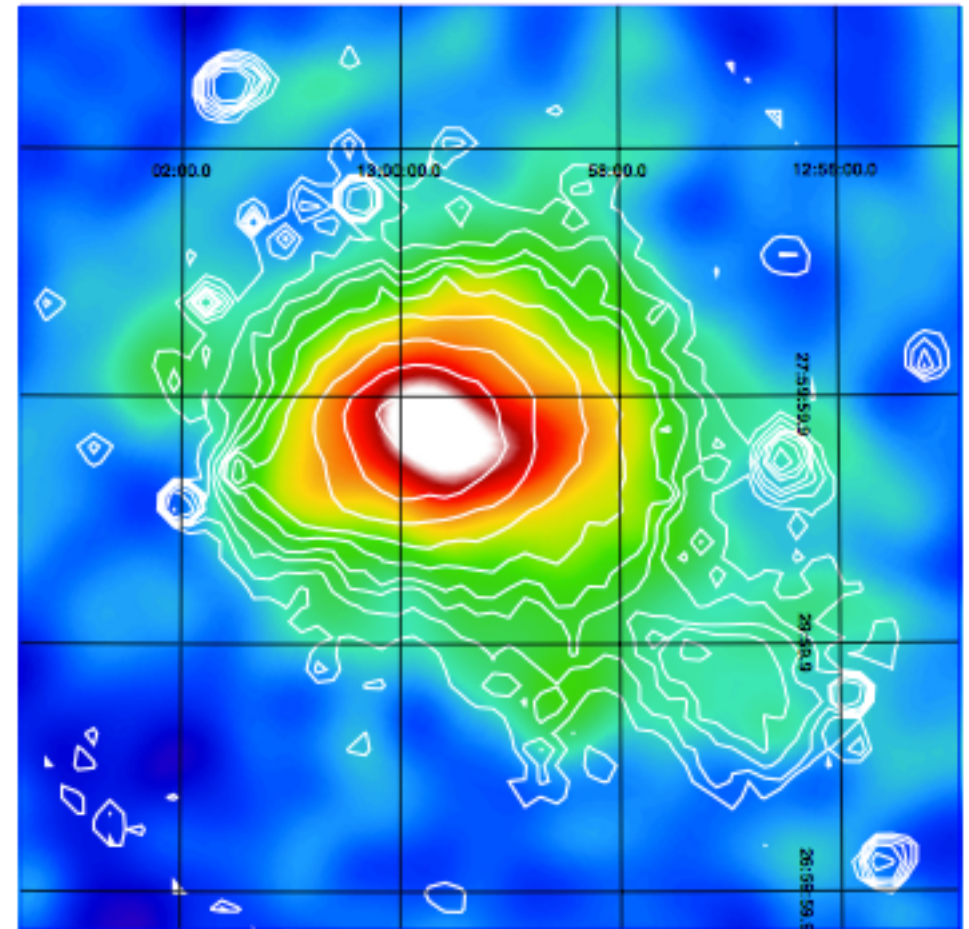
Sunyaev-Zeldovich Effect



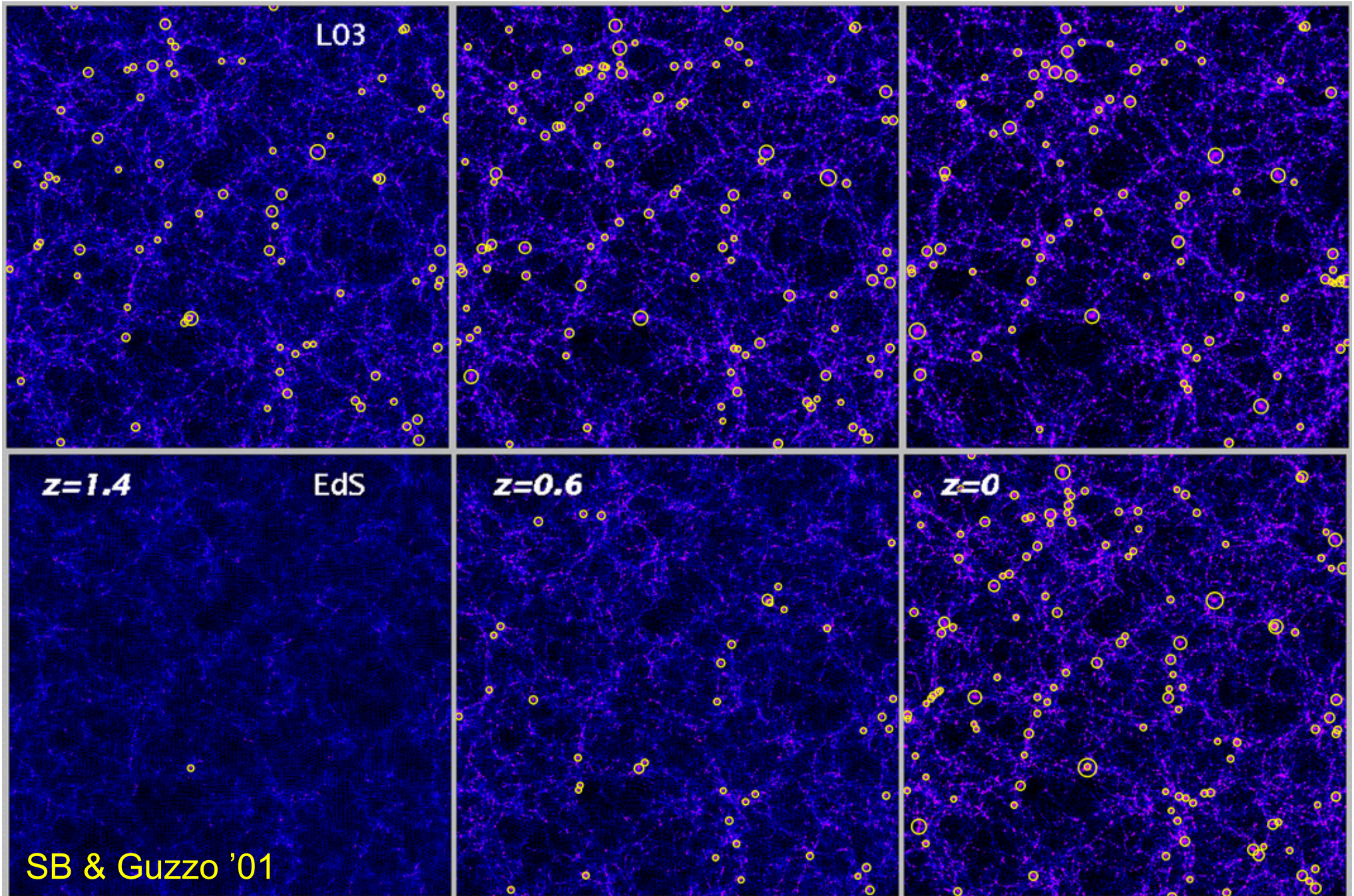
Inverse Compton scattering of CMB photons off the ICM electrons

- ➔ Signal virtually independent of redshift
- ➔ Proportional to the l.o.s. integration of $n_e T_e \sim$ pressure
- ➔ Wider dynamic range accessible
- ➔ We are now in the era of SZ cluster cosmology (e.g. ACT, SPT, Planck)

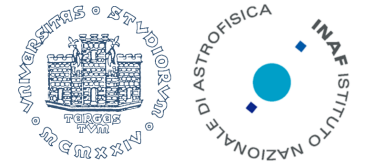
Coma as seen by Planck



Clusters & cosmic growth



Information from a cluster survey



$$\frac{dN(X; z)}{dXdz} = \frac{dV}{dz} f(X, z) \int_0^\infty \frac{dn(M, z)}{dM} \frac{dp(X | M, z)}{dX} dM$$

→ No. of clusters of given observable X and z within the survey area

$$P_{cl}(k; M, z) = b_{cl}^2(k; M, z) P_m(k, z) \rightarrow \text{Clustering of clusters of given mass}$$

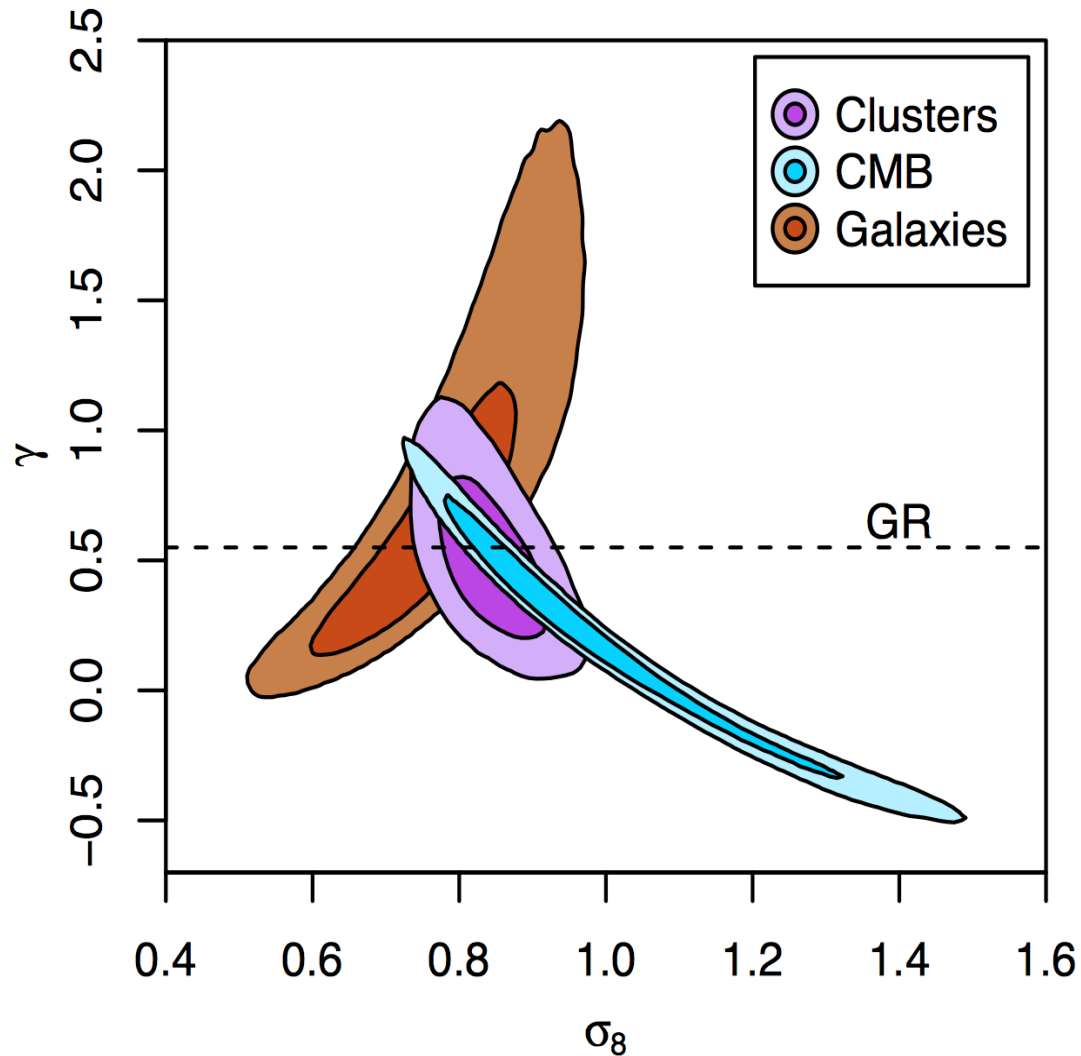
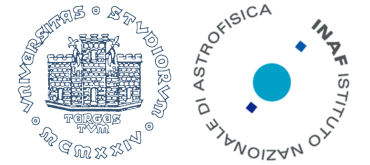
1. Friedmann background: $\frac{dV}{dz}$ → Priors from CMB, BAO, SN-Ia,

2. Selection function: $f(X, z)$ → Observational strategy

3. Growth history and nature of perturbations: $\frac{dn(M, z)}{dM}$ → Precisely calibrated with N-body simulations

4. Astrophysics: $p(X | M, z)$ → Priors on “nuisance parameters” p_j from follow-up observations and/or cosmological simulations

Cluster Cosmology as of today



Reichardt+13

100 SPT clusters at $z > 0.3$

+ Chandra/XMM follow-up for
14 clusters

➔ Fit at the same time
cosmology and mass scaling

Mantz+15

RASS clusters out to $z \sim 0.9$

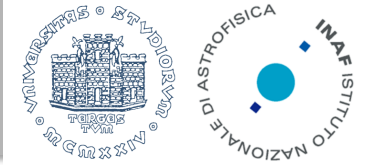
+ Chandra follow-up for M_{gas}

+ mass calibration from WtG WL

➔ Constraints on deviations
from GR:

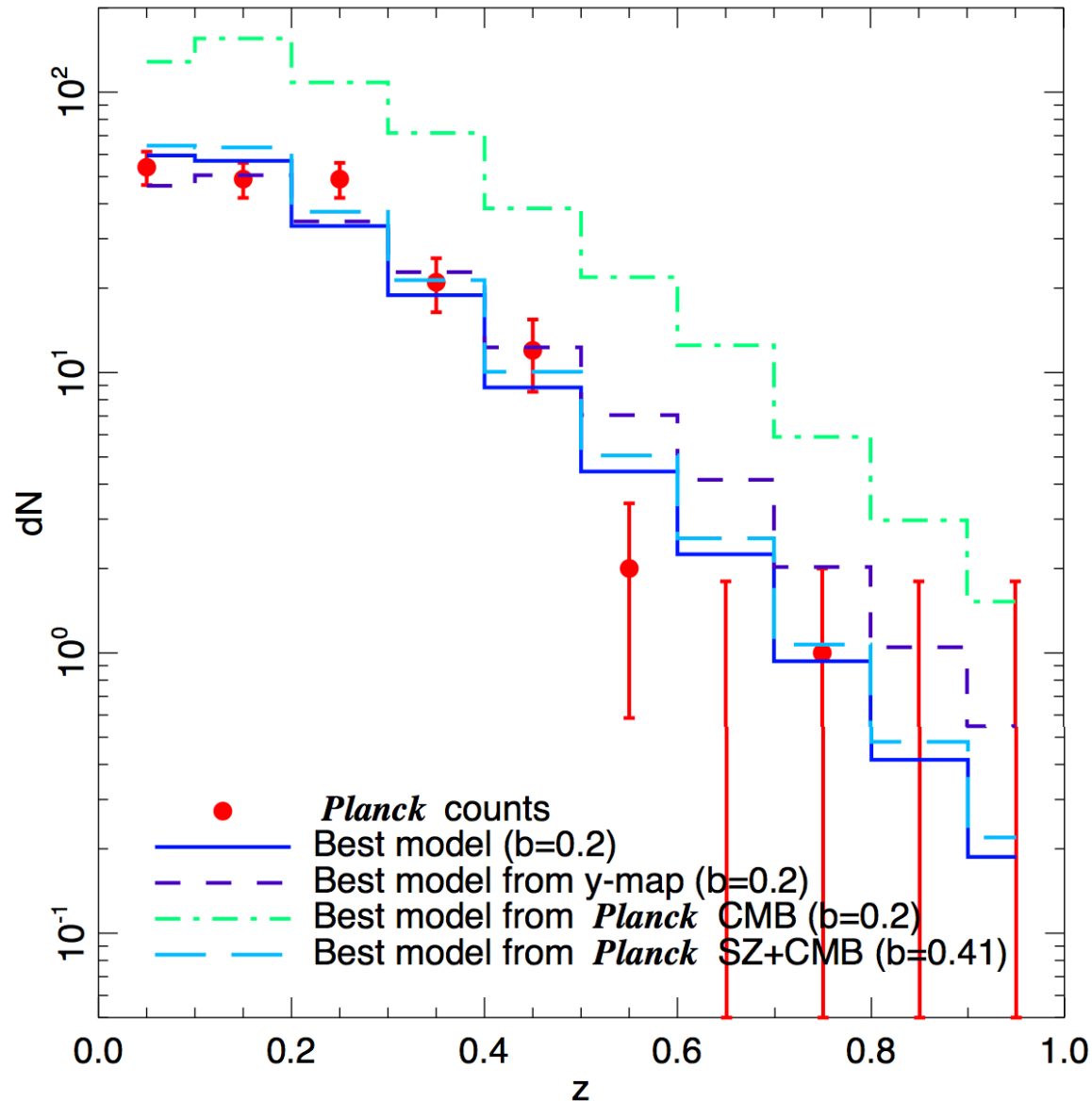
$$f(\Omega_m(z)) \equiv \frac{d \log D_+(a)}{d \log a} = [\Omega_m(z)]^\gamma$$

Planck CMB & clusters



Planck collab XX 2014

Number counts for 189 Planck-SZ clusters



→ X-ray (XMM) calibrated mass scaling

→ Tension with Planck primary CMB

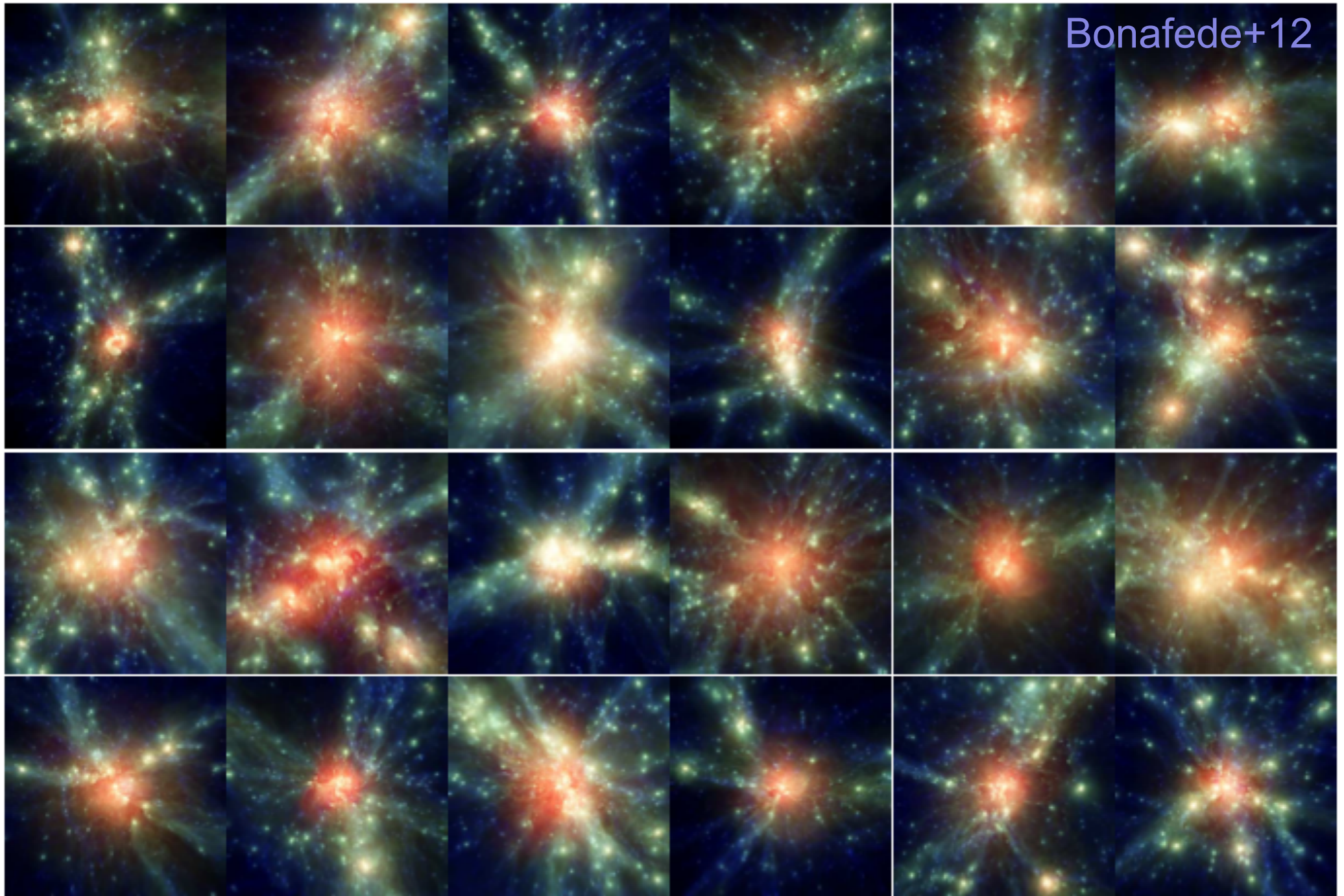
→ **b=0.2** (HE mass bias) suggested by simulations

→ **b=0.4** to recover agreement with CMB cosmology

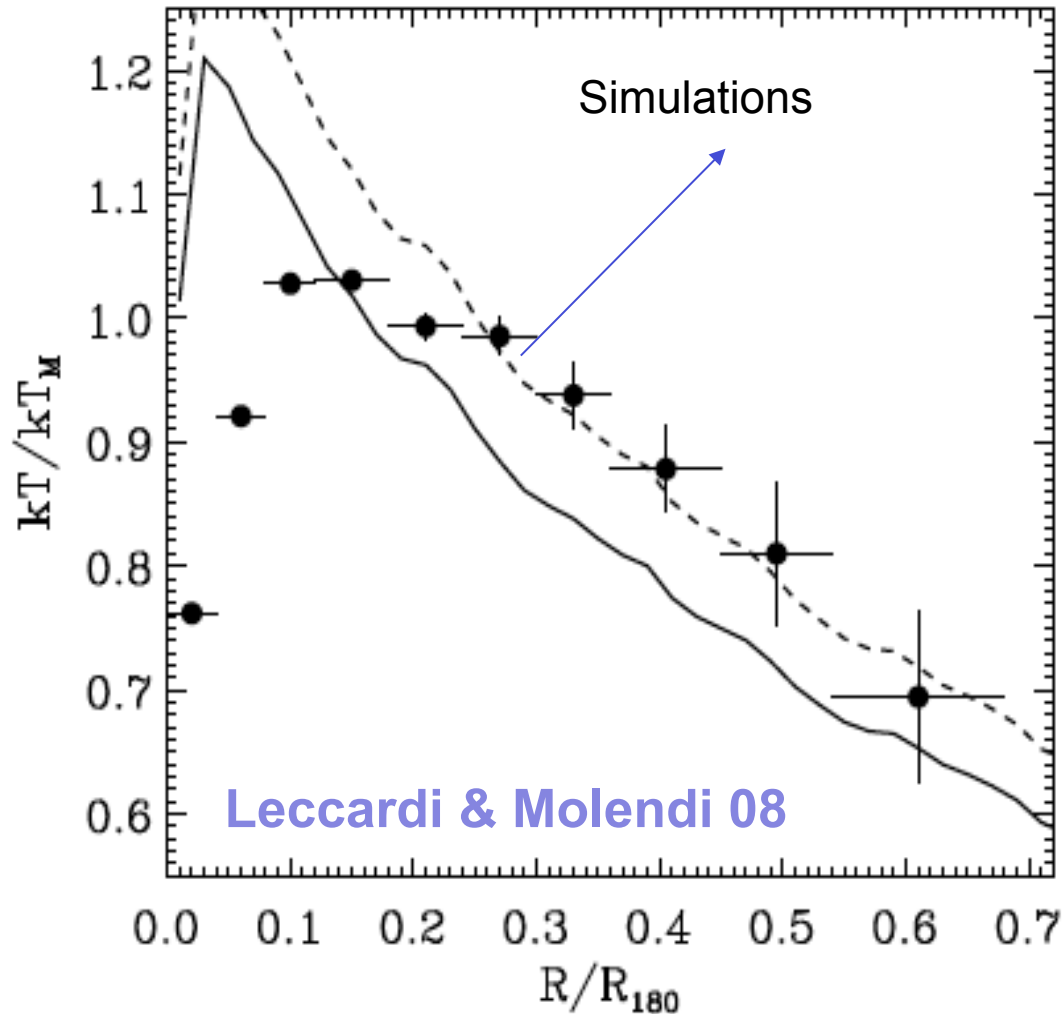
→ Agreement with constraints from:

- Planck-y map
- Other cluster counts
- Cosmic shear

The population of galaxy clusters



Temperature Profiles



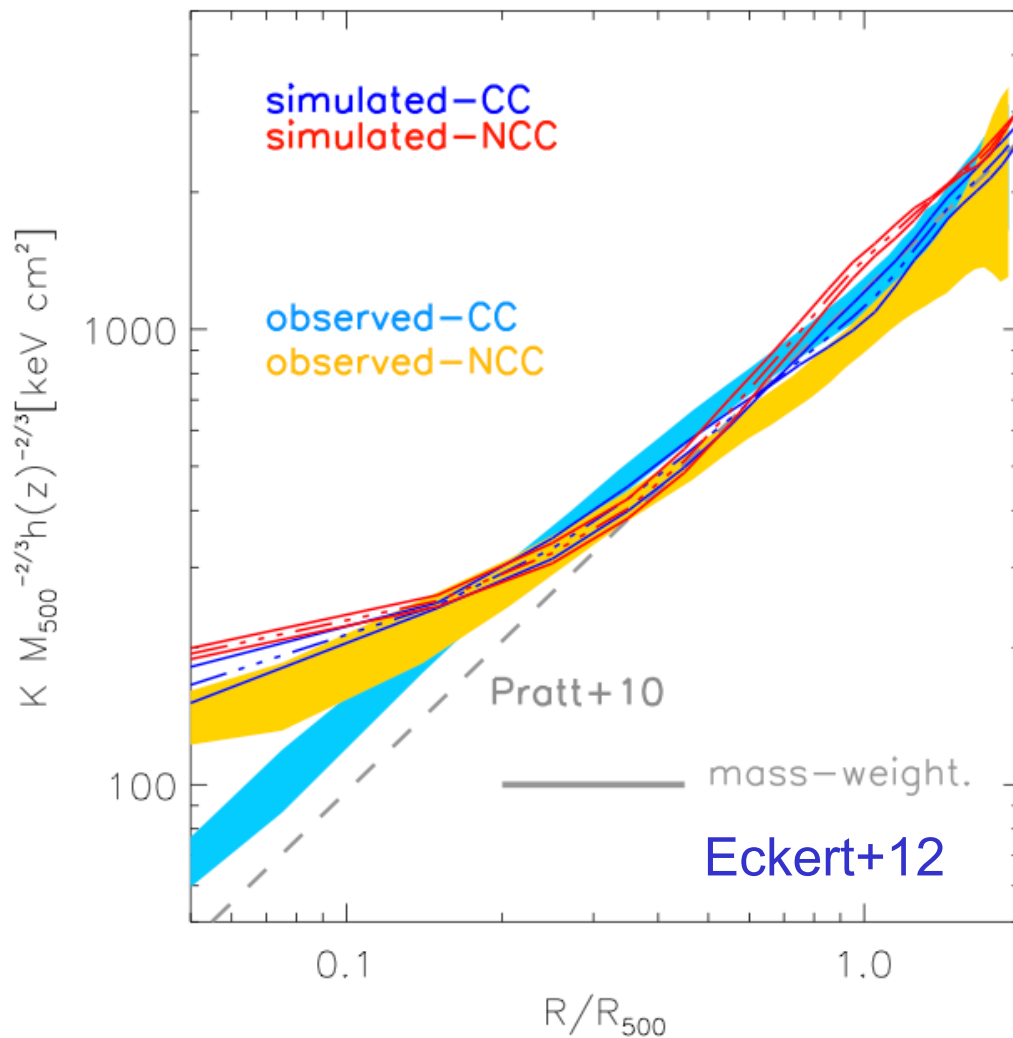
Data: X-ray (XMM) analysis of nearby clusters

Simulations: SPH simulations with star formation and SN feedback (SB+04)

- Central profiles in simulations steep and negative
- Strong disagreement with data
- Requires including AGN feedback

Entropy profiles

$$K = T/n_e^{2/3}$$



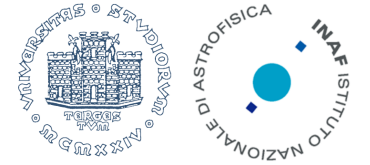
Eckert+12

Data: Joint analysis of X-ray (ROSAT imaging) and SZ (Planck)

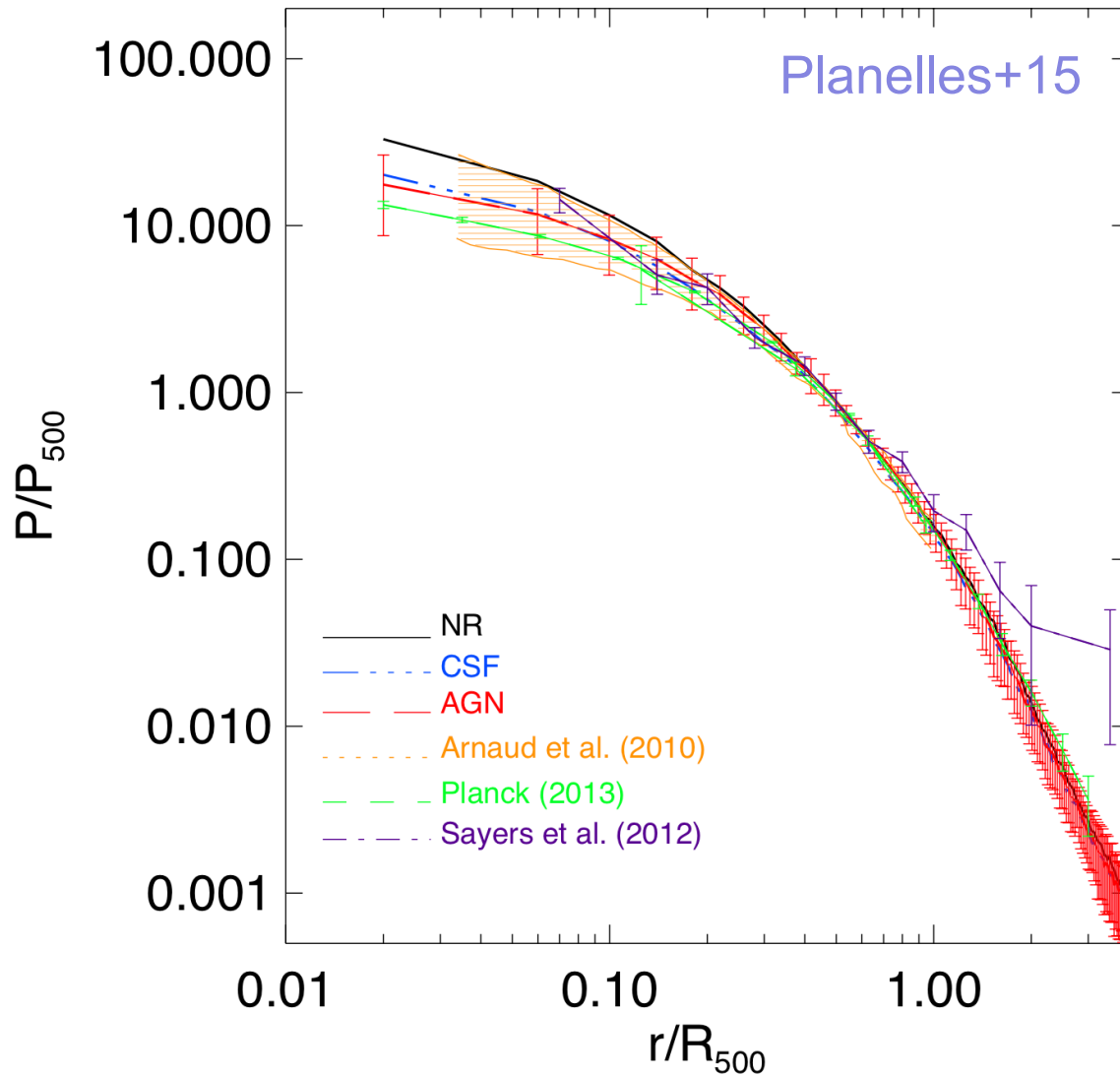
Simulations: Non-radiative with ENZO AMR (Vazza+12)

- Good agreement outside core regions ($r > 0.2 r_{500}$)
- CC vs. non-CC dichotomy from data not reproduced in simulations
- Including radiative cooling not enough to account for the observed diversity in the cluster population

Pressure profiles



$z=0$



➔ Shallower profiles in radiative simulations

• Radiative P-profile consistent with observed profiles from both:

➔ X-ray (XMM); Arnaud+10

➔ SZ from Planck (Planck coll. XX), SPT (McDonald+14) & Bolocam (Sayers+13)

X-ray masses: hydrostatic bias

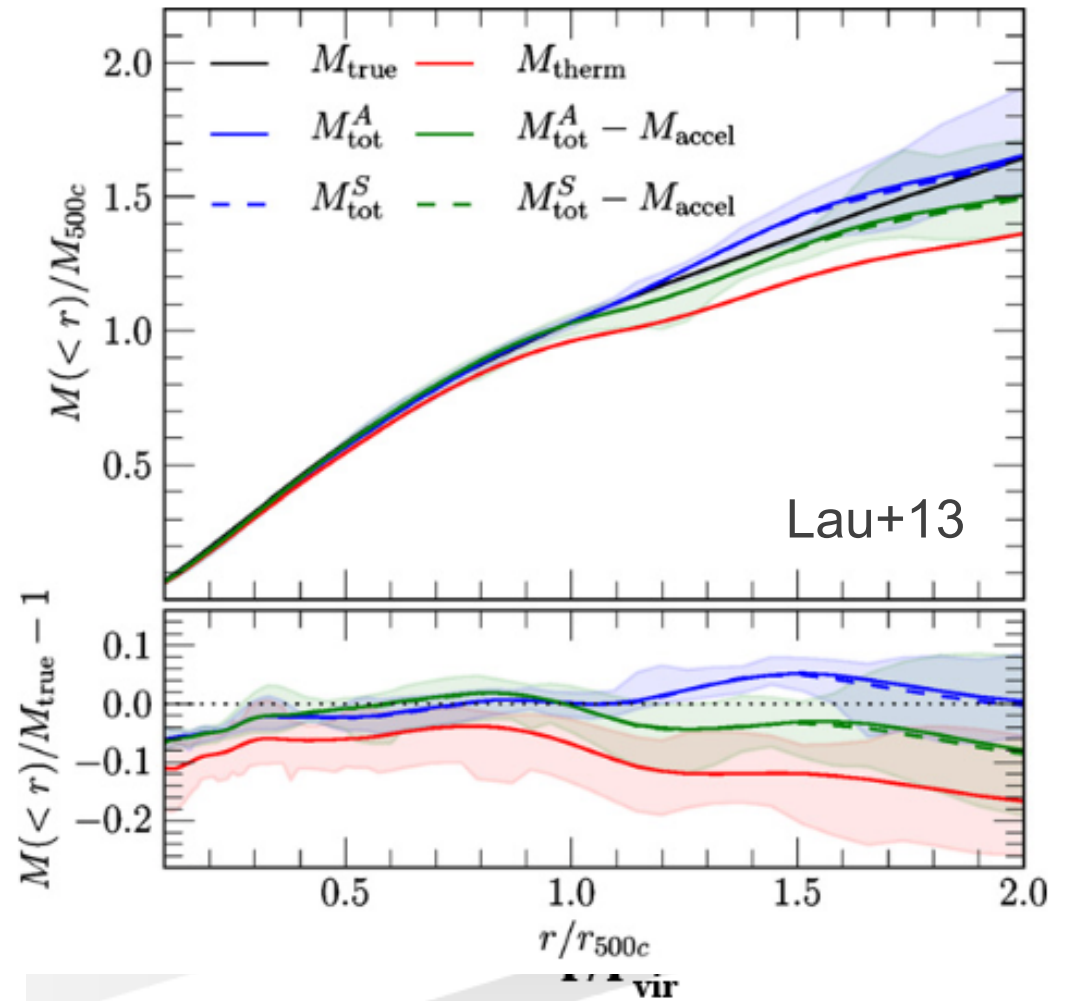
- Hydrostatic equilibrium (HE):

$$M_{hyd}(< r) = -\frac{rkT}{G\mu m_p} \frac{d\ln(nkT)}{d\ln(r)}$$

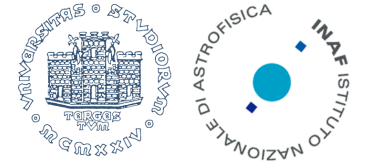
- ➔ HE violated at the ~10% level within r_{500}
- ➔ Larger deviations at larger radii ($>R_{500}$)

Also Rasia+06,12, Nagai+07, Morandi+07, Piffaretti & Valdarnini 08, Meneghetti+09, Lau+09, Kay+11, Suto+13, ...

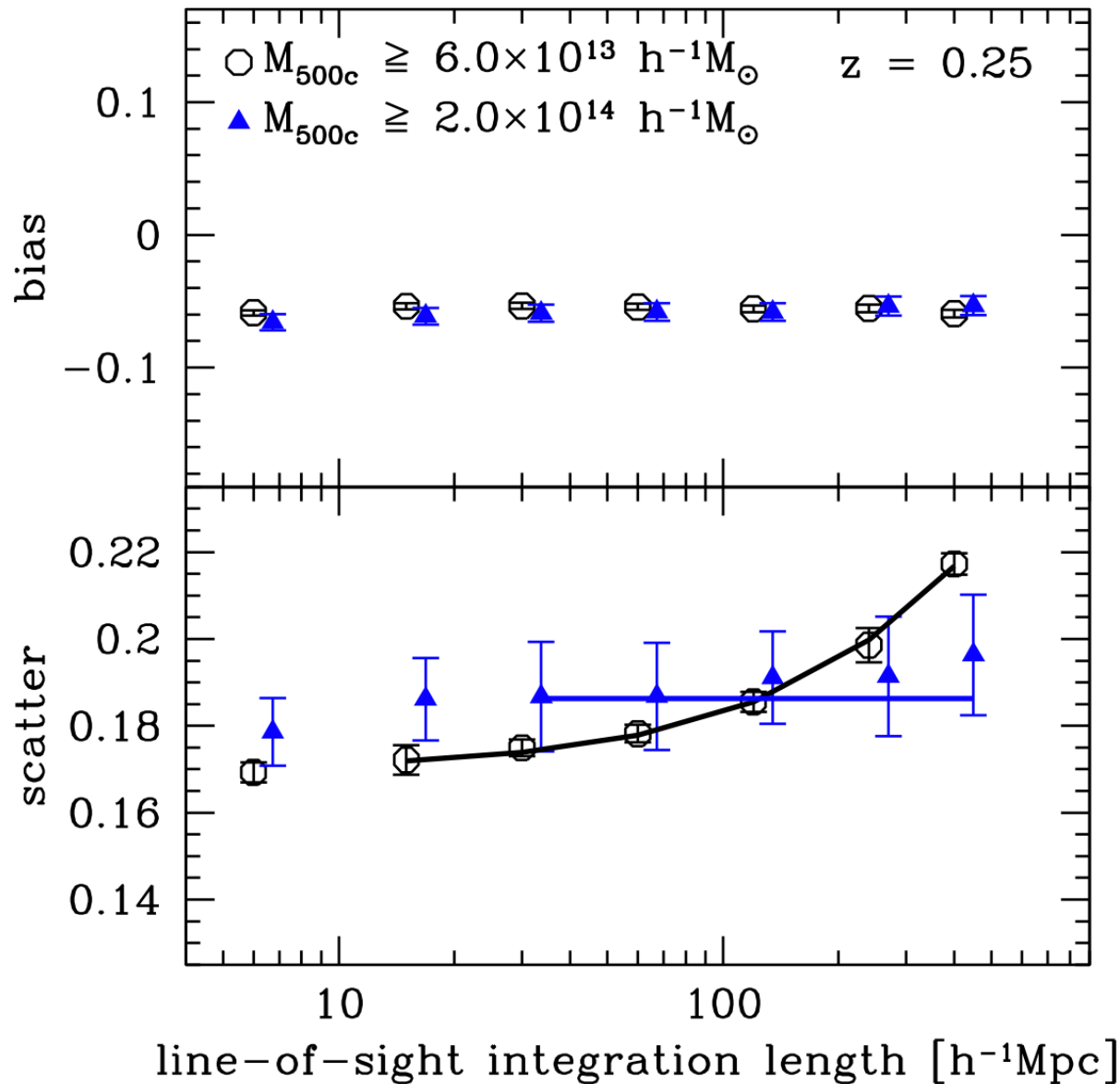
- ➔ Non-thermal pressure support from subsonic turbulent motions
- Acceleration term in the Euler eq. dominates the HE violation (Suto+13; Lau+13)



Reliability of WL masses



Becker & Kravtsov 11

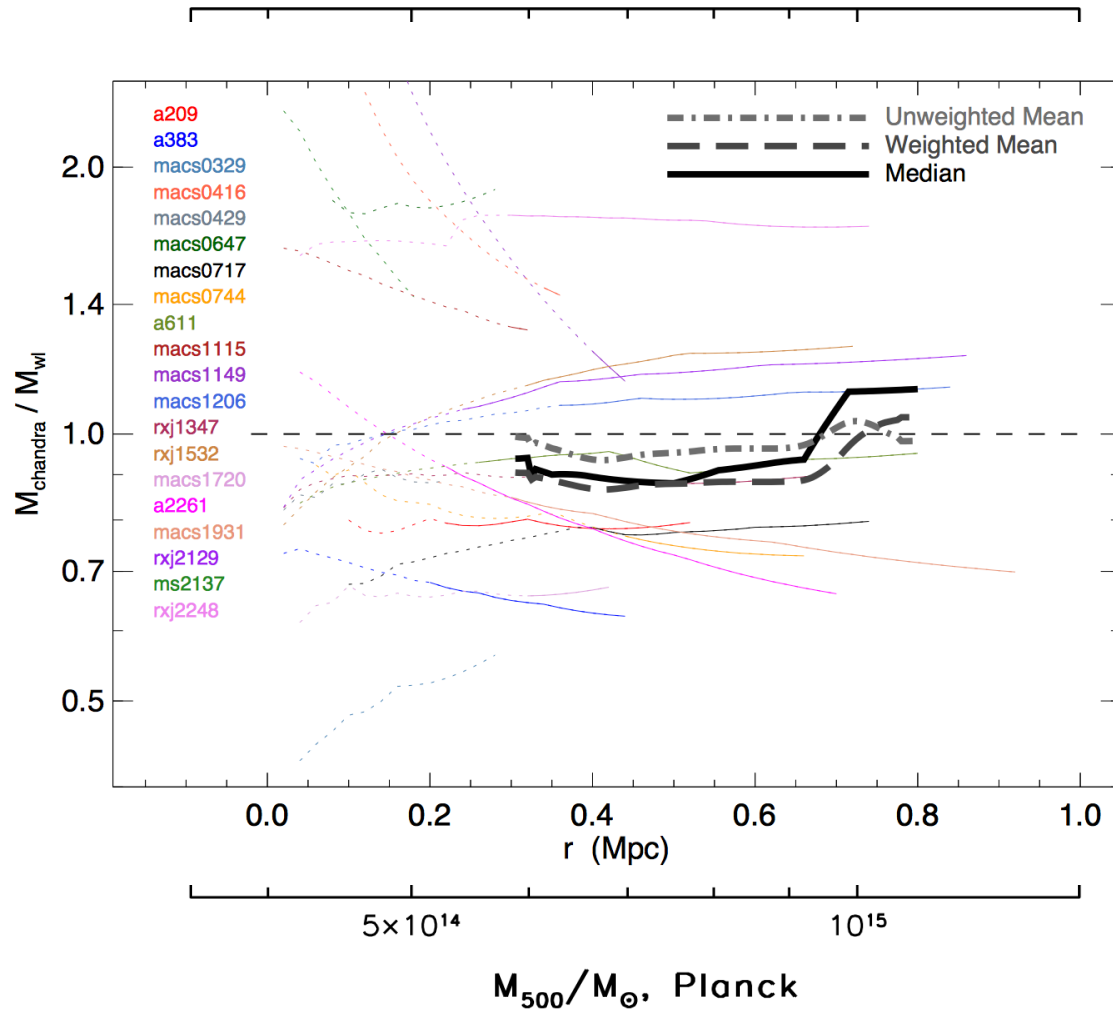


→ Spherical NFW fitting to tangential shear profile

→ 5-10% negative bias in recovered masses

→ Significant bias induced by triaxial halo shape, correlated and uncorrelated structures

Weak-Lensing and X-ray Masses



Von der Linden+14:

Planck clusters with WL (WtG) and X-ray calibrated (XMM) masses

→ $M_X \sim 0.7 M_{WL}$ on average

Donahue+14:

CLASH clusters with WL and X-ray calibrated (Chandra) mass profiles

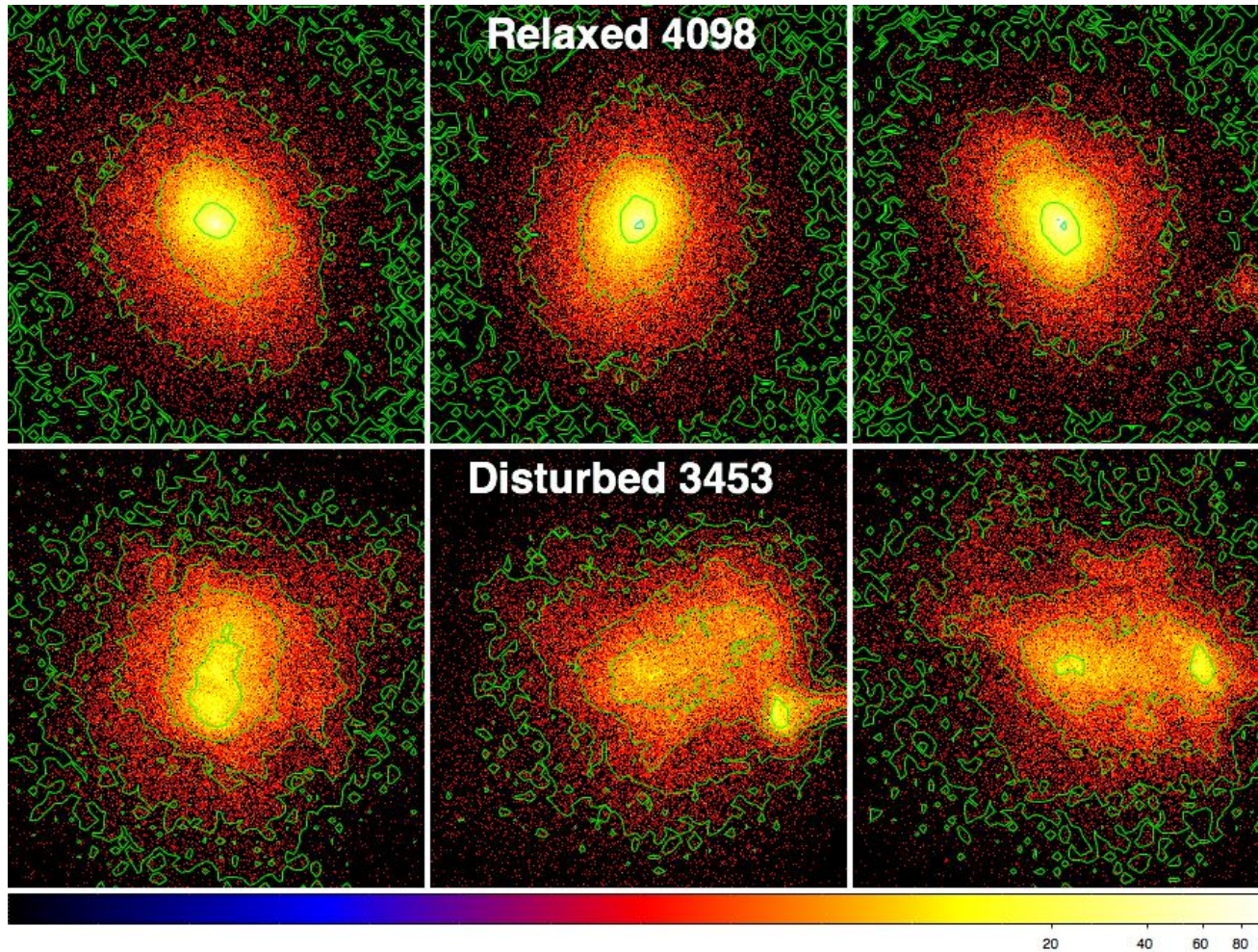
→ $M_X \sim 0.9 M_{WL}$

MIND: different WL mass estimators and **X-ray calibrations!**

E.g. also Zhang+10, Mahdavi+12, Israel+14

Simulating X-ray observations

- Event files from X-MAS Chandra simulator with 100 ks exp. time
- [0.7-2] keV X-ray image (16 x 16 arcmin²)



- 20 clusters @ $z=0.25$ with $M_{200} > 5 \times 10^{14} M_{\odot}$
- 3 projections for each cluster
- Generate mock event files
- Quantitative assessment of observational biases

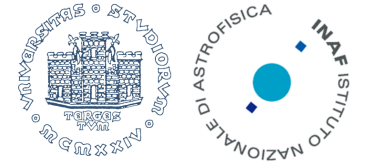
Simulating lensing observations



→ HST-WFC3 lensing of a massive simulated cluster at $z=0.25$

Based on the SkyLens tool (Meneghetti+08)

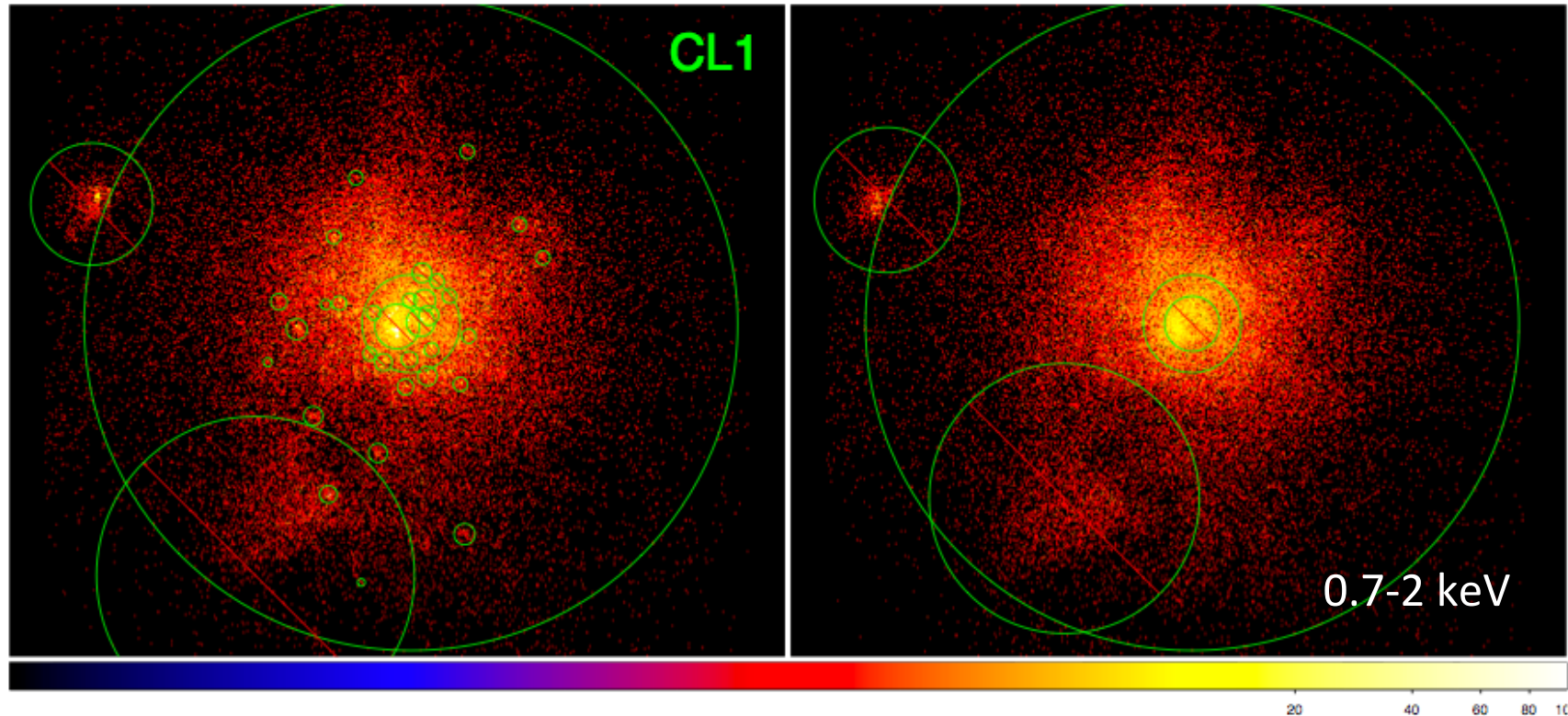
Origin of X-ray mass bias (in SPH simulations)



Black: M_x/M_{true}

Red: M_x/M_{true} using T_{mw}

Green: M_x/M_{WL}



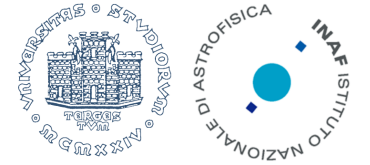
Bias in WL masses: $\sim 10\%$ underestimate at R_{500} (also Becker & Kravtsov 11)

Bias in X-ray masses:

→ 10-15% from violation of hydrostatic equilibrium

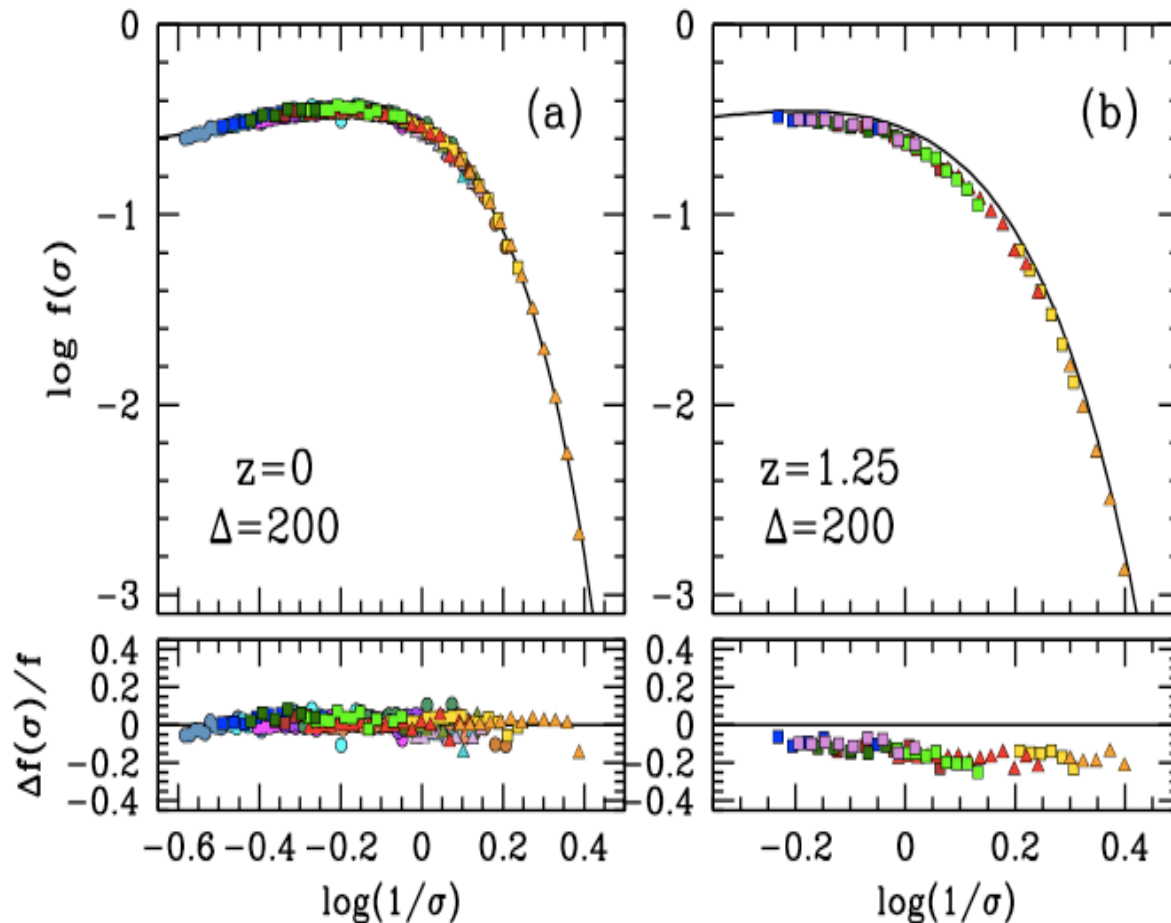
→ $\sim 15-20\%$ from bias in X-ray temperature estimate (but see Nagai+07)

Calibration of the halo mass function



E.g. for Λ CDM: Sheth & Tormen 01, Jenkins+01, Evrard+02, Springel+05, Warren+07, Reed+08, Tinker+09, Crocce+10, Courtin+11, Bhattacharya+11, Angulo+12, Watson+13,

Tinker et al. 09



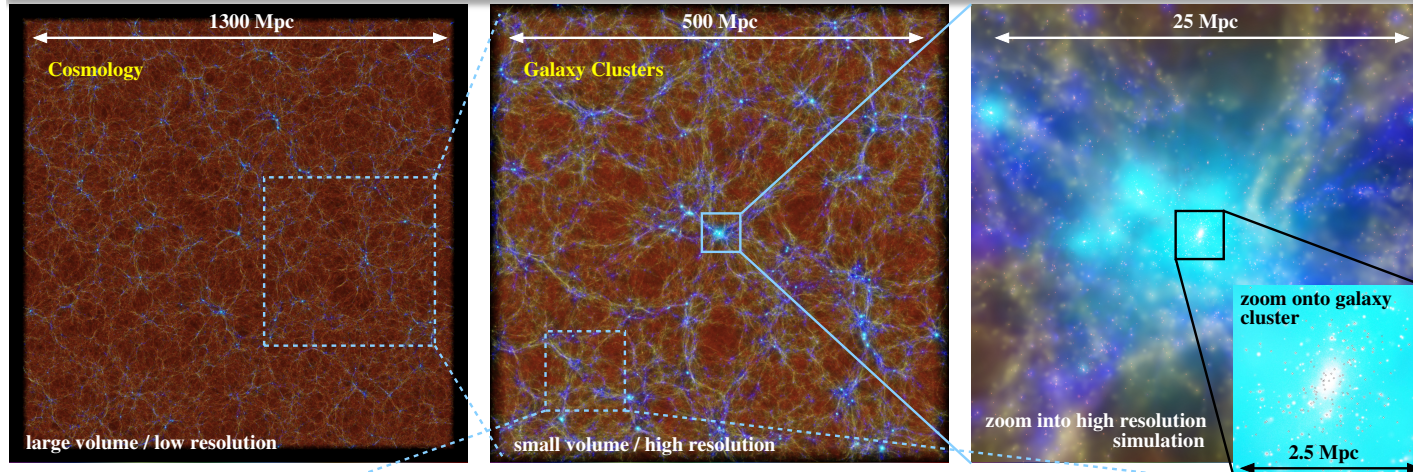
0-th order statements:

(a) N-body simulations provide the DM halo MF to any required precision

(b) Corrections to the Press-Schechter HMF are still almost universal (i.e. independent of cosmology and redshift)

(c) Residuals $<10\%$ at the cluster mass-scale

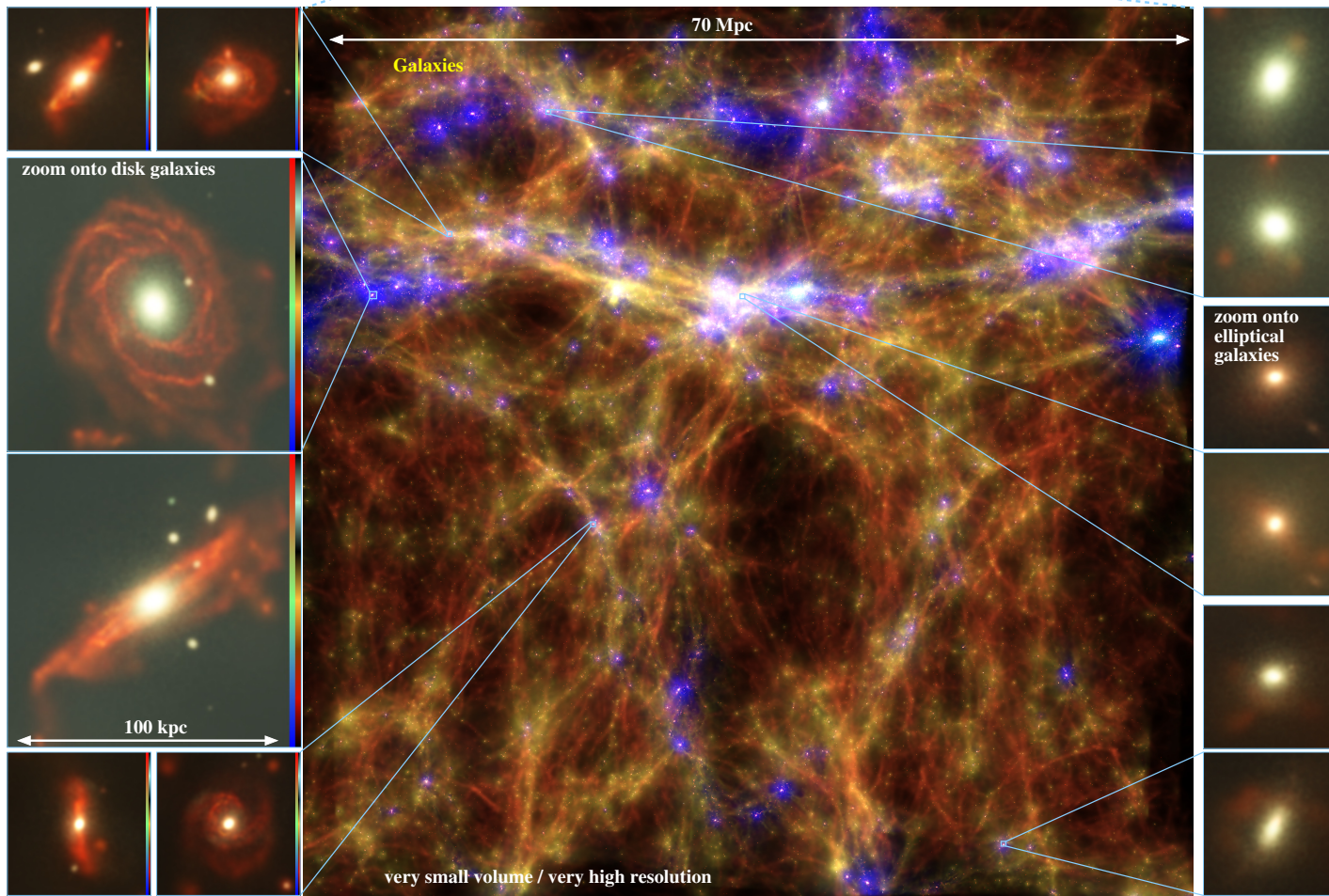
Effects of baryons on the HMF



“Magneticum” simulations

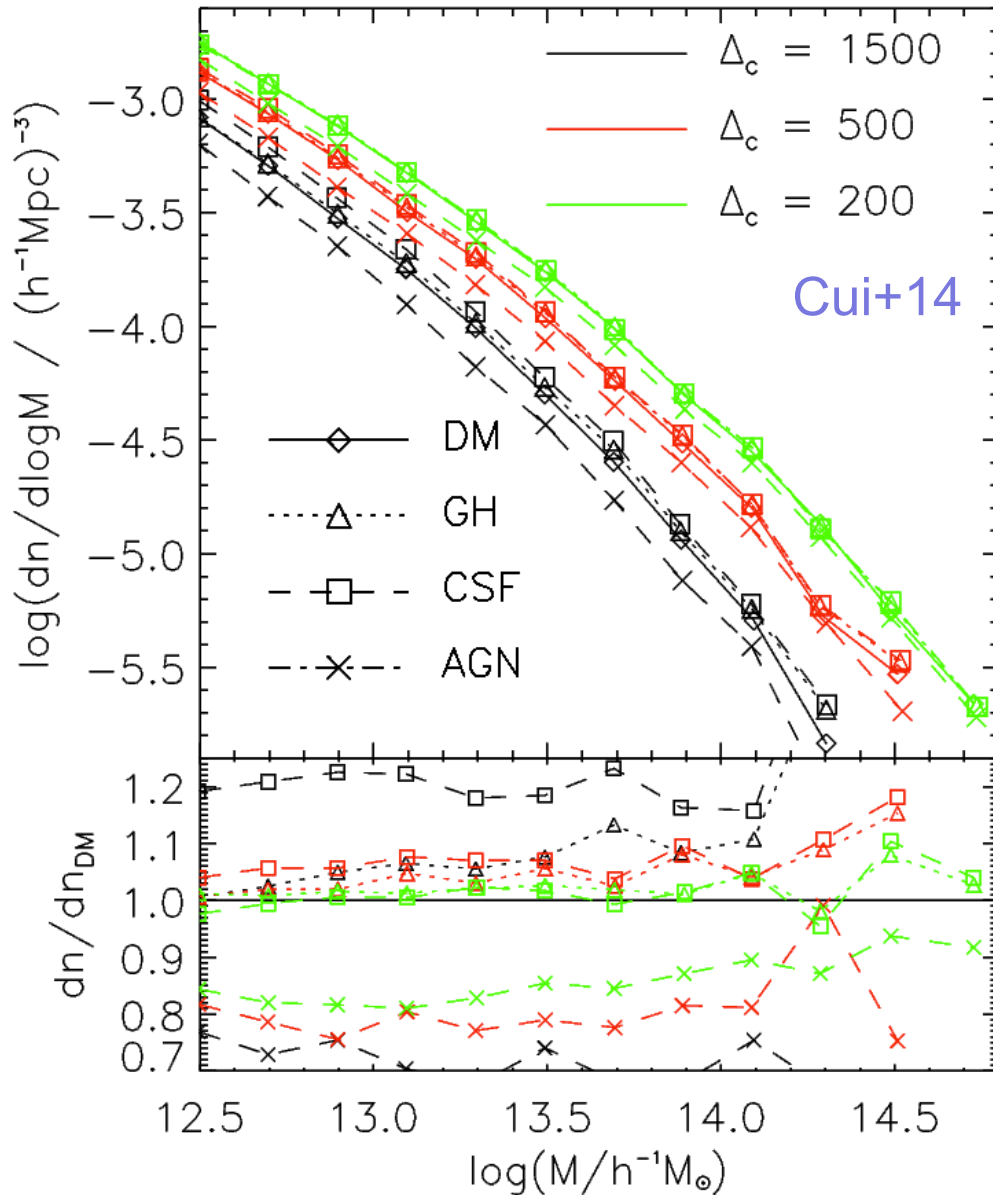
Dolag+14

www.magneticum.org



Effects of baryons on the HMF

Rudd+08, Stanek+08, Cui+12,14, Martizzi+14, Velliscig+14, Vogelsberger+14, Schaller+14, Bocquet+15



Effect of non-radiative gas

➔ Slight increase of the HMF

Effect of radiative hydro

➔ Stronger increase of the HMF

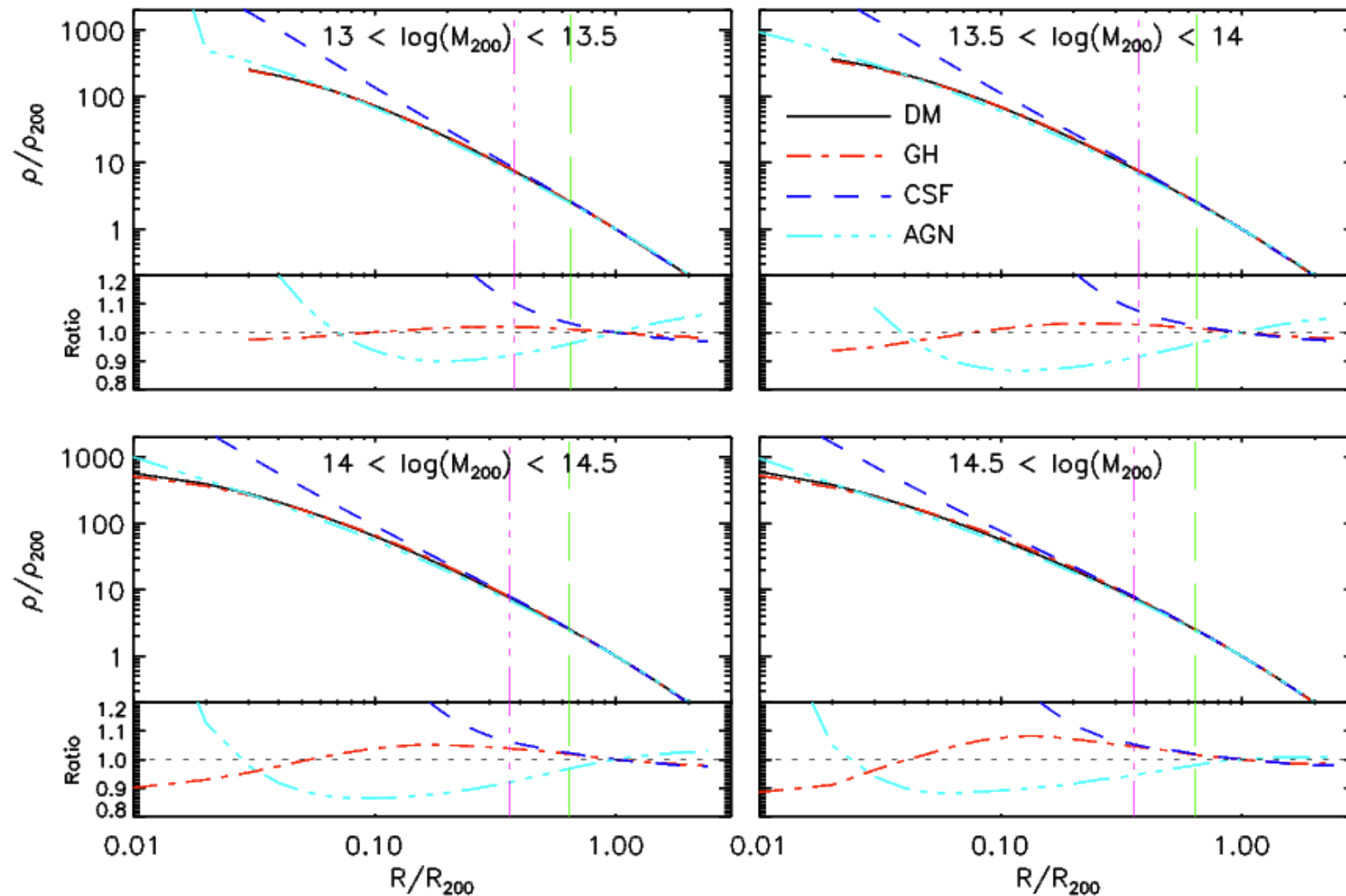
Effect of AGN feedback

➔ Decrease of the HMF

Effect of changing Δ_c

➔ Deviations increase at higher overdensity

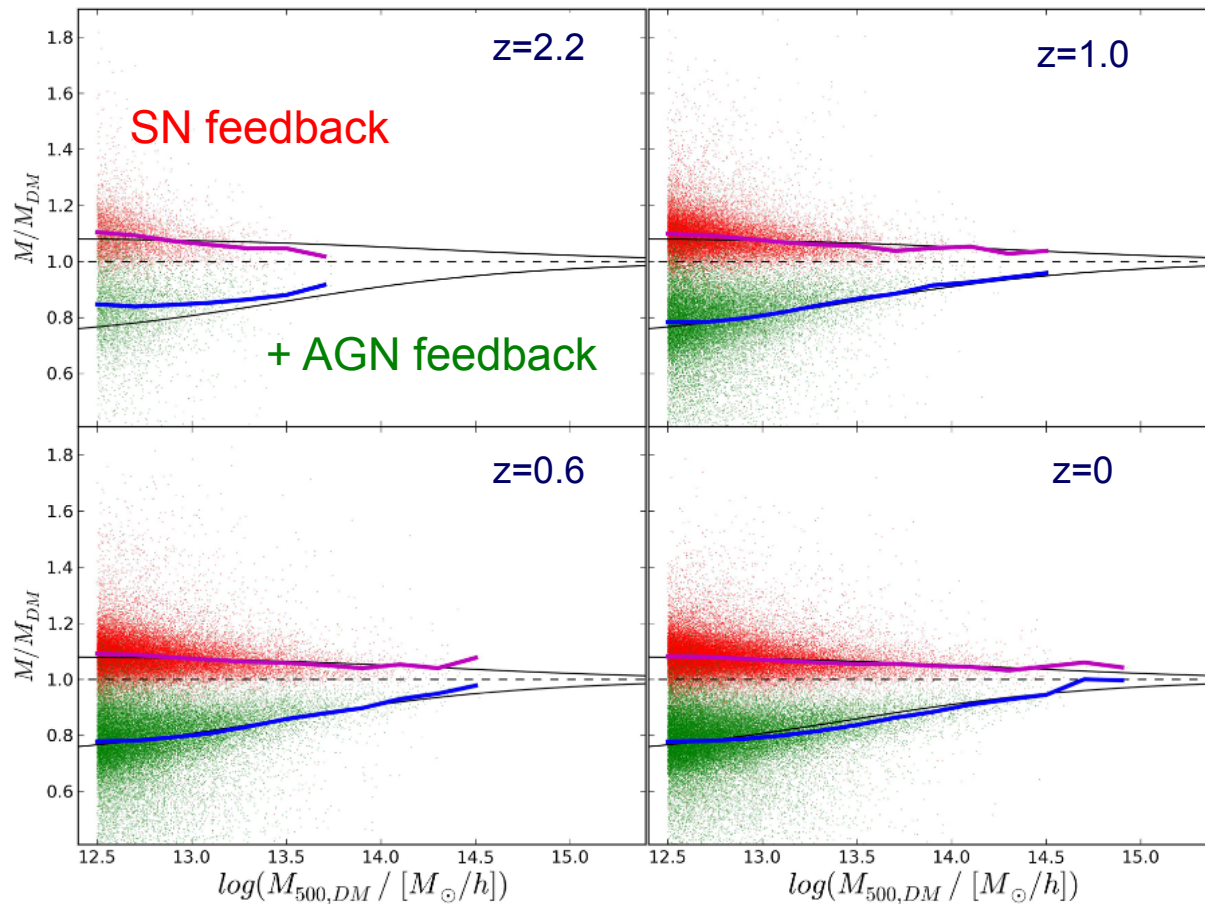
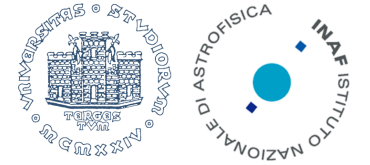
Effects of baryons on density profiles



Simulations with AGN: shallower density profiles (e.g., Cui+14, Martizzi +11; Duffy+10)

➔ Adiabatic expansion of the halo in reaction to sudden gas expulsion at $z \sim 2-3$.

Effects of baryons on the HMF



→ Opposite effects for CSF and AGN simulations

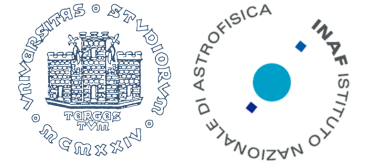
→ AGN: $\sim 20\%$ decrease at $M_{500} = \text{dex}(13.5) h^{-1} M_{\odot}$

→ Independent of redshift

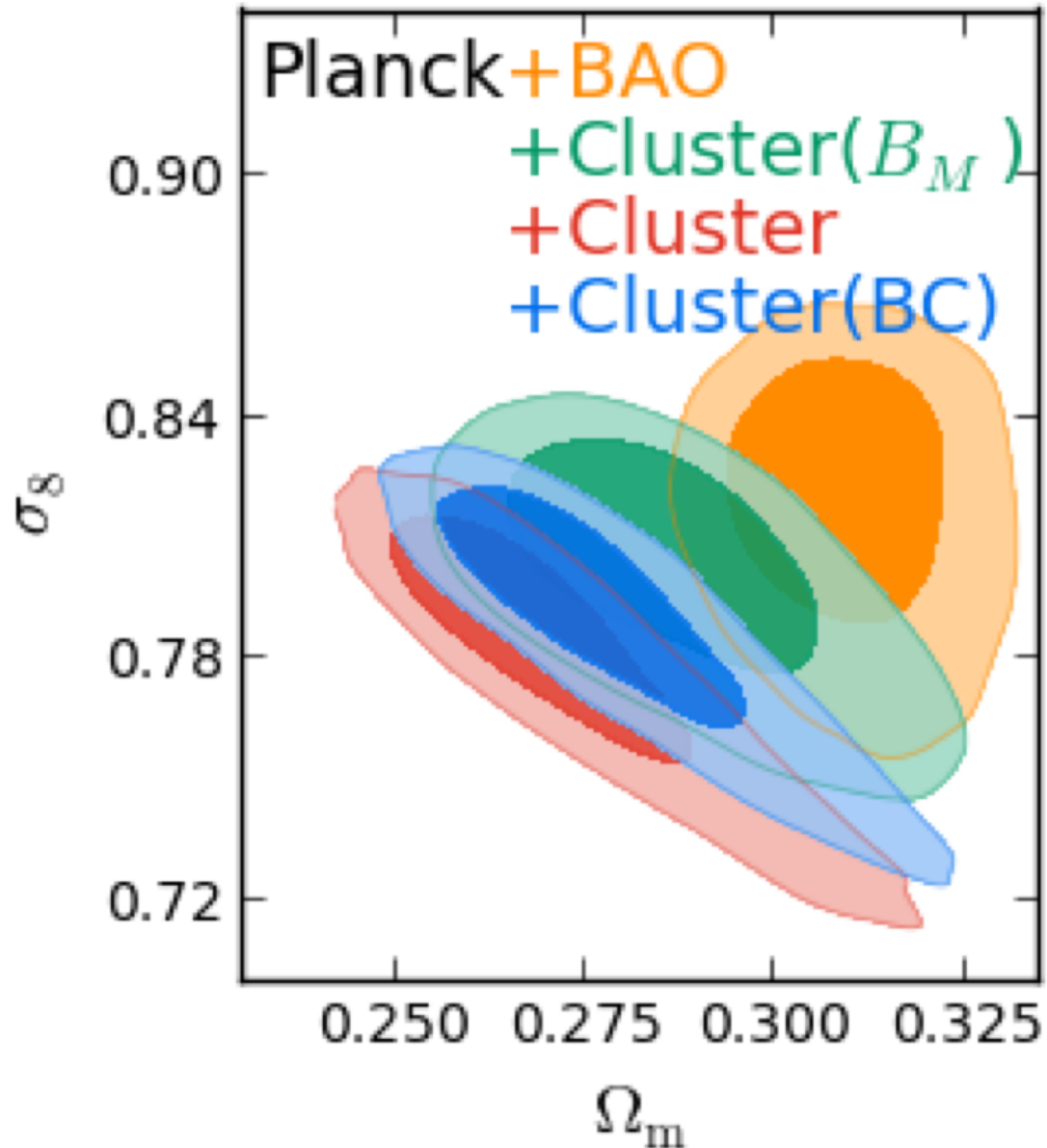
Q1: what's the impact on cosmological constraints?

Q2: how robust is the calibration of the baryon effects on halo masses?

Impact on cosmological constraints



Costanzi+14

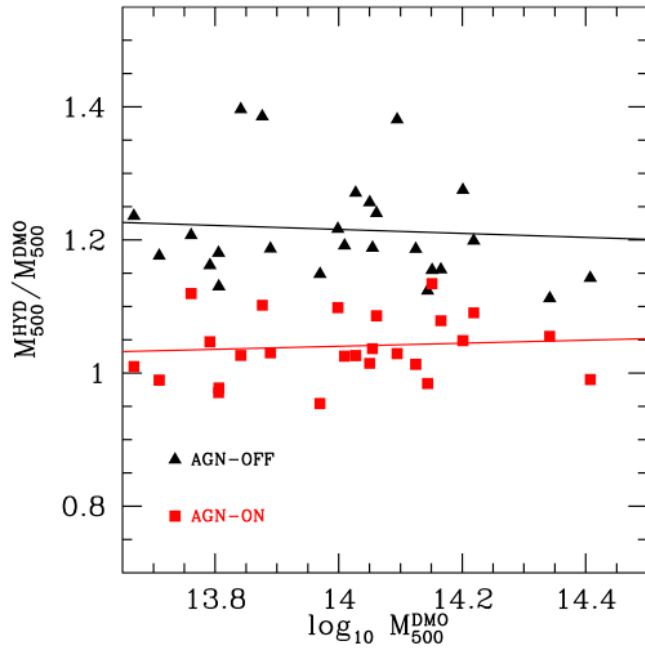


- Planck CMB
- BAO from SDSS-DR11 (Anderson+14)
- CCCP clusters (Vikhlinin+09)
- Massive neutrinos included
- B_M : mass bias = [0.8-1]
- BC: HMF baryonic correction
- Alleviate tension with Planck CMB
- Crucial to calibrate for future surveys

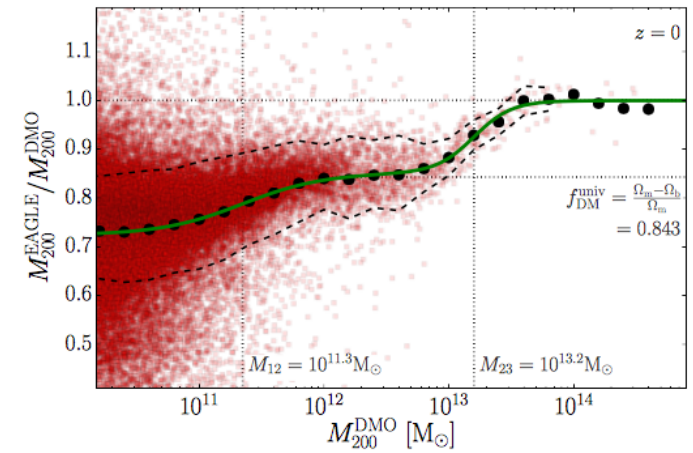
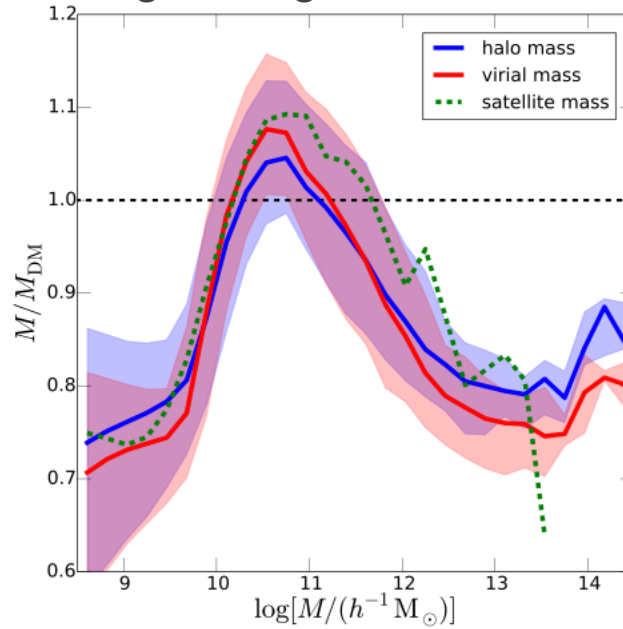
Robustness of calibration



Martizzi+14 : RAMSES

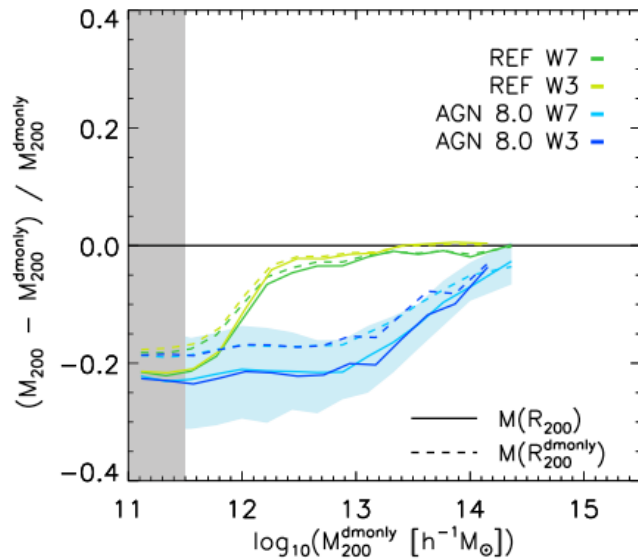
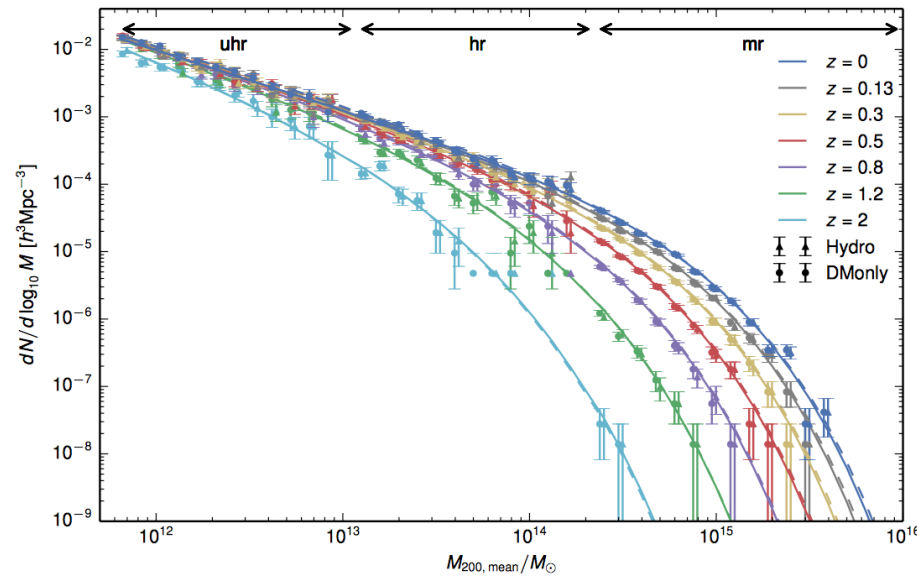


Vogelsberger+14 : AREPO



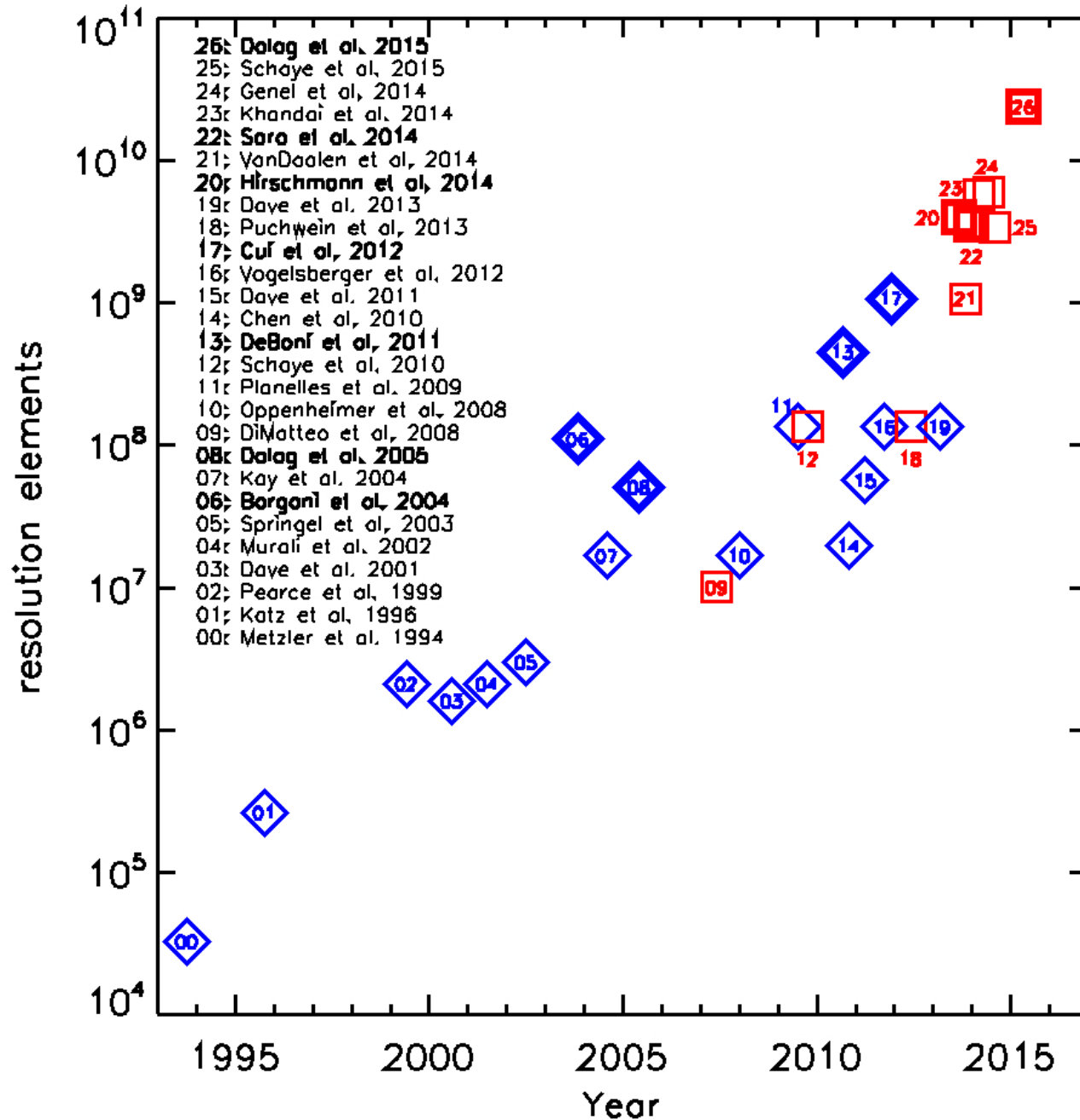
Schaller+14: GADGET-3 (Eagle)

Bocquet+15 : GADGET-3 (Magneticum)



Velliscig+14 : GADGET-3 (OWLS)

Moore's law for hydro simulations



To be kept in mind:

- Different resolutions
- Different physics included
- Trend contributed both by improvement of hardware and code design

Challenge for the future:

➔ Code re-engineering for exa-scale HPC facilities

- **Numerical N-body + hydro simulations:**
 - Ideal framework to capture the complexity of cosmic structure formation
- An exact numerical hydrodynamical method?
 - There is not such a thing.....
- Always test and compare different methods to understand range of validity and limitations
- Astrophysical processes: not self-consistently described
 - Phenomenological sub-resolution models
- Galaxy clusters: simulations help to calibrate as cosmological tools
 - Use simulations “cum grano salis”

INCLUDE IN SIMULATIONS ALL THE
(ASTRO)PHYSICAL PROCESSES?

AS DIFFICULT TO INTERPRET AS
OBSERVATIONS